Higgs potential in the type II seesaw model

A. Arhrib,[1,2] R. Benbrik,[2,3,4] M. Chabab,[2] G. Moultaka,[5,6,*] M. C. Peyranère,[7,8] L. Rahili,[2] and J. Ramadan[2]

[1]*Département de Mathématiques, Faculté des Sciences et Techniques, Tanger, Morocco*
[2]*Laboratoire de Physique des Hautes Energies et Astrophysique, Département de Physique,*
Faculté des Sciences Semlalia, Marrakech, Morocco
[3]*Faculté Polydisciplinaire, Université Cadi Ayyad, Sidi Bouzid, Safi-Morocco*
[4]*Instituto de Fisica de Cantabria (CSIC-UC), Santander, Spain*
[5]*Université Montpellier 2, Laboratoire Charles Coulomb UMR 5221, F-34095 Montpellier, France*
[6]*CNRS, Laboratoire Charles Coulomb UMR 5221, F-34095 Montpellier, France*
[7]*Université Montpellier 2, Laboratoire Univers & Particules de Montpellier UMR 5299, F-34095 Montpellier, France*
[8]*CNRS/IN2P3, Laboratoire Univers & Particules de Montpellier UMR 5299, F-34095 Montpellier, France*

The standard model Higgs sector, extended by one weak gauge triplet of scalar fields with a very small vacuum expectation value, is a very promising setting to account for neutrino masses through the so-called type II seesaw mechanism. In this paper we consider the general renormalizable doublet/triplet Higgs potential of this model. We perform a detailed study of its main dynamical features that depend on five dimensionless couplings and two mass parameters after spontaneous symmetry breaking, and highlight the implications for the Higgs phenomenology. In particular, we determine (i) the complete set of tree-level unitarity constraints on the couplings of the potential and (ii) the exact tree-level boundedness from below constraints on these couplings, valid for *all directions*. When combined, these constraints delineate precisely the theoretically allowed parameter space domain within our perturbative approximation. Among the seven physical Higgs states of this model, the mass of the lighter (heavier) $\mathcal{CP}_{\text{even}}$ state h^0 (H^0) will always satisfy a theoretical *upper (lower) bound* that is reached for a critical value μ_c of μ (the mass parameter controlling triple couplings among the doublet/triplet Higgses). Saturating the unitarity bounds, we find an upper bound $m_{h^0} < \mathcal{O}(0.7\text{–}1 \text{ TeV})$, while the upper bound for the remaining Higgses lies in the range of several tens of TeV. However, the actual masses can be much lighter. We identify two regimes corresponding to $\mu \gtrsim \mu_c$ and $\mu \lesssim \mu_c$. In the first regime the Higgs sector is typically very heavy, and only h^0 that becomes SM-like could be accessible to the LHC. In contrast, in the second regime, somewhat overlooked in the literature, most of the Higgs sector is light. In particular, the heaviest state H^0 becomes SM-like, the lighter states being the $\mathcal{CP}_{\text{odd}}$ Higgs, the (doubly) charged Higgses, and a decoupled h^0, possibly leading to a distinctive phenomenology at the colliders.

I. INTRODUCTION

One of the major goals of the LHC is to uncover the mechanism underlying the electroweak symmetry breaking and thereby the origin of the weak gauge boson and fermion masses. Moreover, observation of neutrino oscillations has shown that neutrinos are massive (for a review see, for instance, [1] and references therein). Such masses do not necessarily require physics beyond the standard model (SM), since one can accommodate a (Dirac) mass through a Yukawa coupling assuming a right-handed neutrino similarly to the other massive fermions. However, the introduction of such a right-handed state, whose only role is to allow for nonzero neutrino masses while being neutral under all the SM interactions, might seem rather mysterious. Furthermore, in contrast with the other right-handed fermion states of the SM, the right-handed neutrino allows also for a Majorana mass that is invariant under the SM gauge group but violates lepton number. These features make plausible

the existence of new flavor physics beyond the SM associated with the neutrino sector. Probably one of the most attractive aspects is the ability to induce naturally the tiny neutrino masses from this new flavor physics sector [2]. The celebrated seesaw mechanism [3–5] relating directly the smallness of the neutrino masses to the presence of a large new scale Λ through $m_\nu \sim \upsilon^2/\Lambda$, when $\Lambda \gg \upsilon$ where υ denotes the electroweak scale, is realized in a grand unified theory (GUT) context comprising right-handed neutrinos and is often dubbed type I seesaw. It can also be achieved without right-handed neutrinos through an extended Higgs sector including an $SU(2)_L$ triplet scalar field, type II seesaw [6–10], or by including two extra matter multiplets in the adjoint of $SU(2)_L$, type III seesaw [11], or a hybrid-type mixture of type I and type III [12–15].

If such extended sectors are too heavy to be directly accessible to TeV scale experiments, they could still be indirectly probed through distinctive low energy effective operators in the neutrino sector [16]. In the present paper we will rather focus on the possibility of accessing directly the Higgs sector *per se* of the type II scenario, studying

*Corresponding author.

general dynamical constraints which originate from the potential that couples the Higgs doublet and the Higgs triplet. However, given the present theoretical uncertainties, we do not commit to any specific GUT or flavor physics scenarios beyond the SM. In particular, mass parameters such as μ and M_Δ will not necessarily take large GUT scale values, even though such a configuration is included in the analysis. We will even consider regimes with very small μ ($\ll G_F^{-1/2}$). As noted in [17], such a small μ makes all the Higgs sector accessible to the LHC. Here we carry out a complete study, taking into account the full set of renormalizable operators present in the potential. The aim is to exhibit the various possible regimes consistent with the dynamical constraints dictated by the potential and their consequences on the phenomenology of the extended Higgs sector. Most of these operators are often neglected in the existing phenomenological studies of the type II seesaw mechanism, based on the fact that after spontaneous symmetry breaking their effects are suppressed by the small Higgs triplet vacuum expectation value (VEV), v_t, when compared to the electroweak scale. This is, however, not justified when studying the small μ regimes just mentioned, where μ can be of order v_t. In this case the detailed dynamics leads to an interesting structure of the Higgs sector.

The paper is organized as follows: In Sec. II, we present the ingredients of the model, the physical Higgs states and mass spectrum, as well as a parametrization of the potential parameters in terms of the physical masses. In Sec. III, we discuss some of the phenomenological and theoretical constraints on the parameters related to precision measurements, the absence of tachyonic Higgs modes, as well as the presence of false vacua. In Sec. IV, we provide a thorough study of the boundedness from below (BFB) of the potential and establish, for the first time simple, necessary and sufficient conditions on the couplings that are valid for all field directions. The unitarity constraints are analyzed in detail in Sec. V, through the study of all the scalar scattering channels. In Sec. VI, we combine, in an analytical compact form, the constraints obtained in Secs. IV and V. Section VII presents the behavior of the $\mathcal{CP}_{\text{even}}$ Higgs masses as functions of the potential parameters, highlighting theoretical upper and lower mass bounds and identifying different regimes that give better insight into the overall Higgs sector phenomenology, as well as the determination of unitarity mass bounds on the lightest Higgs. Section VIII is devoted to a short review of the salient features of the Higgs phenomenology at the colliders as well as to specific illustrations of our results. We conclude in Sec. IX and give some technical details in the appendixes.

II. THE MODEL

We start by recalling the scalar potential and the main properties of the Higgs physical eigenstates after

electroweak symmetry breaking (EWSB), as well as the corresponding eigenmasses and mixing angles. We give the expressions without neglecting any of the couplings appearing in Eq. (2.4) nor making any specific assumption about the magnitudes of μ, m_H^2, and M_Δ^2 which would originate from the unknown underlying high energy theory. The results of this section fix the notations and will serve for the completely model-independent analysis carried out in the subsequent sections.

A. The Higgs potential

The scalar sector consists of the standard Higgs weak doublet H and a colorless scalar field Δ transforming as a triplet under the $SU(2)_L$ gauge group with hypercharge $Y_\Delta = 2$, so that $H \sim (1, 2, 1)$ and $\Delta \sim (1, 3, 2)$ under the $SU(3)_c \times SU(2)_L \times U(1)_Y$.

Under a general gauge transformation $\mathcal{U}(x)$, H and Δ transform as $H \to \mathcal{U}(x)H$ and $\Delta \to \mathcal{U}(x)\Delta\mathcal{U}^\dagger(x)$. One can then write the most general renormalizable and gauge invariant Lagrangian of this scalar sector as follows:

$$\mathcal{L} = (D_\mu H)^\dagger (D^\mu H) + \text{Tr}(D_\mu \Delta)^\dagger (D^\mu \Delta) - V(H, \Delta) + \mathcal{L}_{\text{Yukawa}}, \tag{2.1}$$

where the covariant derivatives are defined by

$$D_\mu H = \partial_\mu H + ig T^a W_\mu^a H + i\frac{g'}{2} B_\mu H, \tag{2.2}$$

$$D_\mu \Delta = \partial_\mu \Delta + ig[T^a W_\mu^a, \Delta] + ig' \frac{Y_\Delta}{2} B_\mu \Delta, \tag{2.3}$$

with (W_μ^a, g) and (B_μ, g') denoting, respectively, the $SU(2)_L$ and $U(1)_Y$ gauge fields and couplings and $T^a \equiv \sigma^a/2$, with σ^a $(a = 1, 2, 3)$ the Pauli matrices. The potential $V(H, \Delta)$ is given by

$$V(H, \Delta) = -m_H^2 H^\dagger H + \frac{\lambda}{4}(H^\dagger H)^2 + M_\Delta^2 \text{Tr}(\Delta^\dagger \Delta)$$
$$+ [\mu(H^T i\sigma^2 \Delta^\dagger H) + \text{H.c.}] + \lambda_1 (H^\dagger H)\text{Tr}(\Delta^\dagger \Delta)$$
$$+ \lambda_2 (\text{Tr}\Delta^\dagger \Delta)^2 + \lambda_3 \text{Tr}(\Delta^\dagger \Delta)^2 + \lambda_4 H^\dagger \Delta\Delta^\dagger H, \tag{2.4}$$

where Tr is the trace over 2×2 matrices. $\mathcal{L}_{\text{Yukawa}}$ contains all the Yukawa sector of the SM plus one extra Yukawa term that leads, after spontaneous symmetry breaking, to (Majorana) mass terms for the neutrinos, without requiring right-handed neutrino states,

$$\mathcal{L}_{\text{Yukawa}} \supset -Y_\nu L^T C \otimes i\sigma^2 \Delta L + \text{H.c.}, \tag{2.5}$$

where L denotes $SU(2)_L$ doublets of left-handed leptons, Y_ν denotes neutrino Yukawa couplings, C the charge

conjugation operator, and we have suppressed flavor indices for simplicity. Although part of the type II seesaw model, we will refer to the above model Eq. (2.1) as the doublet-triplet-Higgs model (DTHM) since in this paper we are mainly interested in the scalar sector, bringing up only occasionally the content of the Yukawa sector $\mathcal{L}_{\text{Yukawa}}$ and the related neutrino masses issue.

Defining the electric charge as usual, $Q = I_3 + \frac{Y}{2}$ where I denotes the isospin, we write the two Higgs multiplets in components as

$$\Delta = \begin{pmatrix} \delta^+/\sqrt{2} & \delta^{++} \\ \delta^0 & -\delta^+/\sqrt{2} \end{pmatrix} \quad \text{and} \quad H = \begin{pmatrix} \phi^+ \\ \phi^0 \end{pmatrix}, \quad (2.6)$$

where we have used, for convenience, the 2×2 traceless matrix representation for the triplet.[1]

The potential defined in Eq. (2.4) exhausts all possible gauge invariant renormalizable operators. For instance, a term of the form $\lambda_5 H^\dagger \Delta^\dagger \Delta H$, which would be legitimate to add if Δ contained a singlet component, can actually be projected on the λ_1 and λ_4 operators appearing in Eq. (2.4) thanks to the identity $H^\dagger \Delta^\dagger \Delta H + H^\dagger \Delta \Delta^\dagger H = H^\dagger H \operatorname{Tr}(\Delta^\dagger \Delta)$ which is valid because Δ is a traceless 2×2 matrix. This simply amounts to redefining λ_1 and λ_4 such as $\lambda_1 + \lambda_5 \rightarrow \lambda_1$, $\lambda_4 - \lambda_5 \rightarrow \lambda_4$. The potential thus depends on five independent dimensionless couplings, λ and λ_i ($i = 1, \ldots, 4$), and three mass parameters, m_H^2, M_Δ^2, and μ. In the present paper we will assume all these parameters to be real valued. Indeed, apart from the μ term, all other operators in V are self-conjugate so that, by hermiticity of the potential, only the real parts of the λ's and the m_H^2, M_Δ^2 mass parameters will be relevant. As for μ, the only parameter that can pick up a would-be CP phase, this phase is unphysical and can always be absorbed in a redefinition of the fields H and Δ. One thus concludes that the DTHM Lagrangian is CP conserving (see also the discussion in [18]). Moreover, V depends on five complex (or ten real) scalar fields.

Assuming that spontaneous EWSB is taking place at some electrically neutral point in the field space, and denoting the corresponding VEVs by

$$\langle \Delta \rangle = \begin{pmatrix} 0 & 0 \\ v_t/\sqrt{2} & 0 \end{pmatrix} \quad \text{and} \quad \langle H \rangle = \begin{pmatrix} 0 \\ v_d/\sqrt{2} \end{pmatrix}, \quad (2.7)$$

one finds, after minimization of the potential Eq. (2.4), the following necessary conditions:

_____

[1]Note that the electric charge assignments for the upper and lower component fields are only conventional and can be interchanged by taking $Y_\Delta = -2$, $Y_H = -1$, entailing an exchange of the upper and lower components of the fermion weak doublets, without affecting the physical content. This seemingly trivial statement is important to keep in mind when discussing possible electric charge breaking minima of the potential.

$$M_\Delta^2 = \frac{2\mu v_d^2 - \sqrt{2}(\lambda_1 + \lambda_4)v_d^2 v_t - 2\sqrt{2}(\lambda_2 + \lambda_3)v_t^3}{2\sqrt{2}v_t},$$
$$(2.8)$$

$$m_H^2 = \frac{\lambda v_d^2}{4} - \sqrt{2}\mu v_t + \frac{(\lambda_1 + \lambda_4)}{2}v_t^2. \quad (2.9)$$

Even though, as we noted above, CP symmetry is realized at the level of the Lagrangian, there remains, in principle, the possibility for a spontaneous breakdown of this symmetry, an issue which we do not address in this paper. We can thus choose in the following v_d and v_t to be real valued; that is, we consider only CP conserving vacua for which complex valued v_d and/or v_t can always be rotated simultaneously to real values through some unphysical phase redefinition of the fields.

These equations, to which we will refer as the EWSB conditions, ensure that the vacuum corresponds to an extremum of the potential [that is, $\partial V/\partial \eta_i|_{\Delta = \langle \Delta \rangle, H = \langle H \rangle} = 0$ for each of the ten real-valued field components denoted here by η_i ($i = 1, \ldots 10$)], but one would still need to check that this extremum is indeed a stable, albeit local, minimum. The corresponding extra conditions are nothing but the absence of tachyonic modes in the Higgs sector, to be considered in a later section. We just anticipate here that the latter conditions will enforce the signs of μ and v_t to be identical. We can thus choose in the following $v_t > 0$, $\mu > 0$ without loss of generality. Furthermore, the two free parameters m_H^2 and M_Δ^2 can now be traded for v_d and v_t through Eqs. (2.8) and (2.9). In the rest of the paper we will take the eight parameters of the potential as being λ, λ_i ($i = 1, \ldots, 4$), μ, v_d, and v_t; requiring the correct electroweak scale will put the further constraint $v \equiv \sqrt{v_d^2 + 2v_t^2} = 246$ GeV on v_d, v_t, reducing this set of free parameters down to seven.

Let us also note that the above EWSB conditions will not necessarily imply that the gauge symmetric vacuum (i.e. at $\eta_i = 0$) is unstable. Indeed the latter instability requires that $M_\Delta^2 < 0$ and/or $m_H^2 > 0$, which are not guaranteed by Eqs. (2.8) and (2.9). Even more so, regimes with large μ will lead, through the EWSB conditions, to a very narrow gauge symmetric local minimum so that metastability issues might have to be considered. (More comments about the structure of the vacua of the model will be deferred to Sec. III C.)

On the other edge of the spectrum, very small values of μ could be favored if one requires the lepton number not to be strongly violated. Indeed, the μ term in Eq. (2.4) is the only source of lepton number violation at the Lagrangian level and *before* spontaneous EWSB. If this term is absent the Yukawa term Eq. (2.5), together with the other standard Yukawa terms, implies a conserved lepton number (where the Δ and H Higgs fields carry, respectively, the lepton

numbers $l_\Delta = -2$ and $l_H = 0$).[2] Then, from the lepton number assignment for H and Δ it follows that the μ term violates lepton number by two units. However, this violation is soft since the μ-induced lepton number violating processes (corresponding either to loop suppressed $2 \to 2$ processes or to propagator suppressed multiparticle processes) will have to involve both the standard and neutrino Yukawa couplings. These features suggest that if the two seemingly independent sources of lepton number violation, namely, the Δ VEV and μ, are assumed to have a common origin such as some spontaneous symmetry breaking of an underlying flavor theory, then it is natural to expect $\mu = \mathcal{O}(v_t)$ up to possible Yukawa coupling factors.

B. Higgs masses and mixing angles

The 10×10 squared mass matrix

$$\mathcal{M}^2 = \frac{1}{2} \frac{\partial^2 V}{\partial \eta_i^2} \bigg|_{\Delta = \langle \Delta \rangle, H = \langle H \rangle} \qquad (2.10)$$

can be recast, using Eqs. (2.8) and (2.9), in a block diagonal form of one doubly degenerate eigenvalue $m_{H^{\pm\pm}}^2$ and four 2×2 matrices denoted in the following by $\mathcal{M}_\pm^2$, $\mathcal{M}_{\mathcal{CP}_{\text{even}}}^2$, and $\mathcal{M}_{\mathcal{CP}_{\text{odd}}}^2$.

1. Mass of the doubly charged field

The double eigenvalue $m_{H^{\pm\pm}}^2$ corresponds to the doubly charged eigenstate $\delta^{\pm\pm}$ and could also be obtained directly by collecting all the coefficients of $\delta^{++}\delta^{--}$ in the potential. It reads

$$m_{H^{\pm\pm}}^2 = \frac{\sqrt{2}\mu v_d^2 - \lambda_4 v_d^2 v_t - 2\lambda_3 v_t^3}{2v_t}. \qquad (2.11)$$

From now on we will denote the doubly charged mass eigenstates $\delta^{\pm\pm}$ by $H^{\pm\pm}$.

2. Mass of the singly charged field

The mass-squared matrix for the singly charged field is

$$\mathcal{M}_\pm^2 = \left(\sqrt{2}\mu - \frac{\lambda_4 v_t}{2}\right) \begin{pmatrix} v_t & -v_d/\sqrt{2} \\ -v_d/\sqrt{2} & v_d^2/2v_t \end{pmatrix}.$$

This matrix is diagonalized by the following matrix $\mathcal{R}_{\beta'}$, given by

$$\mathcal{R}_{\beta'} = \begin{pmatrix} \cos\beta' & -\sin\beta' \\ \sin\beta' & \cos\beta' \end{pmatrix}, \qquad (2.12)$$

---

[2]The processes mediated by Eq. (2.5) and involving Higgs triplet decay or exchange are sometimes misleadingly dubbed "lepton number violating." One can check that the net overall lepton number of any process, comprising such decays or exchange, is conserved. This global symmetry will be violated only spontaneously when Δ acquires a VEV, that is, when the Majorana mass is induced from (2.5).

where β' is a rotation angle. Among the two eigenvalues of $\mathcal{M}_\pm^2$, one is zero and corresponds to the charged Goldstone boson $G^\pm$ while the other corresponds to the singly charged Higgs boson $H^\pm$ and is given by

$$m_{H^\pm}^2 = \frac{(v_d^2 + 2v_t^2)[2\sqrt{2}\mu - \lambda_4 v_t]}{4v_t}. \qquad (2.13)$$

The mass eigenstates $H^\pm$ and $G^\pm$ are rotated from the Lagrangian fields $\phi^\pm$, $\delta^\pm$ and defined by

$$G^\pm = \cos\beta' \phi^\pm + \sin\beta' \delta^\pm, \qquad (2.14)$$

$$H^\pm = -\sin\beta' \phi^\pm + \cos\beta' \delta^\pm. \qquad (2.15)$$

The diagonalization of $\mathcal{M}_\pm^2$ leads to the following relations involving the rotation angle β':

$$\frac{v_d^2}{2v_t}\left[\sqrt{2}\mu - \frac{\lambda_4 v_t}{2}\right] = \cos^2\beta' M_{H^\pm}^2, \qquad (2.16)$$

$$\frac{v_d}{\sqrt{2}}\left[\sqrt{2}\mu - \frac{\lambda_4 v_t}{2}\right] = \frac{\sin 2\beta'}{2} M_{H^\pm}^2, \qquad (2.17)$$

$$v_t\left[\sqrt{2}\mu - \frac{\lambda_4 v_t}{2}\right] = \sin^2\beta' M_{H^\pm}^2. \qquad (2.18)$$

These equations lead to a unique solution for $\sin\beta'$, $\cos\beta'$ up to a global sign ambiguity. Indeed, Eq. (2.16) implies $\sqrt{2}\mu - \frac{\lambda_4 v_t}{2} > 0$ in order not to have a tachyonic $H^\pm$ state and given our convention of $v_t > 0$. Then it follows from Eq. (2.17) that $\sin\beta'$ and $\cos\beta'$ should have the same sign. One finds

$$\sin\beta' = \epsilon_{\beta'} \frac{\sqrt{2}v_t}{\sqrt{v_d^2 + 2v_t^2}}, \qquad \cos\beta' = \epsilon_{\beta'} \frac{v_d}{\sqrt{v_d^2 + 2v_t^2}} \qquad (2.19)$$

with a sign freedom $\epsilon_{\beta'} = \pm 1$, and

$$\tan\beta' = \sqrt{2}\frac{v_t}{v_d}. \qquad (2.20)$$

3. Mass of the neutral fields

The neutral scalar and pseudoscalar mass matrices read

$$\mathcal{M}_{\mathcal{CP}_{\text{even}}}^2 = \begin{pmatrix} A & B \\ B & C \end{pmatrix} \quad \text{and}$$

$$\mathcal{M}_{\mathcal{CP}_{\text{odd}}}^2 = \sqrt{2}\mu \begin{pmatrix} 2v_t & -v_d \\ -v_d & v_d^2/2v_t \end{pmatrix}, \qquad (2.21)$$

where

$$A = \frac{\lambda}{2}v_d^2,$$

$$B = v_d(-\sqrt{2}\mu + (\lambda_1 + \lambda_4)v_t), \qquad (2.22)$$

$$C = \frac{\sqrt{2}\mu v_d^2 + 4(\lambda_2 + \lambda_3)v_t^3}{2v_t}.$$

These symmetric matrices are diagonalized by the following two orthogonal matrices:

$$\mathcal{R}_\alpha = \begin{pmatrix} \cos\alpha & -\sin\alpha \\ \sin\alpha & \cos\alpha \end{pmatrix} \quad \text{and} \quad \mathcal{R}_\beta = \begin{pmatrix} \cos\beta & -\sin\beta \\ \sin\beta & \cos\beta \end{pmatrix},$$
$$(2.23)$$

where α, β denote the rotation angles, respectively, in the $\mathcal{CP}_{\text{even}}$ and $\mathcal{CP}_{\text{odd}}$ sectors.[3] Upon diagonalization of $\mathcal{M}^2_{\mathcal{CP}_{\text{even}}}$ one obtains two massive even-parity physical states h^0 and H^0 defined by

$$h^0 = c_\alpha h + s_\alpha \xi^0, \qquad (2.24)$$

$$H^0 = -s_\alpha h + c_\alpha \xi^0, \qquad (2.25)$$

where h and ξ^0 are the real parts of the ϕ^0 and δ^0 fields shifted by their VEV values,

$$\phi^0 = \frac{1}{\sqrt{2}}(v_d + h + iZ_1) \quad \text{and} \quad \delta^0 = \frac{1}{\sqrt{2}}(v_t + \xi^0 + iZ_2).$$
$$(2.26)$$

The masses are given by the eigenvalues of $\mathcal{M}^2_{\mathcal{CP}_{\text{even}}}$ as follows,

$$m_{h^0}^2 = \frac{1}{2}\left[A + C - \sqrt{(A - C)^2 + 4B^2}\right], \qquad (2.27)$$

$$m_{H^0}^2 = \frac{1}{2}\left[A + C + \sqrt{(A - C)^2 + 4B^2}\right], \qquad (2.28)$$

so that $m_{H^0} > m_{h^0}$. Note that the lighter state h^0 is not necessarily the lightest of the Higgs sector (see Sec. VII).

On the other hand, $\mathcal{M}^2_{\mathcal{CP}_{\text{odd}}}$ leads to one massive physical state A^0 and one massless Goldstone boson G^0 defined by

$$A^0 = -s_\beta Z_1 + c_\beta Z_2, \qquad (2.29)$$

$$G^0 = c_\beta Z_1 + s_\beta Z_2, \qquad (2.30)$$

with masses

$$m_A^2 = \frac{\mu(v_d^2 + 4v_t^2)}{\sqrt{2}v_t}. \qquad (2.31)$$

Knowing the above eigenmasses, one can then determine the rotation angles α and β, which control the field content

of the physical states, from the following diagonalization conditions:

(1) $\mathcal{CP}_{\text{even}}$,

$$C = s_\alpha^2 m_{h^0}^2 + c_\alpha^2 m_{H^0}^2, \qquad (2.32)$$

$$B = \frac{\sin 2\alpha}{2}(m_{h^0}^2 - m_{H^0}^2), \qquad (2.33)$$

$$A = c_\alpha^2 m_{h^0}^2 + s_\alpha^2 m_{H^0}^2. \qquad (2.34)$$

(2) $\mathcal{CP}_{\text{odd}}$,

$$2\sqrt{2}\mu v_t = s_\beta^2 m_A^2, \qquad (2.35)$$

$$\sqrt{2}\mu v_d = \frac{\sin 2\beta}{2}m_A^2, \qquad (2.36)$$

$$\frac{\mu v_d^2}{\sqrt{2}v_t} = c_\beta^2 m_A^2. \qquad (2.37)$$

Of course, Eq. (2.32) should be equivalent to Eq. (2.34) upon use of $s_\alpha^2 + c_\alpha^2 = 1$ and Eqs. (2.27) and (2.28), and similarly for Eqs. (2.35) and (2.37). Furthermore, s_α, c_α, s_β, c_β will all be determined up to a global sign. There is, however, a difference between the two sectors. In the $\mathcal{CP}_{\text{odd}}$ sector s_β and c_β must have the same sign, as can be seen from Eq. (2.36) and the fact that $\mu > 0$ [the latter being due to the absence of the tachyonic A^0 state, Eq. (2.35)]. One then obtains unambiguously

$$\tan\beta = \frac{2v_t}{v_d} \quad \text{and} \quad \tan 2\beta = \frac{4v_t v_d}{v_d^2 - 4v_t^2} \qquad (2.38)$$

from Eqs. (2.35) and (2.37), and

$$s_\beta = \epsilon_\beta \frac{2v_t}{\sqrt{v_d^2 + 4v_t^2}}, \qquad c_\beta = \epsilon_\beta \frac{v_d}{\sqrt{v_d^2 + 4v_t^2}} \qquad (2.39)$$

with a sign freedom $\epsilon_\beta = \pm 1$.

In contrast, the relative sign between s_α and c_α in the $\mathcal{CP}_{\text{even}}$ sector depends on the values of μ, as can be seen from Eqs. (2.22) and (2.33). While they will have the same sign and $\tan\alpha > 0$ for most of the allowed μ and λ_1, λ_4 ranges, there will be a small but interesting domain of small μ values and $\tan\alpha < 0$ which we discuss in detail in Sec. VII. One obtains from Eqs. (2.32), (2.33), and (2.34)

$$s_\alpha = -\frac{\epsilon_\alpha \epsilon}{\sqrt{2}}\left(1 + \frac{(A - C)}{\sqrt{(A - C)^2 + 4B^2}}\right)^{1/2}, \qquad (2.40)$$

$$c_\alpha = \frac{\epsilon_\alpha}{\sqrt{2}}\left(1 - \frac{(A - C)}{\sqrt{(A - C)^2 + 4B^2}}\right)^{1/2}, \qquad (2.41)$$

where $\epsilon_\alpha = \pm 1$ and $\epsilon \equiv \text{sign}[B]$, and

$$\tan 2\alpha = \frac{2B}{A - C}. \tag{2.42}$$

Let us finally note that the angles β and β' are correlated since they depend exclusively on v_d and v_t. For instance, one always has

$$\tan\beta = \sqrt{2}\tan\beta', \tag{2.43}$$

as can be seen from Eqs. (2.20) and (2.38).

4. Lagrangian parameters from physical masses and couplings

The full experimental determination of the DTHM would require not only evidence for the neutral and (doubly) charged Higgs states, but also the experimental determination of the masses and couplings of these states among themselves as well as to the gauge and matter sectors of the model. Crucial tests would then be driven by the predicted correlations among these measurable quantities. For instance, one can easily express the Lagrangian parameters μ and the λ's in terms of the physical Higgs masses and the mixing angle α as well as the VEVs v_d, v_t, using Eqs. (2.11), (2.13), (2.31), (2.32), (2.33), and (2.34). One finds

$$\lambda_1 = -\frac{2}{v_d^2 + 4v_t^2} \cdot m_A^2 + \frac{4}{v_d^2 + 2v_t^2} \cdot m_{H^\pm}^2$$
$$+ \frac{\sin 2\alpha}{2 v_d v_t} \cdot (m_{h^0}^2 - m_{H^0}^2), \tag{2.44}$$

$$\lambda_2 = \frac{1}{v_t^2}\left\{ \frac{s_\alpha^2 m_{h^0}^2 + c_\alpha^2 m_{H^0}^2}{2} + \frac{1}{2} \cdot \frac{v_d^2}{v_d^2 + 4v_t^2} \cdot m_A^2 \right.$$
$$\left. - \frac{2 v_d^2}{v_d^2 + 2v_t^2} \cdot m_{H^\pm}^2 + m_{H^{\pm\pm}}^2 \right\}, \tag{2.45}$$

$$\lambda_3 = \frac{1}{v_t^2}\left\{ \frac{-v_d^2}{v_d^2 + 4v_t^2} \cdot m_A^2 + \frac{2 v_d^2}{v_d^2 + 2v_t^2} \cdot m_{H^\pm}^2 - m_{H^{\pm\pm}}^2 \right\}, \tag{2.46}$$

$$\lambda_4 = \frac{4}{v_d^2 + 4v_t^2} \cdot m_A^2 - \frac{4}{v_d^2 + 2v_t^2} \cdot m_{H^\pm}^2, \tag{2.47}$$

$$\lambda = \frac{2}{v_d^2}\{c_\alpha^2 m_{h^0}^2 + s_\alpha^2 m_{H^0}^2\}, \tag{2.48}$$

$$\mu = \frac{\sqrt{2} v_t}{v_d^2 + 4v_t^2} \cdot m_A^2. \tag{2.49}$$

The remaining two Lagrangian parameters m_H^2 and M_Δ^2 are then related to the physical parameters through the EWSB conditions Eqs. (2.8) and (2.9). To complete the determination in terms of physical quantities, one should further extract the mixing angle α from the measurement of some

couplings (see also Appendix C) and v_d and v_t from the W (or Z) masses. Using Eqs. (2.38), (3.1), and (3.2), one finds

$$v_d^2 = \frac{1}{(1 + \frac{1}{2}\tan^2\beta)} \frac{\sin^2\theta_W M_W^2}{\pi\alpha_{\text{QED}}},$$
$$v_t^2 = \frac{\tan^2\beta}{(1 + \frac{1}{2}\tan^2\beta)} \frac{\sin^2\theta_W M_W^2}{4\pi\alpha_{\text{QED}}} \tag{2.50}$$

or

$$v_d^2 = \frac{1}{(1 + \tan^2\beta)} \frac{\sin 2\theta_W M_Z^2}{2\pi\alpha_{\text{QED}}},$$
$$v_t^2 = \frac{\tan^2\beta}{(1 + \tan^2\beta)} \frac{\sin 2\theta_W M_Z^2}{8\pi\alpha_{\text{QED}}} \tag{2.51}$$

or

$$v_d^2 = \frac{\sin^2\theta_W}{\pi\alpha_{\text{QED}}}(2M_W^2 - \cos^2\theta_W M_Z^2),$$
$$v_t^2 = \frac{\sin^2\theta_W}{2\pi\alpha_{\text{QED}}}(\cos^2\theta_W M_Z^2 - M_W^2). \tag{2.52}$$

Using any of the above equations to substitute for v_d, v_t in Eqs. (2.44) and (2.49) allows us to obtain the Lagrangian parameters solely in terms of experimentally measurable quantities. Although Eqs. (2.50), (2.51), and (2.52) are theoretically trivially equivalent, they involve different sets of experimental observables and can thus lead to non-equivalent reconstruction strategies depending on the achieved accuracies in the measurement of these observables. Similarly, trading $\tan\beta$ for $\tan\beta'$ through Eq. (2.43) can be useful, depending on which of the two quantities is experimentally better determined through some coupling measurements. We should also note that Eqs. (2.44), (2.45), (2.46), (2.47), (2.48), (2.49), (2.50), (2.51), and (2.52) not only allow us to reconstruct the Lagrangian parameters from the measurable Higgs masses, α, β, M_Z, and/or M_W, but can also serve as consistency checks among observable quantities for the model when the λ's and μ are determined independently through the measurement of couplings in the purely Higgs sector (see also Appendix C). Finally, as can be seen from Eq. (2.52), the magnitude of v_t entails the deviation of the ρ parameter from its SM tree-level value, a point we will discuss further in the following section.

III. MISCELLANEOUS CONSTRAINTS

A. Constraints from electroweak precision measurements

In the standard model the custodial symmetry ensures that the ρ parameter, $\rho \equiv \frac{M_W^2}{M_Z^2\cos^2\theta_W}$, is equal to 1 at tree level. In the DTHM one obtains the Z and W gauge boson masses readily from Eq. (2.7) and the kinetic terms in Eq. (2.1) as

$$M_Z^2 = \frac{(g^2 + g'^2)(v_d^2 + 4v_t^2)}{4} = \frac{g^2(v_d^2 + 4v_t^2)}{4\cos^2\theta_W}, \quad (3.1)$$

$$M_W^2 = \frac{g^2(v_d^2 + 2v_t^2)}{4}, \quad (3.2)$$

hence the modified form of the ρ parameter:

$$\rho = \frac{v_d^2 + 2v_t^2}{v_d^2 + 4v_t^2} \neq 1 \quad (3.3)$$

and actually $\rho < 1$ at the tree level. Since we are interested in the limit $v_t \ll v_d$ we rewrite

$$\rho \simeq 1 - 2\frac{v_t^2}{v_d^2} = 1 + \delta\rho \quad (3.4)$$

with $\delta\rho = -2\frac{v_t^2}{v_d^2} < 0$ and $\sqrt{v_d^2 + 2v_t^2} = 246$ GeV. Thus the model will remain viable as long as the experimentally driven values of $\delta\rho$ are compatible with a negative number. The implication for the DTHM has already been studied in the literature [17]. Here we only discuss briefly this point, taking into account the latest updates of the electroweak observable fits as reported by the PDG [19]. One should compare the theoretical value with the experimental value after having subtracted from the latter all the known standard model contributions to the ρ parameter. The quoted number after this subtraction, $\rho_0 = 1.0008^{+0.0017}_{-0.0007}$, obtained from a global fit including the direct search limits on the standard Higgs boson, is not compatible with a negative $\delta\rho$ and would exclude the DTHM. However, at the 2σ level, one obtains $\rho_0 = 1.0004^{+0.0029}_{-0.0011}$ [19], which is again compatible with $\delta\rho < 0$. Moreover, relaxing the Higgs direct limit leads to $\rho_0 = 1.0008^{+0.0017}_{-0.0010}$, again compatible with $\delta\rho < 0$. From the last two numbers one gets an upper bound on v_t of order 2.5–4.6 GeV. In the present study we will thus be contented by the conservative assumption that an upper bound of 2.5 GeV guarantees consistency with the experimental constraints. We should note, though, that the tree-level DTHM value of $\delta\rho$ being of order 10^{-4}, it is legitimate to ask about the effects of radiative corrections to this quantity within the DTHM. As far as we know, radiative corrections to $\delta\rho$ are not available in the literature in the case of $Y_\Delta = 2$ that concerns us here, while several studies have been dedicated to this question in the framework of a $Y_\Delta = 0$ triplet Higgs [20–23]. In [20], it has been shown that the tree-level bound on the triplet VEV could be pushed to higher values by one-loop radiative corrections. Whether this will happen also in our case is still to be investigated and deserves a study that is out of the scope of the present paper, including for that matter all other CERN LEP/Stanford Linear Collider SM observables.

B. Absence of tachyonic modes

From Eq. (2.31), the requirement that m_A^2 should be positive implies $\mu v_t > 0$. The same positivity requirement in the singly charged and doubly charged sectors, Eqs. (2.11) and (2.13), together with our phase convention $v_t > 0$ discussed in Sec. II, leads to the following bounds on μ:

$$\mu > 0, \quad (3.5)$$

$$\mu > \frac{\lambda_4 v_t}{2\sqrt{2}}, \quad (3.6)$$

$$\mu > \frac{\lambda_4 v_t}{\sqrt{2}} + \sqrt{2}\frac{\lambda_3 v_t^3}{v_d^2}. \quad (3.7)$$

The tachyonless condition in the $\mathcal{CP}_{\text{even}}$ sector, Eqs. (2.27) and (2.28), is somewhat more involved and reads

$$\sqrt{2}\mu v_d^2 + \lambda v_d^2 v_t + 4(\lambda_2 + \lambda_3)v_t^3 > 0, \quad (3.8)$$

$$-8\mu^2 v_t + \sqrt{2}\mu(\lambda v_d^2 + 8(\lambda_1 + \lambda_4)v_t^2)$$
$$+ 4(\lambda(\lambda_2 + \lambda_3) - (\lambda_1 + \lambda_4)^2)v_t^3 > 0. \quad (3.9)$$

The first of these two equations is actually always satisfied as a consequence of Eq. (3.5) and the boundedness from below conditions for the potential [see Sec. IV and Eq. (4.21)]. The second equation, quadratic in μ, will lead to new constraints on μ in the form of an allowed range

$$\mu_- < \mu < \mu_+. \quad (3.10)$$

The full expressions of $\mu_\pm$ and a discussion of their real valuedness are given in Appendix A. Here we discuss their behavior in the regime $v_t \ll v_d$. In this case one finds a vanishingly small μ_- given by

$$\mu_- = ((\lambda_1 + \lambda_4)^2 - \lambda(\lambda_2 + \lambda_3))\frac{2\sqrt{2}}{\lambda}\frac{v_t^3}{v_d^2} + \mathcal{O}(v_t^4) \quad (3.11)$$

and a large μ_+ given by

$$\mu_+ = \frac{\lambda}{4\sqrt{2}}\frac{v_d^2}{v_t} + \sqrt{2}(\lambda_1 + \lambda_4)v_t + \mathcal{O}(v_t^2). \quad (3.12)$$

Depending on the signs and magnitudes of the λ's, one of the lower bounds (3.5), (3.6), and (3.7) or μ_- will overwhelm the others. Moreover, these no-tachyon bounds will eventually have to be amended by taking into account the existing experimental exclusion limits. This is straightforward for A^0, $H^\pm$, and $H^{\pm\pm}$. We thus define, for later reference,

$$\mu_{\min} = \max \begin{bmatrix} \frac{\sqrt{2}v_t}{v_d^2 + 4v_t^2}(m_A^2)_{\exp} \\ \frac{\lambda_4 v_t}{2\sqrt{2}} + \frac{\sqrt{2}v_t}{v_d^2 + 2v_t^2}(m_{H^\pm}^2)_{\exp} \\ \frac{\lambda_4 v_t}{\sqrt{2}} + \sqrt{2}\frac{\lambda_3 v_t^3}{v_d^2} + \frac{\sqrt{2}v_t}{v_d^2}(m_{H^{\pm\pm}}^2)_{\exp} \end{bmatrix}, \quad (3.13)$$

where $(m_A)_{\text{exp}}$, $(m_{H^\pm})_{\text{exp}}$, $(m_{H^{\pm\pm}})_{\text{exp}}$ denote some experimental lower exclusion limits for the Higgs masses. Equations (3.5), (3.6), and (3.7) are then replaced by

$$\mu > \mu_{\text{min}} \qquad (3.14)$$

in order for the masses to satisfy these exclusion limits. Similar modifications on $\mu_\pm$ taking into account experimental exclusion limits in the $\mathcal{CP}_{\text{even}}$ sector are more involved and will be differed to Sec. VII after having established the theoretical upper (lower) bounds on the h^0 (H^0) masses. Furthermore, the upper bound μ_+ will be instrumental in determining the maximally allowed values of the six Higgs masses m_{H^0}, m_A, $m_{H^\pm}$, $m_{H^{\pm\pm}}$, as we will see in Sec. VII.

C. The vacuum structure

Obviously, violation of any of the constraints discussed in the previous subsection is a signal that the would-be electroweak vacuum is not a minimum (but rather a saddle point or a local maximum) for the given set of values λ, λ_i, v_d, v_t when μ is either very small or very large. However, since Eqs. (2.8) and (2.9) are nonlinear in v_d, v_t, it could still be possible to find a different set of values v'_d, v'_t, for the same input values of m_H^2, M_Δ^2, where the true electroweak minimum is obtained at a lower point of the potential than the previous one. More generally, and depending on the values of the parameters of the potential, one expects, on top of the electroweak minimum, a rich structure of extrema that can affect the interpretation and viability of this minimum and thus possibly lead to additional constraints on these parameters. A complete study of such extrema can be very involved since the potential depends on ten independent real fields. Here we only provide a partial qualitative discussion.

Upon use of Eqs. (2.7), (2.8), and (2.9) in Eq. (2.4), one readily finds that the value of the potential at the electroweak minimum, $\langle V \rangle_{\text{EWSB}}$, is given by

$$\langle V \rangle_{\text{EWSB}} = -\frac{1}{16}(\lambda v_d^4 + 4(\lambda_2 + \lambda_3)v_t^4 \\ + 4v_d^2 v_t((\lambda_1 + \lambda_4)v_t - \sqrt{2}\mu)). \qquad (3.15)$$

Since the potential vanishes at the gauge invariant origin of the field space, $V_{H=0,\Delta=0} = 0$, then spontaneous electroweak symmetry breaking would be energetically disfavored if $\langle V \rangle_{\text{EWSB}} > 0$.[4] One can thus require as a first approximation the naive bound on μ,

$$\mu < \mu_{\text{max}} \equiv \frac{\lambda}{4\sqrt{2}}\frac{v_d^2}{v_t} + (\lambda_1 + \lambda_4)\frac{v_t}{\sqrt{2}} + \mathcal{O}(v_t^2), \quad (3.16)$$

---

[4]We should, however, keep in mind the possibility that a long-lived metastable vacuum could still be physically acceptable, even when $\langle V \rangle_{\text{EWSB}} > 0$, thus altering our constraints; these issues are not addressed further in the present paper.

to ensure $V_{\text{EWSB}} < 0$. As can be seen from Eq. (3.12) one has either $\mu_{\text{max}} < \mu_+$ or $\mu_{\text{max}} > \mu_+$ depending on the sign of $\lambda_1 + \lambda_4$. But for all practical purposes $\mu_{\text{max}} \simeq \mu_+$ in the regime $v_t/v_d \ll 1$, so that the proviso stated above concerning the relevance of the tachyonless conditions is weakened for the upper bound μ_+ which can be replaced by μ_{max}. There is, however, yet another critical value of μ. As mentioned at the end of Sec. II A, M_Δ^2 and $-m_H^2$ can both be positive for sufficiently large values of μ, thus making the gauge invariant point $H = 0$, $\Delta = 0$ a local minimum. This happens when $\mu > \mu_H$, where

$$\mu_H = \frac{\lambda}{4\sqrt{2}}v_d^2 + (\lambda_1 + \lambda_4)\frac{v_t}{2\sqrt{2}}. \qquad (3.17)$$

If $\lambda_1 + \lambda_4 > 0$ then $\mu_H < \mu_{\text{max}} < \mu_+$. To delineate some consistency constraints in this case, it would be necessary to look more closely at the decay rate from a metastable gauge invariant vacuum to the EWSB vacuum, if $\mu_H < \mu < \mu_{\text{max}}$, and vice versa, from a metastable EWSB vacuum to the gauge invariant vacuum when $\mu_{\text{max}} < \mu < \mu_+$. Fortunately, however, these configurations altogether are already excluded if we take into account the experimental mass limits on the standard model Higgs. Indeed, as will be shown in Secs. VII and VIII, the lightest $\mathcal{CP}_{\text{even}}$ Higgs state h^0 becomes purely SM-like for such large values of μ, irrespective of the values of the couplings λ, λ_i, while m_{h^0} becomes very small for these values [e.g. $m_{h^0} = \sqrt{3(\lambda_1 + \lambda_4)}v_t$ for $\mu = \mu_H$] and thus experimentally excluded.

Nonetheless, the structure of the potential Eq. (2.4) is sufficiently rich to provide dangerous extrema configurations which are not excluded by the above-mentioned experimental limits. We exhibit here, without many details, one example among a manifold of possibilities. There is an extremum in the field space direction defined by $\text{Re}\phi^0 = \text{Re}\phi^+ \equiv \frac{v_d^c}{\sqrt{2}}$ and $\text{Re}\delta^0 = -\text{Re}\delta^{++} \equiv \frac{v_t^c}{\sqrt{2}}$, and all other fields put to zero.

This requires

$$\mu = -\frac{\lambda_4 v_t^c}{\sqrt{2}}, \qquad (3.18)$$

$$m_H^2 = \tfrac{1}{2}(\lambda v_d^{c2} + (2\lambda_1 - \lambda_4)v_t^{c2}), \qquad (3.19)$$

$$M_\Delta^2 = -\lambda_1 v_d^{c2} - (2\lambda_2 + \lambda_3)v_t^{c2}. \qquad (3.20)$$

Note that this direction, and thus the corresponding extremum, spontaneously breaks charge conservation. We will refer to this extremum as charge breaking (CB). Furthermore, in contrast with the EWSB point, Eqs. (2.8) and (2.9), here μ is not a free parameter. We can then seek a region in parameter space where this CB extremum coexists with an EWSB minimum, and check what happens at the gauge invariant extremum point as well. Requiring Eqs. (2.8), (2.9), (3.18), (3.19), and (3.20) to be

simultaneously satisfied leads to correlations among v_d, v_t, v_d^c, v_t^c. These lead in turn to constraints on the λ, λ_i parameter space in order for all these VEVs to be real valued (modulo gauge transformations), together with the immediate constraint $\lambda_4 v_t^c < 0$ originating from Eq. (3.18) and $\mu > 0$.[5] The ensuing correlations allow us to write $m_{h^0}^2$, $\langle V \rangle_{\rm EWSB}$, and $\langle V \rangle_{\rm CB}$ (the value of the potential at the CB extremum) in the following form:

$$m_{h^0}^2 = (\lambda(2\lambda_2 + \lambda_3) + 2\lambda_4^2 + \lambda_1(\lambda_4 - 2\lambda_1)) \frac{v_t v_t^c}{\lambda_4} + \mathcal{O}(v_t^2)$$

$$= 2m_H^2 + \mathcal{O}(v_t^2), \qquad (3.21)$$

$$\langle V \rangle_{\rm EWSB} = -(\lambda(2\lambda_2 + \lambda_3) + 2\lambda_4^2 + \lambda_1(\lambda_4 - 2\lambda_1))$$
$$\times (\lambda(2\lambda_2 + \lambda_3) + \lambda_1(-2\lambda_1 + \lambda_4))$$
$$\times \frac{v_t^2 v_t^{c2}}{4\lambda\lambda_4^2} + \mathcal{O}(v_t^3), \qquad (3.22)$$

$$\langle V \rangle_{\rm CB} = (4\lambda_1^2 - 2\lambda(2\lambda_2 + \lambda_3) - \lambda_4^2) \frac{v_t^{c4}}{4\lambda} + \mathcal{O}(v_t^2). \qquad (3.23)$$

Various interesting conclusions can be drawn from the above equations. As can be seen from Eq. (3.21), a physical h^0, i.e. $m_{h^0}^2 > 0$, implies a positive m_H^2 and thus an *unstable* gauge invariant point at the origin of the fields ($H = 0$, $\Delta = 0$). Furthermore, in the consistent (λ, λ_i) domain (given in footnote 2) $m_{h^0}^2$ is indeed positive and, furthermore, one finds from Eq. (3.22) that $\langle V \rangle_{\rm EWSB} < 0$. The EWSB vacuum is thus energetically favored over the gauge symmetry preserving one which lies at $V = 0$. It then remains to compare the EWSB point with the CB point. Close inspection of Eq. (3.23) shows that $\langle V \rangle_{\rm CB} > 0$ in all the (λ, λ_i) domain given in footnote 2, if and only if $\lambda_4 < 0$, in which case the EWSB is energetically favored over the CB. However, if $\lambda_4 > 0$ (and thus $v_t^c < 0$), there are regions in the (λ, λ_i) consistent domain where $\langle V \rangle_{\rm CB} < 0$, provided that $4\lambda_4^2 < \lambda(2\lambda_2 + \lambda_3)$. Moreover, the potential at this CB point becomes much deeper than at the EWSB point since we are in the regime $v_t \ll |v_t^c|$. This is a dangerous configuration since it makes the EWSB vacuum potentially very short-lived due to tunneling effects [24,25]. We stress here that this EWSB point is a true local minimum in this configuration; i.e. there are no tachyonic Higgs states which could have signaled its nonrelevance beforehand. (This is easily seen from the fact that h^0 is nontachyonic and is the lightest Higgs state when

$\mu \sim |v_t^c| \gg v_t$; see also Sec. VII.) Even more so, the potential is bounded from below, as can be shown by comparing the corresponding (λ, λ_1) domain with the boundedness from below constraints that we will derive in the following section. We have thus exhibited an example of a configuration where μ can be very large, consistent with the experimental h^0 mass limit, and *a fortiori* with all the nontachyon constraints, corresponding locally to an acceptable EWSB vacuum, but still nonviable due to the existence of lower (charge breaking) points akin to what happens in two-Higgs-doublet models (see, for instance, [26]).

We end this section with a general comment concerning the neutrino mass seesaw mechanism. The common lore is to assume a GUT origin for μ and M_Δ, and taking $\mu \sim M_\Delta \sim \mathcal{O}(M_{\rm GUT})$ leads, through Eq. (2.8), naturally to a tiny v_t. However, as noted in the Introduction we do not commit, in the present study, to specific high energy physics scenarios, so that M_Δ and/or μ could be smaller than a hypothetical GUT scale. It is then interesting to note that even in this case a kind of seesaw mechanism is actually still at work model-independently due to the dynamics of the potential. This is simply due to the form of the μ upper bound μ_+, Eq. (3.12): The larger μ is, the smaller v_t should be in order to avoid a tachyonic h^0. For instance, taking $\lambda \simeq 0.5$ and $\mu_+ \simeq 2 \times 10^{12}$ GeV leads to $v_t \simeq 1$ eV and $M_\Delta \simeq 10^{13}$ GeV.

IV. BOUNDEDNESS OF THE POTENTIAL

A necessary condition for the stability of the vacuum comes from requiring that the potential given in Eq. (2.4) be bounded from below when the scalar fields become large in any direction of the field space. The constraints ensuring BFB of the DTHM potential have been studied in the literature so far only partially (see e.g. [18]), and at the tree level. It would thus be somewhat premature to invoke possible quantum modifications of these constraints before fully settling the tree-level issue first. This section is devoted to this issue and aims at deriving, at the tree level, the complete *necessary and sufficient* BFB conditions valid for *all* directions in field space.[6]

Obviously, at large field values the potential Eq. (2.4) is generically dominated by the part containing the terms that are quartic in the fields,

$$V^{(4)}(H, \Delta) = \frac{\lambda}{4}(H^\dagger H)^2 + \lambda_1 (H^\dagger H) {\rm Tr}(\Delta^\dagger \Delta)$$
$$+ \lambda_2 ({\rm Tr}\Delta^\dagger \Delta)^2 + \lambda_3 {\rm Tr}(\Delta^\dagger \Delta)^2$$
$$+ \lambda_4 H^\dagger \Delta\Delta^\dagger H. \qquad (4.1)$$

---

[5]Working in the regime $v_t \ll v_d$, $|v_t^c|$, $|v_d^c|$ and keeping only terms $\mathcal{O}(v_t)$, the constraint in the (λ, λ_i) space satisfying all these requirements is found to be $\lambda_1 < \frac{1}{4} \times (\lambda_4 - \sqrt{8\lambda(2\lambda_2 + \lambda_3) + 17\lambda_4^2})$. Note that $\lambda > 0$ and $2\lambda_2 + \lambda_3 > 0$ for a bounded from below potential (see Sec. IV).

[6]We will thus not address in this paper the possibility that loop corrections could lift the potential in some otherwise unbounded from below directions, nor the issues related to metastability of the vacuum which could relax some of the constraints. See also Sec. IIIC.

The study of $V^{(4)}(H, \Delta)$ will thus be sufficient to obtain the main constraints. To obtain BFB conditions it is common in the literature to pick up specific field directions or to put some of the couplings to zero. Consider, for instance, the following two cases:

(1) In the absence of any coupling between doublet and triplet Higgs bosons, i.e. $\lambda_1 = \lambda_4 = 0$, it is obvious that

$$\lambda > 0 \quad \& \quad \lambda_2 > 0 \quad \& \quad \lambda_3 > 0 \qquad (4.2)$$

will ensure that the potential is bounded from below.

(2) If one picks up the field space directions where only the electrically neutral components are nonvanishing, one finds

$$V_0^{(4)} = \frac{\lambda}{4}|\phi^0|^4 + (\lambda_2 + \lambda_3)|\delta^0|^4 + (\lambda_1 + \lambda_4)|\phi^0|^2|\delta^0|^2. \qquad (4.3)$$

In order for the potential to be bounded from below in this subspace, $V_0^{(4)}$ should be positive for any values of $|\phi^0|$ and $|\delta^0|$, including when one or the other is vanishing. The latter cases imply the necessary conditions $\lambda > 0$ and $\lambda_2 + \lambda_3 > 0$. It is then possible to rewrite Eq. (4.3) in the form

$$V_0^{(4)} = \left[\frac{\sqrt{\lambda}}{2}|\phi^0|^2 - \sqrt{\lambda_2 + \lambda_3}|\delta^0|^2\right]^2 + \left(\lambda_1 + \lambda_4 + \sqrt{\lambda(\lambda_2 + \lambda_3)}\right)|\phi^0|^2|\delta^0|^2. \quad (4.4)$$

Since the first term is non-negative and vanishes in the direction $|\phi^0|^2/|\delta^0|^2 = 2\sqrt{(\lambda_2 + \lambda_3)/\lambda}$, then the necessary and sufficient conditions for the BFB of the potential in *this* direction are

$$\lambda > 0,$$
$$\lambda_2 + \lambda_3 > 0, \qquad (4.5)$$
$$\lambda_1 + \lambda_4 + \sqrt{\lambda(\lambda_2 + \lambda_3)} > 0.$$

As it will become clear later on in this section, the conditions in case 1 are sufficient but not necessary, even for this special case. Furthermore, while the conditions in case 2 are necessary and sufficient for the corresponding direction, they obviously remain necessary for the general potential, but it is *a priori* not clear whether they can be sufficient. By looking at other special cases in two-field and three-field directions, we will show that they are generally not sufficient. Before doing so, let us first point out a more convenient method to obtain positivity constraints like Eq. (4.5) directly from Eq. (4.3) rather than writing it first in the form of Eq. (4.4). The potential Eq. (4.3) can be cast in the form

$$V(\chi) = a + b\chi^2 + c\chi^4 \qquad (4.6)$$

by the change of variable $\chi = |\phi^0|/|\delta^0|$. Since χ is, by definition, real valued and the moduli $|\phi^0|$ and $|\delta^0|$ can have any value, then the problem of finding the necessary and sufficient BFB conditions for Eq. (4.3) is equivalent to finding the conditions on a, b, c such that $V(\chi) > 0$ for any $\chi \in [0, \infty[$. Since $V(\chi)$ has no linear or cubic terms in χ, it is easy to find these conditions by studying $V(\chi)$ as a biquadratic function:

$$a > 0,$$
$$c > 0, \qquad (4.7)$$
$$b + 2\sqrt{ac} > 0.$$

Applied to Eq. (4.3) these conditions reproduce immediately Eq. (4.5). We can now easily study other field directions. For instance, the direction where only δ^{++} and ϕ^0 are nonvanishing yields

$$V = (\lambda_2 + \lambda_3)|\delta^{++}|^4 + \lambda_1|\delta^{++}|^2|\phi^0|^2 + \frac{\lambda}{4}|\phi^0|^4 \quad (4.8)$$

for which the BFB constraints are readily obtained from Eq. (4.7) as

$$\lambda > 0 \quad \& \quad \lambda_2 + \lambda_3 > 0 \quad \& \quad \lambda_1 + \sqrt{\lambda(\lambda_2 + \lambda_3)} > 0. \qquad (4.9)$$

Similarly, if we consider the field direction with nonvanishing δ^+ and ϕ^+, then

$$V = \left(\lambda_2 + \frac{\lambda_3}{2}\right)|\delta^+|^4 + \left(\lambda_1 + \frac{\lambda_4}{2}\right)|\delta^+|^2|\phi^+|^2 + \frac{\lambda}{4}|\phi^+|^4 \qquad (4.10)$$

and the corresponding BFB conditions read

$$\lambda > 0 \quad \& \quad \lambda_2 + \frac{\lambda_3}{2} > 0 \quad \& \quad \lambda_1 + \frac{\lambda_4}{2} + \sqrt{\lambda\left(\lambda_2 + \frac{\lambda_3}{2}\right)} > 0. \qquad (4.11)$$

It is then obvious that these two sets of conditions are neither equivalent nor contained in the conditions of Eq. (4.5). This shows that the BFB conditions derived only from the neutral direction Eq. (4.3) are neither necessary nor sufficient to ensure boundedness from below of the full potential Eq. (2.4). In Appendix B we have listed the potentials for all the field directions with only two nonvanishing fields, together with the corresponding BFB conditions. Adding these conditions, we come closer to the real sufficient and necessary conditions. But one can get more conditions by going now to field directions where three fields are nonvanishing. We give the exhaustive list of all these three-field direction potentials in Appendix B. In these more complicated configurations, an iteration of the method described above allowed us to treat all of them, although the results become somewhat complicated and not so telling. For instance, the three-field direction with nonvanishing ϕ^0, ϕ^+, δ^+ [see Eq. (B24)] yields some of the simplest BFB conditions,

$$\lambda > 0 \wedge 2\lambda_2 + \lambda_3 > 0 \wedge \sqrt{\lambda(4\lambda_2 + 2\lambda_3)} + 2\lambda_1 + \lambda_4$$
$$> 0 \wedge (2\lambda(2\lambda_2 + \lambda_3) > (2\lambda_1 + \lambda_4)^2 \vee 2\lambda_1 + \lambda_4 > 0),$$

$$(4.12)$$

where $\wedge$, $\vee$ stand, respectively, for the logical AND, OR. These conditions are obtained by first defining the reduced variables $\chi_1 = |\phi^+|/|\phi^0|$, $\chi_2 = |\delta^+|/|\phi^0|$, and then using iteratively the constraints Eqs. (4.7). By the same method we could obtain even more complicated BFB conditions as given in Eqs. (B26)–(B35). Analyzing them numerically we confirm that Eqs. (4.5) are far from being the full story. However, and despite their apparently complicated structure, the intersection of the regions they delineate in the space of the λ's has a form similar to Eqs. (4.5) and (B14). Moreover, the true BFB conditions will be obtained only if all field directions are taken into account, up to some arbitrary $SU(2) \times U(1)$ gauge transformations, but in this case the method used so far is not tractable anymore.

To proceed to the most general case, we adopt a different parametrization of the fields that will turn out to be particularly convenient to entirely solve the problem. Without loss of generality we can define

$$r \equiv \sqrt{H^\dagger H + \mathrm{Tr}\Delta^\dagger\Delta}, \tag{4.13}$$

$$H^\dagger H \equiv r^2 \cos^2\gamma, \tag{4.14}$$

$$\mathrm{Tr}(\Delta^\dagger\Delta) \equiv r^2 \sin^2\gamma, \tag{4.15}$$

$$\mathrm{Tr}(\Delta^\dagger\Delta)^2/(\mathrm{Tr}\Delta^\dagger\Delta)^2 \equiv \zeta, \tag{4.16}$$

$$(H^\dagger\Delta\Delta^\dagger H)/(H^\dagger H \,\mathrm{Tr}\Delta^\dagger\Delta) \equiv \xi \tag{4.17}$$

(where we adopted here a parametrization similar to the one used in [27] to study two-Higgs-doublet models, although for the latter models the problem is not fully solved by such a parametrization). Obviously, when H and Δ scan all the field space, the radius r scans the domain $[0, \infty[$ and the angle $\gamma \in [0, \frac{\pi}{2}]$. Moreover, one can show that

$$0 \le \xi \le 1 \quad \text{and} \quad \tfrac{1}{2} \le \zeta \le 1. \tag{4.18}$$

With this parametrization it is straightforward to cast $V^{(4)}(H, \Delta)$ in the following simple form,

$$V^{(4)}(r, \tan\gamma, \xi, \zeta) = \frac{r^4}{4(1 + \tan^2\gamma)^2}(\lambda + 4(\lambda_1 + \xi\lambda_4)\tan^2\gamma + 4(\lambda_2 + \zeta\lambda_3)\tan^4\gamma).$$

$$(4.19)$$

Because of the bi-quadratic dependence in $\tan\gamma$, one can indeed consider only the range $0 \le \tan\gamma < +\infty$ in accordance with the above-stated range for γ. We have thus

written $V^{(4)}$ in the form of Eq. (4.6). Boundedness from below is then equivalent to requiring $V^{(4)} > 0$ *for all* $\tan\gamma \in [0, \infty[$ and *all* ξ, ζ satisfying Eq. (4.18). Now applying directly the conditions Eqs. (4.7), one obtains

$$\lambda > 0 \ \& \ \lambda_2 + \zeta\lambda_3 > 0 \ \&$$
$$\lambda_1 + \xi\lambda_4 + \sqrt{\lambda(\lambda_2 + \zeta\lambda_3)} > 0 \ \ \forall\zeta \in [\tfrac{1}{2}, 1], \ \ \forall \xi[0, 1].$$

$$(4.20)$$

Because of the monotonic dependence in ζ and ξ, it is easy to show that these conditions can be rewritten as

$$\lambda > 0 \ \& \ \lambda_2 + \lambda_3 > 0 \ \& \ \lambda_2 + \frac{\lambda_3}{2} > 0 \tag{4.21}$$

$$\& \ \lambda_1 + \sqrt{\lambda(\lambda_2 + \lambda_3)} > 0 \ \& \ \lambda_1 + \sqrt{\lambda\left(\lambda_2 + \frac{\lambda_3}{2}\right)} > 0$$

$$(4.22)$$

$$\& \ \lambda_1 + \lambda_4 + \sqrt{\lambda(\lambda_2 + \lambda_3)} > 0 \ \&$$
$$\lambda_1 + \lambda_4 + \sqrt{\lambda\left(\lambda_2 + \frac{\lambda_3}{2}\right)} > 0.$$

$$(4.23)$$

We stress here that the above conditions ensure BFB for all possible directions in field space and thus provide the most general "all directions necessary and sufficient BFB conditions" that solve completely the issue at the tree level. Note that all the two-field direction conditions given in Eqs. (B11)–(B15) are special cases of the above conditions. We also checked numerically that this is the case for all ten three-field direction conditions, Eqs. (B26)–(B35).

V. UNITARITY CONSTRAINTS

Constraints on the scalar potential parameters can be obtained by demanding that tree-level unitarity be preserved in a variety of scattering processes: scalar-scalar scattering, gauge-boson–gauge-boson scattering, and scalar–gauge-boson scattering, as was initially done for the SM [28–30]. The generalizations of such constraints to various extended Higgs sector scenarios have been studied in the literature; see, for instance, [31–34]. Here we treat such constraints in the DTHM at the tree level, limiting ourselves to two-body scalar scattering processes dominated by quartic interactions. This is justified by the fact that we are interested in the leading unitarity constraints, that is, in the limit where $\sqrt{s}$ is much larger than any other mass scale involved. In particular, this means that we disregard here unitarity constraints that would involve the μ parameter when the latter is very large. Indeed, this parameter contributes to the scalar scattering processes through the cubic interactions entering the Feynman diagrams with scalar exchange in the s, t, and u channels.

Furthermore, the ratio μ/v_t controls the size of the exchanged scalar masses so that some of the aforementioned diagrams can be important in the vicinity of the resonance pole in the limit of large $\sqrt{s} \sim \mu v_d/v_t$.

In order to derive the unitarity constraints on the scalar masses, we adopt the basis of unrotated states, corresponding to the fields before electroweak symmetry breaking. The quartic scalar vertices have, in this case, a much simpler form than the complicated functions of λ_i, α, and β obtained in the physical basis ($H^{\pm\pm}$, $H^\pm$, $G^\pm$, h^0, H^0, A^0, and G^0) of mass eigenstate fields. The S matrix for the physical fields is related, by a unitary transformation, to the S matrix for the unrotated fields. Close inspection shows that the full set of two-body scalar scattering processes leads to a 35×35 S matrix which can be decomposed into seven block submatrices corresponding to mutually unmixed sets of channels with definite charge and CP states. One has the following submatrix dimensions, structured in terms of net electric charge in the initial/final states: $S^{(1)}(6 \times 6)$, $S^{(2)}(7 \times 7)$, and $S^{(3)}(2 \times 2)$ corresponding to zero-charge channels, $S^{(4)}(10 \times 10)$ corresponding to the one-charge channels, $S^{(5)}(7 \times 7)$ corresponding to the two-charge channels, $S^{(6)}(2 \times 2)$ corresponding to the three-charge channels, and $S^{(7)}(1 \times 1)$ corresponding to the unique four-charge channel. The corresponding T-matrix submatrices $T^{(1)}, \ldots, T^{(7)}$—with a momentum conservation factor $(2\pi)^4 \delta^4(\sum \text{momenta})$ properly factored out– are then easily extracted using the pure scalar quartic interactions expressed in terms of the nonphysical fields $\phi^\pm$, $\delta^\pm$, $\delta^{\pm\pm}$, h, ξ^0, and $Z_i (i = 1, 2)$, as listed in Appendix C.

One can then, in principle, extract the unitarity constraints on each component of the T matrix through the unitarity equation, which we write here in a shorthand form as

$$-i(T - T^\dagger) \sim \int ``TT^\dagger"$$
(5.1)

where $\int$ denotes, symbolically, the phase space integral over each intermediate state channel (see, for instance, [35]). However, it proves more efficient to define a modified matrix in such a way that its diagonalized form still satisfies Eq. (5.1). The usual unitarity bound on partial-wave amplitudes that is valid for *elastic* scattering would then apply readily to all the eigenvalues, thus encoding indirectly the bounds on all the components of the T matrix.[7] The proper redefinition is a $\tilde{T}$ matrix having the same entries as T but

---

[7] This, however, cannot be achieved, in general, by simply diagonalizing T, since on the right-hand side of Eq. (5.1) the phase space factor is not the same for all the two-particle channels, even in the high energy massless limit we are considering. It picks up a factor $1/2$ only for internal states with identical particles so as to avoid double counting. The right-hand side of Eq. (5.1) is thus not a proper matrix multiplication of T by $T^\dagger$, a fact emphasized by the quotation marks in the equation.

with an extra $1/\sqrt{2}$ factor for each initial or final state channel having two identical particles. $\tilde{T}$ now satisfies Eq. (5.1) with the same phase space for *all* channels and a true matrix multiplication of $\tilde{T}$ by $\tilde{T}^\dagger$. Its diagonalized form will thus satisfy the same equation. Defining $\mathcal{M}_n \equiv i\tilde{T}^{(n)}$, with $n = 1, \ldots, 7$, we give hereafter the resulting submatrices whose entries correspond to the quartic couplings that mediate the $2 \to 2$ scalar processes. These submatrices are Hermitian; thus the sought for eigenvalues will all be real valued.

The first submatrix $\mathcal{M}_1$ corresponds to the scattering whose initial and final states are one of the following: $(\phi^+ \delta^-, \delta^+ \phi^-, hZ_2, \xi^0 Z_1, Z_1 Z_2, h\xi^0)$. With the help of Appendix C one finds

$$\mathcal{M}_1 = \begin{pmatrix} \lambda_1 + \frac{\lambda_4}{2} & 0 & -\frac{i\lambda_4}{2\sqrt{2}} & \frac{i\lambda_4}{2\sqrt{2}} & \frac{\lambda_4}{2\sqrt{2}} & \frac{\lambda_4}{2\sqrt{2}} \\ 0 & \lambda_1 + \frac{\lambda_4}{2} & \frac{i\lambda_4}{2\sqrt{2}} & -\frac{i\lambda_4}{2\sqrt{2}} & \frac{\lambda_4}{2\sqrt{2}} & \frac{\lambda_4}{2\sqrt{2}} \\ \frac{i\lambda_4}{2\sqrt{2}} & -\frac{i\lambda_4}{2\sqrt{2}} & \lambda_{14}^+ & 0 & 0 & 0 \\ -\frac{i\lambda_4}{2\sqrt{2}} & \frac{i\lambda_4}{2\sqrt{2}} & 0 & \lambda_{14}^+ & 0 & 0 \\ \frac{\lambda_4}{2\sqrt{2}} & \frac{\lambda_4}{2\sqrt{2}} & 0 & 0 & \lambda_{14}^+ & 0 \\ \frac{\lambda_4}{2\sqrt{2}} & \frac{\lambda_4}{2\sqrt{2}} & 0 & 0 & 0 & \lambda_{14}^+ \end{pmatrix},$$
(5.2)

where $\lambda_{ij}^\pm = \lambda_i \pm \lambda_j$. We find that $\mathcal{M}_1$ has the following three double eigenvalues:

$$e_1 = \lambda_1 + \lambda_4,$$
(5.3)

$$e_2 = \lambda_1,$$
(5.4)

$$e_3 = \tfrac{1}{2}(2\lambda_1 + 3\lambda_4).$$
(5.5)

The second submatrix $\mathcal{M}_2$ corresponds to the scattering with one of the following initial and final states: $(\phi^+ \phi^-, \delta^+ \delta^-, \delta^{++} \delta^{--}, \frac{Z_1 Z_1}{\sqrt{2}}, \frac{Z_2 Z_2}{\sqrt{2}}, \frac{hh}{\sqrt{2}}, \frac{\xi^0 \xi^0}{\sqrt{2}})$, where the $\sqrt{2}$ accounts for identical particle statistics. Again, with the help of Appendix C, one finds that $\mathcal{M}_2$ is given by

$$\mathcal{M}_2 = \begin{pmatrix} \lambda & \frac{\tilde{\lambda}_{14}}{2} & \lambda_{14}^+ & \frac{\lambda}{2\sqrt{2}} & \frac{\lambda_1}{\sqrt{2}} & \frac{\lambda}{2\sqrt{2}} & \frac{\lambda_1}{\sqrt{2}} \\ \frac{\tilde{\lambda}_{14}}{2} & 2\tilde{\lambda}_{23} & 2\lambda_{23}^+ & \frac{\tilde{\lambda}_{14}}{2\sqrt{2}} & \sqrt{2}\lambda_{23}^+ & \frac{\tilde{\lambda}_{14}}{2\sqrt{2}} & \sqrt{2}\lambda_{23}^+ \\ \lambda_{14}^+ & 2\lambda_{23}^+ & 4\lambda_{23}^+ & \frac{\lambda_1}{\sqrt{2}} & \sqrt{2}\lambda_2 & \frac{\lambda_1}{\sqrt{2}} & \sqrt{2}\lambda_2 \\ \frac{\lambda}{2\sqrt{2}} & \frac{\tilde{\lambda}_{14}}{2\sqrt{2}} & \frac{\lambda_1}{\sqrt{2}} & \frac{3}{4}\lambda & \frac{\lambda_{14}^+}{2} & \frac{\lambda}{4} & \frac{\lambda_{14}^+}{2} \\ \frac{\lambda_1}{\sqrt{2}} & \sqrt{2}\lambda_{23}^+ & \sqrt{2}\lambda_2 & \frac{\lambda_{14}^+}{2} & 3\lambda_{23}^+ & \frac{\lambda_{14}^+}{2} & \lambda_{23}^+ \\ \frac{\lambda}{2\sqrt{2}} & \frac{\tilde{\lambda}_{14}}{2\sqrt{2}} & \frac{\lambda_1}{\sqrt{2}} & \frac{\lambda}{4} & \frac{\lambda_{14}^+}{2} & \frac{3\lambda}{4} & \frac{\lambda_{14}^+}{2} \\ \frac{\lambda_1}{\sqrt{2}} & \sqrt{2}\lambda_{23}^+ & \sqrt{2}\lambda_2 & \frac{\lambda_{14}^+}{2} & \lambda_{23}^+ & \frac{\lambda_{14}^+}{2} & 3\lambda_{23}^+ \end{pmatrix},$$
(5.6)

where $\tilde{\lambda}_{14} = 2\lambda_1 + \lambda_4$ and $\tilde{\lambda}_{23} = 2\lambda_2 + \lambda_3$. Despite its apparently complicated structure, one can easily determine the seven eigenvalues of $\mathcal{M}_2$ as follows:

$$f_1 = \frac{\lambda}{2}, \qquad (5.7)$$

$$f_2 = 2\lambda_2, \qquad (5.8)$$

$$f_3 = 2(\lambda_2 + \lambda_3), \qquad (5.9)$$

$$a_\pm = \frac{1}{4}\left[\lambda + 4\lambda_2 + 8\lambda_3 \pm \sqrt{(\lambda - 4\lambda_2 - 8\lambda_3)^2 + 16\lambda_4^2}\right], \qquad (5.10)$$

$$b_\pm = \frac{1}{4}\left[3\lambda + 16\lambda_2 + 12\lambda_3 \right.$$
$$\left. \pm \sqrt{(3\lambda - 16\lambda_2 - 12\lambda_3)^2 + 24(2\lambda_1 + \lambda_4)^2}\right]. \qquad (5.11)$$

The third submatrix $\mathcal{M}_3$ corresponds to the basis $(hZ_1, \xi^0 Z_2)$ and is given by

$$\mathcal{M}_3 = \begin{pmatrix} \frac{\lambda}{2} & 0 \\ 0 & 2\lambda_{23}^+ \end{pmatrix} \qquad (5.12)$$

with eigenvalues $k_1 = f_1$ and $k_2 = f_3$.

The one-charge channels occur for two-by-two body scattering between the ten charged states ($h\phi^+$, $\xi^0\phi^+$, $Z_1\phi^+$, $Z_2\phi^+$, $h\delta^+$, $\xi^0\delta^+$, $Z_1\delta^+$, $Z_2\delta^+$, $\delta^{++}\delta^-$, $\delta^{++}\phi^-$). The 10×10 submatrix $\mathcal{M}_4$ obtained from the above scattering processes is given by

$$\mathcal{M}_4 = \begin{pmatrix} \frac{\lambda}{2} & 0 & 0 & 0 & 0 & \frac{\lambda_4}{2\sqrt{2}} & 0 & \frac{-i\lambda_4}{2\sqrt{2}} & \frac{-\lambda_4}{2} & 0 \\ 0 & \lambda_1 & 0 & 0 & \frac{\lambda_4}{2\sqrt{2}} & 0 & \frac{i\lambda_4}{2\sqrt{2}} & 0 & 0 & 0 \\ 0 & 0 & \frac{\lambda}{2} & 0 & 0 & \frac{i\lambda_4}{2\sqrt{2}} & 0 & \frac{\lambda_4}{2\sqrt{2}} & \frac{-i\lambda_4}{2} & 0 \\ 0 & 0 & 0 & \lambda_1 & \frac{-i\lambda_4}{2\sqrt{2}} & 0 & \frac{\lambda_4}{2\sqrt{2}} & 0 & 0 & 0 \\ 0 & \frac{\lambda_4}{2\sqrt{2}} & 0 & \frac{i\lambda_4}{2\sqrt{2}} & \frac{1}{2}\tilde{\lambda}_{14} & 0 & 0 & 0 & 0 & \frac{-\lambda_4}{2} \\ \frac{\lambda_4}{2\sqrt{2}} & 0 & \frac{-i\lambda_4}{2\sqrt{2}} & 0 & 0 & 2\lambda_{23}^+ & 0 & 0 & -\sqrt{2}\lambda_3 & 0 \\ 0 & \frac{-i\lambda_4}{2\sqrt{2}} & 0 & \frac{\lambda_4}{2\sqrt{2}} & 0 & 0 & \frac{1}{2}\tilde{\lambda}_{14} & 0 & 0 & \frac{-i\lambda_4}{2} \\ \frac{i\lambda_4}{2\sqrt{2}} & 0 & \frac{\lambda_4}{2\sqrt{2}} & 0 & 0 & 0 & 0 & 2\lambda_{23}^+ & -i\sqrt{2}\lambda_3 & 0 \\ \frac{-\lambda_4}{2} & 0 & \frac{i\lambda_4}{2} & 0 & 0 & -\sqrt{2}\lambda_3 & 0 & i\sqrt{2}\lambda_3 & 2\lambda_{23}^+ & 0 \\ 0 & 0 & 0 & 0 & \frac{-\lambda_4}{2} & 0 & \frac{i\lambda_4}{2} & 0 & 0 & \lambda_{14}^+ \end{pmatrix}. \qquad (5.13)$$

As one can see, this matrix contains many vanishing elements, and the ten eigenvalues are straightforward to obtain analytically. They read as follows:

$$d_1 = e_1, \qquad (5.14)$$

$$d_2 = e_2 \quad \text{(twice)}, \qquad (5.15)$$

$$d_3 = e_3, \qquad (5.16)$$

$$d_4 = f_1, \qquad (5.17)$$

$$d_5 = f_2, \qquad (5.18)$$

$$d_6 = f_3, \qquad (5.19)$$

$$d_7 = \lambda_1 - \frac{\lambda_4}{2}, \qquad (5.20)$$

$$d_\pm = a_\pm. \qquad (5.21)$$

The fifth submatrix $\mathcal{M}_5$ corresponds to the scattering with initial and final states being one of the following seven states: ($\frac{\phi^+\phi^+}{\sqrt{2}}, \frac{\delta^+\delta^+}{\sqrt{2}}, \delta^+\phi^+, \delta^{++}\xi^0, \delta^{++}Z_2, \delta^{++}Z_1, \delta^{++}h$). It reads

$$\mathcal{M}_5 = \begin{pmatrix} \frac{\lambda}{2} & 0 & 0 & 0 & 0 & 0 & 0 \\ 0 & \tilde{\lambda}_{23} & 0 & -\lambda_3 & -i\lambda_3 & 0 & 0 \\ 0 & 0 & \frac{\tilde{\lambda}_{14}}{2} & 0 & 0 & \frac{-i\lambda_4}{2} & \frac{-\lambda_4}{2} \\ 0 & -\lambda_3 & 0 & 2\lambda_2 & 0 & 0 & 0 \\ 0 & i\lambda_3 & 0 & 0 & 2\lambda_2 & 0 & 0 \\ 0 & 0 & \frac{i\lambda_4}{2} & 0 & 0 & \lambda_1 & 0 \\ 0 & 0 & \frac{-\lambda_4}{2} & 0 & 0 & 0 & \lambda_1 \end{pmatrix} \qquad (5.22)$$

and possesses the following seven distinct eigenvalues:

$$c_1 = e_1, \tag{5.23}$$

$$c_2 = e_2, \tag{5.24}$$

$$c_3 = f_1, \tag{5.25}$$

$$c_4 = f_2, \tag{5.26}$$

$$c_5 = f_3, \tag{5.27}$$

$$c_6 = d_7, \tag{5.28}$$

$$c_7 = 2\lambda_2 - \lambda_3. \tag{5.29}$$

There are also triply charged states. The submatrix $\mathcal{M}_6$ corresponding to this case generates the scattering with initial and final states being one of the following $(\delta^{++}\phi^+, \delta^{++}\delta^+)$, and is given by

$$\mathcal{M}_6 = \begin{pmatrix} \lambda_{14}^+ & 0 \\ 0 & 2\lambda_{23}^+ \end{pmatrix} \tag{5.30}$$

with eigenvalues $k_1 = e_1$ and $k_2 = f_3$. Finally, it is easy to check that there is just one quadruply charged state $\frac{1}{\sqrt{2}}\delta^{++}\delta^{++}$, leading to

$$\mathcal{M}_7 = f_3 \tag{5.31}$$

with f_3 an eigenvalue.

From the usual expansion in terms of partial-wave amplitudes a_J, we write, following our notations,

$$\mathcal{M}^{(kf)} = i\tilde{T}_{kf} = 16i\pi \sum_{J \geq 0} (2J + 1)a_J^{(kf)}(s)P_J(\cos\theta), \tag{5.32}$$

where $\mathcal{M}^{(kf)}$ denotes the entries of the $\mathcal{M}$ matrix, the subscripts k and f run over all possible initial and final states of the above 35-state basis, θ denotes the scattering angle of the corresponding processes, and the P_J's are the Legendre polynomials. Since we considered only the leading high energy (massless limit) contributions that are s and θ independent, all the partial waves with $J \neq 0$ vanish, and one is left with

$$a_0^{(kf)} = -\frac{i}{16\pi}\mathcal{M}^{(kf)} \tag{5.33}$$

for each channel. The S-matrix unitarity constraint for elastic scattering $|a_0^{(kk)}| \leq 1$ [or alternatively $|\mathrm{Re}(a_0^{(kk)})| \leq \frac{1}{2}$ [36,37]] applies to the diagonal entries of $\mathcal{M}$. It encodes as well the constraints for nonelastic scattering, provided that it is applied to the eigenchannels of the 35-state basis as noted previously. Thus, this constraint translates through Eq. (5.33) directly to all the eigenvalues we determined above. We defer to the next section, Eqs. (6.4), (6.5), (6.6),

(6.7), (6.8), (6.9), (6.10), (6.11), (6.12), and (6.13), the list of all the resulting constraints.

VI. COMBINED UNITARITY AND POTENTIAL STABILITY CONSTRAINTS

Let us first recall all the constraints obtained in Secs. IV and V.

BFB:

$$\lambda \geq 0 \quad \& \quad \lambda_2 + \lambda_3 \geq 0 \quad \& \quad \lambda_2 + \frac{\lambda_3}{2} \geq 0 \tag{6.1}$$

$$\& \quad \lambda_1 + \sqrt{\lambda(\lambda_2 + \lambda_3)} \geq 0 \quad \& \quad \lambda_1 + \sqrt{\lambda\left(\lambda_2 + \frac{\lambda_3}{2}\right)} \geq 0 \tag{6.2}$$

$$\& \quad \lambda_1 + \lambda_4 + \sqrt{\lambda(\lambda_2 + \lambda_3)} \geq 0 \quad \&$$

$$\lambda_1 + \lambda_4 + \sqrt{\lambda\left(\lambda_2 + \frac{\lambda_3}{2}\right)} \geq 0. \tag{6.3}$$

Unitarity:

$$|\lambda_1 + \lambda_4| \leq \kappa\pi, \tag{6.4}$$

$$|\lambda_1| \leq \kappa\pi, \tag{6.5}$$

$$|2\lambda_1 + 3\lambda_4| \leq 2\kappa\pi, \tag{6.6}$$

$$|\lambda| \leq 2\kappa\pi, \tag{6.7}$$

$$|\lambda_2| \leq \frac{\kappa}{2}\pi, \tag{6.8}$$

$$|\lambda_2 + \lambda_3| \leq \frac{\kappa}{2}\pi, \tag{6.9}$$

$$|\lambda + 4\lambda_2 + 8\lambda_3 \pm \sqrt{(\lambda - 4\lambda_2 - 8\lambda_3)^2 + 16\lambda_4^2}| \leq 4\kappa\pi, \tag{6.10}$$

$$|3\lambda + 16\lambda_2 + 12\lambda_3$$
$$\pm \sqrt{(3\lambda - 16\lambda_2 - 12\lambda_3)^2 + 24(2\lambda_1 + \lambda_4)^2}| \leq 4\kappa\pi, \tag{6.11}$$

$$|2\lambda_1 - \lambda_4| \leq 2\kappa\pi, \tag{6.12}$$

$$|2\lambda_2 - \lambda_3| \leq \kappa\pi, \tag{6.13}$$

where we introduced the parameter κ which takes the values $\kappa = 16$ or 8, depending on whether we choose $|a_0| \leq 1$ or $|\mathrm{Re}(a_0)| \leq \frac{1}{2}$, as pointed out at the end of Sec. V.

Working out analytically these two sets of BFB and unitarity constraints, one can reduce them to a more compact system where the allowed ranges for the λ's are easily identified. One can obtain a necessary domain for λ, λ_2, λ_3 that does not depend on λ_1 and λ_4, by considering simultaneously Eqs. (6.7), (6.8), (6.9), (6.10), (6.11), (6.12), and (6.13) together with Eq. (6.1). It then turns out that Eqs. (6.8) and (6.9) as well as the lower part of Eq. (6.13) are weaker than the actually allowed domains for λ_2, λ_3, and similarly, Eq. (6.7) is weaker than the constraint on λ coming from Eq. (6.11). We find

$$0 \leq \lambda \leq \frac{2}{3}\kappa\pi, \tag{6.14}$$

$$\lambda_2 + \lambda_3 \geq 0 \quad \& \quad \lambda_2 + \frac{\lambda_3}{2} \geq 0, \tag{6.15}$$

$$\lambda_2 + 2\lambda_3 \leq \frac{\kappa}{2}\pi, \tag{6.16}$$

$$4\lambda_2 + 3\lambda_3 \leq \frac{\kappa}{2}\pi, \tag{6.17}$$

$$2\lambda_2 - \lambda_3 \leq \kappa\pi. \tag{6.18}$$

We stress here that the above constraints define the largest possible domain for λ, λ_2, λ_3 for any set of allowed values of λ_1, λ_4, although Eqs. (6.10) and (6.11) have been used to determine this domain. It is noteworthy that the upper bound on λ, Eq. (6.14), is reduced by a factor 3 with respect to the naive expectation, Eq. (6.7). Studying further Eqs. (6.10) and (6.11), one can rewrite them in the following simple form where the dependence on λ_1, λ_4 has been explicitly separated from that on λ, λ_2, λ_3:

$$|\lambda_4| \leq \min\sqrt{\left(\lambda \pm 2\kappa\pi\right)\left(\lambda_2 + 2\lambda_3 \pm \frac{\kappa}{2}\pi\right)}, \tag{6.19}$$

$$|2\lambda_1 + \lambda_4| \leq \sqrt{2\left(\lambda - \frac{2}{3}\kappa\pi\right)\left(4\lambda_2 + 3\lambda_3 - \frac{\kappa}{2}\pi\right)}, \tag{6.20}$$

where Eqs. (6.14) and (6.18) have been used in deriving Eq. (6.20).[8] Various comments are in order here. First, to obtain the full domain for λ_1, λ_4, one has to add to the above two equations Eqs. (6.4), (6.5), (6.6), and (6.12) as

well as Eqs. (6.2) and (6.3). Thus for each set of values of λ, λ_2, λ_3, the allowed domain for λ_1, λ_4 is easily determined as the overlap of a set of linear bands, as illustrated in Fig. 1.

As stated earlier, Eqs. (6.15), (6.16), (6.17), and (6.18) define the largest possible domain for λ_2, λ_3 allowed by the combined unitarity and BFB constraints. The reason is seen from Eqs. (6.19) and (6.20) which are the only extra constraints on λ_2, λ_3 depending on the actual values of λ, λ_1, λ_4. As one can easily check, these constraints become trivially satisfied when $\lambda_1 = \lambda_4 = 0$ and thus correspond to the case of the largest λ_2, λ_3 domain. For each set of nonvanishing values for λ_1, λ_4, the domain of λ_2, λ_3 given by Eqs. (6.15), (6.16), (6.17), and (6.18) will be further reduced according to Eqs. (6.19) and (6.20). We illustrate the largest (λ_2, λ_3) domain in Fig. 2.

To summarize, the boundaries of the combined unitarity and general BFB domains for the five couplings are now given by the reduced set of Eqs. (6.2), (6.3), (6.4), (6.5), (6.6), (6.14), (6.15), (6.16), (6.17), (6.18), (6.19), and (6.20), which moreover have an analytically simpler form. In particular, one readily finds from Eq. (6.20) that saturating the unitarity bound on λ, i.e. $\lambda = \frac{2}{3}\kappa\pi$, reduces the two-dimensional (λ_1, λ_4) domain to the one-dimensional (straight line) $\lambda_4 = -2\lambda_1$. This, as well as other features, will be useful in determining lower and upper bounds on the Higgs masses in the next section.
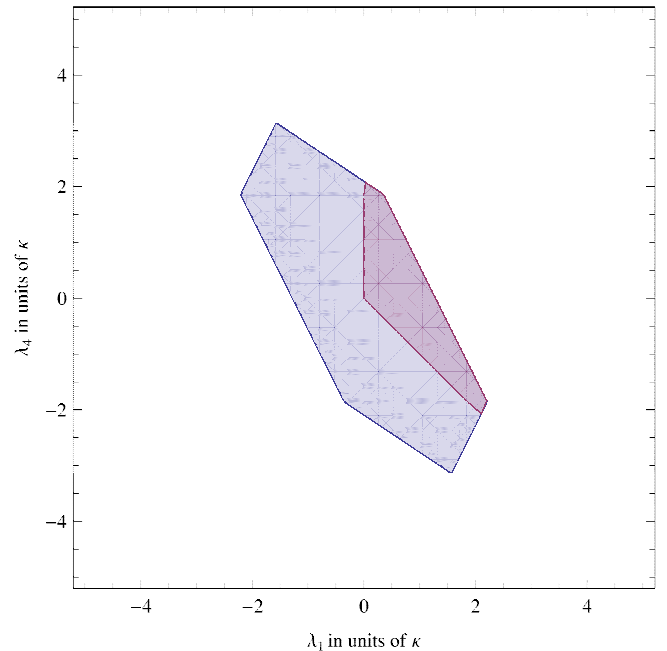
---

[8]In writing Eq. (6.20) we relied on the fact that the minimum of $\sqrt{2(\lambda \pm \frac{2}{3}\kappa\pi)(4\lambda_2 + 3\lambda_3 \pm \frac{\kappa}{2}\pi)}$ is given by $\sqrt{2(\lambda - \frac{2}{3}\kappa\pi)(4\lambda_2 + 3\lambda_3 - \frac{\kappa}{2}\pi)}$ in all the domain allowed by λ, λ_2, λ_3. In contrast, $\min\sqrt{(\lambda \pm 2\kappa\pi)(\lambda_2 + 2\lambda_3 \pm \frac{\kappa}{2}\pi)}$ appearing in Eq. (6.19) cannot be written in a closed form in this domain.

FIG. 1 (color online). An illustration of a section of the (λ_1, λ_4) domain (light gray) in units of κ as determined by Eqs. (6.4), (6.5), (6.6), (6.12), (6.19), and (6.20), where we fixed $\lambda = \lambda_2 = \lambda_3 = 0$. Adding the BFB constraints, Eqs. (6.2) and (6.3), one obtains the reduced domain shown (gray).
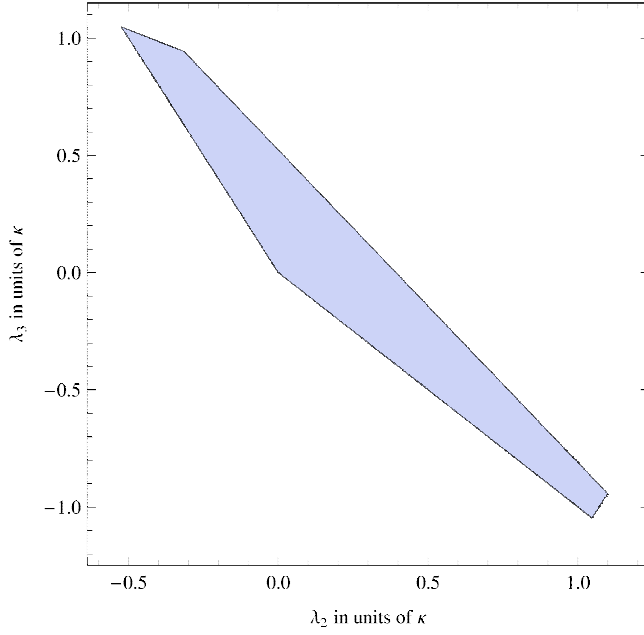
FIG. 2 (color online). We illustrate here the *largest* $\lambda_2 - \lambda_3$ domain allowed by the combined unitarity and BFB constraints in units of κ. This domain corresponds to Eqs. (6.15), (6.16), (6.17), and (6.18) and is attained for $\lambda_1 = \lambda_4 = 0$, in which case Eqs. (6.19) and (6.20) are trivially satisfied. As can be seen from Eqs. (6.19) and (6.20), a smaller domain is obtained as soon as λ_1 and/or λ_4 are nonzero, irrespective of the value of λ satisfying Eq. (6.14).

VII. HIGGS MASS THEORETICAL BOUNDS

In this section we rely on the results of the previous sections to study the theoretically allowed ranges of the Higgs masses when varying the $\lambda_i's$ and the μ parameter in their allowed domains. Rather than assuming that μ is very large, i.e. of the order of the GUT scale together with $\mu \simeq M_\Delta$, we will study all the phenomenologically allowed range. We stress here that even very small values of μ are consistent with a tiny value of v_t necessary for realistic neutrino masses [and $\mathcal{O}(1)$ Yukawa couplings], provided that we take into account consistently Eq. (2.8).

Let us first describe qualitatively the generic behavior of the masses when μ is varied. We will show that, as a function of μ, the h^0 mass features a *maximum* $m_{h^0}^{\max}$ for a specific value $\mu = \mu_c$. This maximum will translate into an upper bound on m_{h^0} when the unitarity bound on λ is saturated. Similarly, the H^0 mass reaches a *minimum* $m_{H^0}^{\min}$ at a nearby value which we momentarily also denote $\mu = \mu_c$ for the sake of the qualitative discussion. In the range $\mu < \mu_c$, H^0 is the heaviest among all the Higgses, decreasing very slowly with increasing μ towards its minimum value $m_{H^0}^{\min}$, while m_{h^0} increases very quickly with μ to $m_{h^0}^{\max}$. The other Higgs masses can have various hierarchies and, in particular, the unusual one where the $m_{H^{\pm\pm}}$ is the lightest state, $m_{H^{\pm\pm}} < m_{H^\pm} < m_A \simeq m_{h^0}$. In contrast, in

the range $\mu_c < \mu < \mu_{\max}$, m_{H^0} now increases quickly with μ while m_{h^0} decreases very slowly from its maximal value. This sharply different behavior of m_{h^0} and m_{H^0} below and above μ_c can be traced back to the smallness of v_t. We illustrate numerically such a behavior in Fig. 3, where the seemingly constant $m_{h^0}^2$ for $\mu > \mu_c$ and constant $m_{H^0}^2$ for $\mu < \mu_c$ are artifacts of the very small ratio v_t/v_d. In fact, $m_{h^0}^2$ is decreasing very slowly to the right of μ_c and reaches zero when $\mu = \mu_+$ (cf. Sec. III B and Appendix A), while $m_{H^0}^2$ starts off at $\mu = \mu_{\min}$ and decreases very slowly until its minimum value at $\mu = \mu_c$, then increases very slowly between μ_c and approximately $\mu = \bar{\mu} \simeq \lambda v_t/\sqrt{2}$, and increases very quickly afterwards.[9]

More quantitatively, we find that there are two different values of μ_c, which we dub $\mu_c^{(1)}$, $\mu_c^{(2)}$, that are uniquely determined in terms of v_d, v_t and the λ's. When one of these two critical values corresponds to $m_{h^0}^{\max}$, the other will correspond to $m_{H^0}^{\min}$, and vice versa, depending on the sign of the following quantity:

$$\mathcal{V}_\lambda \equiv (-\lambda + \lambda_1 + \lambda_4)v_d^2 + 4(\lambda_2 + \lambda_3)v_t^2. \qquad (7.1)$$

Moreover, it turns out that at these extrema one of the two h^0 or H^0 states will correspond to a purely SM-like Higgs state, and this too is controlled by the sign of $\mathcal{V}_\lambda$. One can summarize the behavior analytically as follows.

(i) $\mathcal{V}_\lambda > 0$:

In this case m_{h^0} reaches a maximum given by

$$m_{h^0\,(1)}^{2\,\max} = m_{(1)}^2 \equiv \frac{\lambda v_d^2}{2} \qquad (7.2)$$

when μ takes the value

$$\mu = \mu_c^{(1)} \equiv (\lambda_1 + \lambda_4)\frac{v_t}{\sqrt{2}}, \qquad (7.3)$$

and $m_{H^0}^2$ reaches a minimum given by

$$\begin{aligned} m_{H^0\,(1)}^{2\,\min} = m_{(2)}^2 &\equiv \frac{1}{2(v_d^2 + 16v_t^2)} \\ &\times (\lambda v_d^4 + 16v_t^2((\lambda_1 + \lambda_4)v_d^2 \\ &+ 4(\lambda_2 + \lambda_3)v_t^2)) \\ &= \frac{\lambda v_d^2}{2} + \mathcal{O}(v_t^2) \qquad (7.4) \end{aligned}$$

when μ takes the value

$$\begin{aligned} \mu = \mu_c^{(2)} &\equiv \frac{v_t}{\sqrt{2}(v_d^2 + 16v_t^2)}((2\lambda - \lambda_1 - \lambda_4)v_d^2 \\ &+ 8(2\lambda_1 + 2\lambda_4 - \lambda_2 - \lambda_3)v_t^2). \qquad (7.5) \end{aligned}$$

---

[9]The precise value is $\bar{\mu} = v_t(\lambda v_d^2 + 4(4\lambda_1 - \lambda_2 - \lambda_3 + 4\lambda_4)v_t^2)/\sqrt{2}(v_d^2 + 16v_t^2)$. In fact, $\bar{\mu}$ is the common value of μ at which the slopes of the variations of $m_{h^0}^2$ and $m_{H^0}^2$ as functions of μ experience a sudden change.
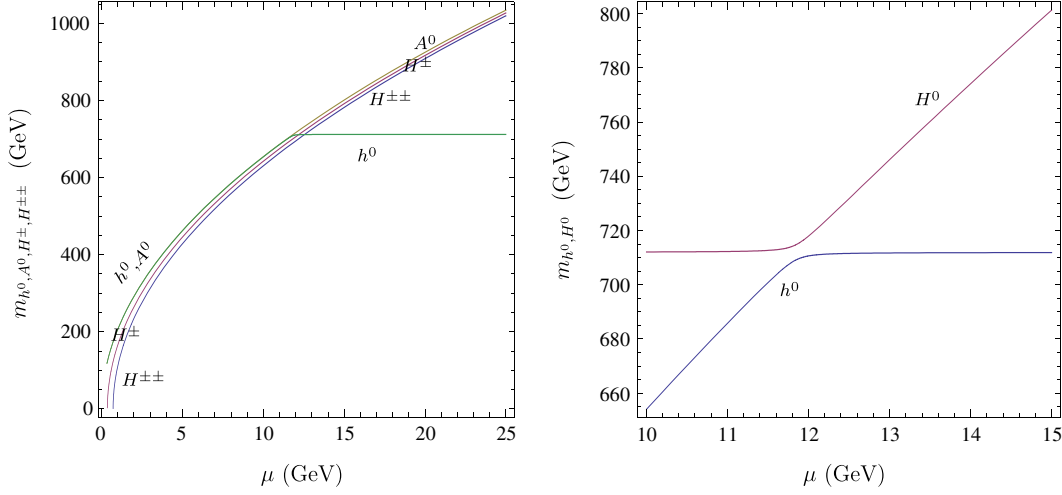
FIG. 3 (color online).   Illustration of the regime $\mathcal{V}_\lambda < 0$ with $\lambda = \frac{16\pi}{3}$, $\lambda_2 = 10^{-1}$, $\lambda_3 = 2 \times 10^{-1}$, $\lambda_1 = -\frac{1}{2}$, $\lambda_4 = 1$, $v_t = 1$ GeV, $v = 246$ GeV, $v_d = \sqrt{v^2 - 2v_t^2}$, $\kappa = 8$, leading to $\mu_c^{(2)} \simeq 23$ GeV. See Eq. (7.5).

Expanding the Higgs masses squared around $\mu_c^{(1)}$, one finds

$$m_{h^0}^2 = m_{h^0\,(1)}^{2\,\max} - \frac{4v_d^2}{\mathcal{V}_\lambda}\delta_{\mu 1}^2 + \mathcal{O}(\delta_{\mu 1}^3), \qquad (7.6)$$

$$\Delta_{H^0}^2 = (-\lambda + \lambda_1 + \lambda_4)\frac{v_d^2}{2} + 2(\lambda_2 + \lambda_3)v_t^2$$
$$+ \frac{v_d^2}{\sqrt{2}v_t}\delta_{\mu 1} + \mathcal{O}(\delta_{\mu 1}^2), \qquad (7.7)$$

$$\Delta_{A^0}^2 = (-\lambda + \lambda_1 + \lambda_4)\frac{v_d^2}{2} + 2(\lambda_1 + \lambda_4)v_t^2$$
$$+ \frac{(v_d^2 + 4v_t^2)}{\sqrt{2}v_t}\delta_{\mu 1} + \mathcal{O}(\delta_{\mu 1}^2), \qquad (7.8)$$

$$\Delta_{H^\pm}^2 = \left(-\lambda + \lambda_1 + \frac{\lambda_4}{2}\right)\frac{v_d^2}{2} + (2\lambda_1 + \lambda_4)\frac{v_t^2}{2}$$
$$+ \frac{(v_d^2 + 2v_t^2)}{\sqrt{2}v_t}\delta_{\mu 1} + \mathcal{O}(\delta_{\mu 1}^2), \qquad (7.9)$$

$$\Delta_{H^{\pm\pm}}^2 = (-\lambda + \lambda_1)\frac{v_d^2}{2} - \lambda_3 v_t^2 + \frac{v_d^2}{\sqrt{2}v_t}\delta_{\mu 1} + \mathcal{O}(\delta_{\mu 1}^2), \qquad (7.10)$$

where $\Delta_X^2 \equiv m_X^2 - m_{h^0}^{2\,\max}$ denotes the various squared mass splittings from $m_{h^0}^{2\,\max}$ and $\delta_{\mu 1} \equiv \mu - \mu_c^{(1)}$.

(ii) $\mathcal{V}_\lambda < 0$:
   In this case the reversed configuration occurs. m_{h^0} reaches a maximum given by

$$m_{h^0\,(2)}^{2\,\max} = m_{(2)}^2 \qquad (7.11)$$

at $\mu = \mu_c^{(2)}$, while m_{H^0} reaches a minimum given by

$$m_{H^0\,(2)}^{2\,\min} = m_{(1)}^2 \qquad (7.12)$$

at $\mu = \mu_c^{(1)}$, where $m_{(1)}^2$, $m_{(2)}^2$, $\mu_c^{(1)}$, $\mu_c^{(2)}$ are as defined in Eqs. (7.2), (7.3), (7.4), and (7.5). Again, expanding around $\mu_c^{(2)}$ we find

$$m_{h^0}^2 = m_{h^0\,(2)}^{2\,\max} + \frac{4v_d^2}{\mathcal{V}_\lambda}\delta_{\mu 2}^2 + \mathcal{O}(\delta_{\mu 2}^3) \qquad (7.13)$$

and the squared mass splittings

$$\Delta_{H^0}^2 = (\lambda - \lambda_1 - \lambda_4)\frac{v_d^2}{2} - 2(\lambda_2 + \lambda_3)v_t^2 + \frac{v_d^2}{\sqrt{2}v_t}\delta_{\mu 2} + \mathcal{O}(\delta_{\mu 2}^2), \qquad (7.14)$$

$$\Delta_{A^0}^2 = \frac{v_d^2}{(v_d^2 + 16v_t^2)}\left((\lambda - \lambda_1 - \lambda_4)\frac{v_d^2}{2} + 2(2(\lambda - \lambda_2 - \lambda_3) - \lambda_1 - \lambda_4)v_t^2\right) + \frac{(v_d^2 + 4v_t^2)}{\sqrt{2}v_t}\delta_{\mu 2} + \mathcal{O}(\delta_{\mu 2}^2, v_t^4/v_d^2), \qquad (7.15)$$

$$\Delta^2_{H^\pm} = \frac{v_d^2}{(v_d^2 + 16v_t^2)}\left(\left(\lambda - \lambda_1 - \frac{3}{2}\lambda_4\right)\frac{v_d^2}{2} + \left(2\lambda - \lambda_1 - 4\lambda_2 - 4\lambda_3 - \frac{11}{2}\lambda_4\right)v_t^2\right) + \frac{(v_d^2 + 2v_t^2)}{\sqrt{2}v_t}\delta_{\mu2} + \mathcal{O}(\delta^2_{\mu2}, v_t^4/v_d^2),$$

$$(7.16)$$

$$\Delta^2_{H^{\pm\pm}} = \frac{v_d^2}{(v_d^2 + 16v_t^2)}\left(\left(\lambda - \lambda_1 - 2\lambda_4\right)\frac{v_d^2}{2} - (4\lambda_2 + 5\lambda_3 + 8\lambda_4)v_t^2\right) + \frac{v_d^2}{\sqrt{2}v_t}\delta_{\mu2} + \mathcal{O}(\delta^2_{\mu2}, v_t^4/v_d^2), \qquad (7.17)$$

where $\delta_{\mu2} \equiv \mu - \mu_c^{(2)}$.

Noting that $\mu_c^{(1)} - \mu_c^{(2)}$, $m^2_{(2)} - m^2_{(1)}$, and $\mathcal{V}_\lambda$ have the same sign, and defining

$$\mu_c^{\min} \equiv \min\{\mu_c^{(1)}, \mu_c^{(2)}\}, \qquad (7.18)$$

$$\mu_c^{\max} \equiv \max\{\mu_c^{(1)}, \mu_c^{(2)}\}, \qquad (7.19)$$

one can recast the results of Eqs. (7.2), (7.4), (7.11), and (7.12) in a more compact form as

$$m^{2\,\max}_{h^0} = m^2_{h^0}(\mu = \mu_c^{\max}) = \min\{m^2_{(1)}, m^2_{(2)}\}, \qquad (7.20)$$

$$m^{2\,\min}_{H^0} = m^2_{H^0}(\mu = \mu_c^{\min}) = \max\{m^2_{(1)}, m^2_{(2)}\}, \qquad (7.21)$$

with an implicit reference to the two regimes (i) and (ii) if one keeps in mind that $m^2_{(i)}$ is reached for $\mu = \mu_c^{(i)}$. A numerical illustration of the above features is given in Figs. 3 and 4.

The mixing pattern.—For $\mu = \mu_c^{(1)}$, h^0 and H^0 become pure doublet or triplet states, since in this case $B = 0$, as can be seen from Eq. (2.22). However, a close inspection of Eq. (2.40) shows that in regime (i) [respectively, (ii)] one has $s_\alpha = 0$ (respectively, $s_\alpha = 1$) for this value of μ. Thus, at $\mu = \mu_c^{(1)}$, h^0 becomes a pure SM-like Higgs in regime (i), but it is H^0 that becomes a pure SM-like Higgs in regime (ii). The fact that the SM-like state is not always associated with the lightest $\mathcal{CP}_{\rm even}$ state is important when discussing the Higgs phenomenology and the interpretation of the experimental limits and is consistent with the fact that $m^2_{(1)}$ is indeed the SM-Higgs squared mass,

Eq. (7.2). In fact, due to the smallness of v_t/v_d, the behavior of the mixing angle α over the full range of the μ parameter follows closely the generic pattern discussed above: In both regimes (i) and (ii) one has essentially $s_\alpha \simeq \pm 1$ or $s_\alpha \simeq 0$ over most of the μ range, except for a very narrow region in the vicinity of $\bar{\mu}$ defined in footnote 9 and satisfying

$$\bar{\mu} = \tfrac{1}{2}(\mu_c^{(1)} + \mu_c^{(2)}), \qquad (7.22)$$

where $|s_\alpha|$ changes quickly from $\simeq 0$ to $\simeq 1$. The generic dominance of no-mixing regimes can be understood from the asymptotic behavior at small and large μ values, i.e. $|\sin\alpha|_{\mu\to 0}| = 1 - 2\frac{(\lambda_1+\lambda_4)^2}{\lambda^2}(v_t^2/v_d^2) + \mathcal{O}(v_t^3)$ and $\sin\alpha|_{\mu\to\mu_+} = 2(v_t/v_d) + \mathcal{O}(v_t^2)$, together with the fact that $ds_\alpha/d\mu = \mathcal{O}(v_t^3)$. We illustrated this behavior in Fig. 5, adopting the sign convention $\epsilon_\alpha = +1$. As seen in Fig. 5(b), s_α remains positive in all the μ range since $B < 0$ [cf. Eqs. (2.22) and (2.40)]. And in accordance with the asymptotic behavior, s_α tends to $\mathcal{O}(10^{-2})$ at large $\mu(>\bar{\mu})$, where h^0 is nearly SM-like, and to $\mathcal{O}(1)$ at small $\mu(<\bar{\mu})$, where H^0 is nearly SM-like. (Note that in this numerical example $\mu_c^{(1)}$ becomes negative and is never reached.) In contrast, for the regime illustrated in Fig. 5(a), s_α remains negative for $\mu < \mu_c^{(1)}$, crosses zero at $\mu_c^{(1)}$, and again tends to a positive value $\mathcal{O}(10^{-2})$ for $\mu \gg \mu_c^{(1)}$.

The exact magnitude of $|s_\alpha|$ at the three critical values of μ can be summarized as follows:

$$
\begin{array}{rcll}
 & & \mathcal{V}_\lambda > 0: & \mathcal{V}_\lambda < 0: \\
|s_\alpha(\mu = \mu_c^{(1)})| & = & 0, & 1 \\
|s_\alpha(\mu = \bar{\mu})| & = & \left(\frac{1}{2} - \frac{2v_t}{\sqrt{v_d^2+16v_t^2}}\right)^{1/2}, & \left(\frac{1}{2} + \frac{2v_t}{\sqrt{v_d^2+16v_t^2}}\right)^{1/2} \\
 & = & \frac{1}{\sqrt{2}} - \sqrt{2}\frac{v_t}{v_d} + \mathcal{O}\left(\frac{v_t^2}{v_d^2}\right), & \frac{1}{\sqrt{2}} + \sqrt{2}\frac{v_t}{v_d} + \mathcal{O}\left(\frac{v_t^2}{v_d^2}\right) \\
|s_\alpha(\mu = \mu_c^{(2)})| & = & \frac{v_d}{\sqrt{v_d^2+16v_t^2}}, & \frac{4v_t}{\sqrt{v_d^2+16v_t^2}} \\
 & = & 1 - 8\frac{v_t^2}{v_d^2} + \mathcal{O}\left(\frac{v_t^3}{v_d^3}\right), & 4\frac{v_t}{v_d} + \mathcal{O}\left(\frac{v_t^3}{v_d^3}\right)
\end{array}
$$

$$(7.23)$$

Large mixing scenarios have been discussed previously in [18,38], while here we quantify more precisely the regions where such a large mixing takes place. For later analyses it is useful to characterize the μ range in the large $|s_\alpha|$

regime. One sees from the above equations that the size of this range is $\mathcal{O}(v_t)$. As a first approximation one can characterize it by the interval $0 < \mu < \mu_c^{\min}$, with $\mu_c^{\min}$ given by Eq. (7.18). However, depending on the values

of λ and $\lambda_1 + \lambda_4$, $|s_\alpha|$ can still be very close to 1 in the range $\mu_c^{\min} < \mu < \bar\mu$, especially when $\mu_c^{\min}$ is not positive definite [it becomes negative when $\lambda_1 + \lambda_4 < 0$ or $2\lambda - (\lambda_1 + \lambda_4) < 0$]. It is more sensible to base this characterization on the amount of deviation from the value $|s_\alpha| = 1$. Defining $\hat\mu$ in the vicinity of $\bar\mu$ in the form $\hat\mu \equiv \bar\mu - \delta \times v_t$, with δ strictly >0, one finds $|s_\alpha(\hat\mu)| = 1 - k(\delta)\frac{v_t^2}{v_d^2} + \mathcal{O}(\frac{v_t^3}{v_d^3})$. For each given *positive* value of k, there corresponds a value of $\hat\mu$ given by

$$\hat\mu_{(\pm)} = \left(\frac{\lambda}{\sqrt2} - \frac{\lambda - \lambda_1 - \lambda_4}{\sqrt2 \pm \sqrt k}\right)v_t + \mathcal{O}\left(\frac{v_t^3}{v_d^2}\right). \quad (7.24)$$

The twofold ambiguity in this expression is resolved as follows: Requiring consistently $\mu_c^{\min} \le \hat\mu < \bar\mu$ to hold, one should take for $\mathcal{V}_\lambda > 0$, $\hat\mu = \hat\mu_{(-)}$ with $k \ge 8$, and for $\mathcal{V}_\lambda < 0$, $\hat\mu = \hat\mu_{(+)}$ for any $k \ge 0$.[10] In particular, $\hat\mu$ reproduces, respectively, $\mu_c^{(1)}$ and $\mu_c^{(2)}$ for the special values $k = 0$ and $k = 8$ as expected, while $\bar\mu$ cannot be reached for any finite value of k [consistently with the fact that $|s_\alpha(\hat\mu)| \simeq 1$ and $|s_\alpha(\hat\mu)| \simeq 1/\sqrt2$ are not perturbatively close to each other in terms of powers of v_t/v_d].

With the above prescription one can characterize the μ range in the large $|s_\alpha|$ regime by $0 < \mu < \hat\mu(k)$, where k can now be interpreted as triggering the experimental sensitivity to the deviation of $|s_\alpha|$ from its maximal value $|s_\alpha| = 1$. Equation (7.24) shows that the lower the sensitivity to large $|s_\alpha|$ (i.e. the larger k), the lower the sensitivity of the size of the μ domain to $\lambda_1 + \lambda_4$. We will come back to the above issues in the phenomenological discussion of Sec. VIII.

Unitarity bounds.—Relying on the above properties we can now easily derive the theoretical upper bounds on the various Higgs masses. From Eq. (7.2), and using the maximal value allowed by the tree-level unitarity constraint for λ, Eq. (6.14), and $v_d \simeq 246$ GeV, we determine an upper bound on m_{h^0},

$$m_{h^0} \lesssim 712 \text{ GeV} \quad (\text{for } \kappa = 8), \quad (7.25)$$

$$\lesssim 1 \text{ TeV} \quad (\text{for } \kappa = 16). \quad (7.26)$$

If Eq. (7.11) is used instead, then the saturation of unitarity and BFB bounds on $\lambda_1 + \lambda_4$ should also be considered. However, due to the smallness of v_t/v_d, this would lead to only a few GeV change in the above upper bounds. As far as m_{H^0} is concerned, the above bounds are essentially the minimally allowed values, as is obvious from Eqs. (7.20)

and (7.21), in the unitarity saturation limit. To obtain its theoretical upper bound as well as those of the other Higgs masses, one should rather take μ at its maximally allowed value, $\mu_{\max} \simeq \mu_+ \simeq \frac{\lambda}{4\sqrt2}\frac{v_d^2}{v_t}$, since all these masses increase monotonically with μ. For instance, with the set of parameters chosen in Figs. 3 and 4 and $v_t = 1$ GeV, one finds the upper bounds

$$m_{H^{\pm\pm}} \simeq m_{H^\pm} \simeq m_A \simeq m_{H^0} \simeq 88 \text{ TeV} \quad (\text{for } \kappa = 8), \quad (7.27)$$

$$\simeq 124 \text{ TeV} \quad (\text{for } \kappa = 16), \quad (7.28)$$

which are not phenomenologically compelling. Actually, somewhat lower bounds are obtained when taking into account the experimental exclusion limits on a light Higgs m_{h^0} but remain too high to be useful. In contrast, phenomenologically interesting scenarios with light charged, doubly charged, $\mathcal{CP}_{\text{odd}}$ and $\mathcal{CP}_{\text{even}}$ Higgses are possible for small values of μ. For instance, as illustrated in Figs. 3 and 4, such a light spectrum occurs when $\mu \ll \mu_c^{(2)} \simeq 23$ GeV. More generally, the analytical expressions given above for the mass splittings show that in the vicinity of μ_c and, in particular, for $\mu < \mu_c$, the neutral $\mathcal{CP}_{\text{even}}$ h^0 is not necessarily the lightest Higgs.[11] The detailed patterns will depend on the actual values of the λ's and will be studied more thoroughly in the next section, but one can already see some generic features in regimes (i) and (ii) at $\mu \simeq \mu_c$. In regime (i), where $-\lambda + \lambda_1 + \lambda_4 > 0$, one expects $H^{\pm\pm}$ to become the lightest Higgs if $-\lambda + \lambda_1 < 0$, that is, when $\lambda_1 < \lambda < \lambda_1 + \lambda_4$. Similarly, in regime (ii), where typically $\lambda - \lambda_1 - \lambda_4 > 0$, one again expects $H^{\pm\pm}$ to be the lightest Higgs when $\lambda_1 + \lambda_4 < \lambda < \lambda_1 + 2\lambda_4$. More generally, a close inspection of Eqs. (2.11) and (2.27) shows that $m_{H^{\pm\pm}} < m_{h^0}$ when $\mu < \mu^\star = (\lambda + \lambda_4)v_t/\sqrt2 + \mathcal{O}(v_t^3/v_d^2)$, and only if $\lambda_4 > 0$.[12] Furthermore, it immediately follows from Eqs. (2.13) and (2.31) that $m_{H^{\pm\pm}} < m_{H^\pm} < m_A$ when $\lambda_4 > 0$ so that the necessary and sufficient condition for $H^{\pm\pm}$ to be the lightest Higgs is

$$\mu < \mu^\star \quad \text{with} \quad \lambda_4 > 0. \quad (7.29)$$

Phenomenological bounds.—In order to prepare for a phenomenological study, we discussed in Sec. III B the modification on the tachyonic bounds of μ when experimental exclusion limits are available for m_{A^0}, $m_{H^\pm}$, and $m_{H^{\pm\pm}}$, cf. Eqs. (3.13) and (3.14). Here we address the same question concerning m_{h^0} and m_{H^0}. For each given experimental bound $(m_{h^0})_{\exp}$ [respectively, $(m_{H^0})_{\exp}$] there correspond two values $\mu_\pm^{h^0}$ [respectively, $\mu_\pm^{H^0}$], namely,

---

[10]Strictly speaking, in the case $\mathcal{V}_\lambda > 0$ one can still choose k in the interval $2 < k < 8$ if $\mathcal{V}_\lambda$ is sufficiently close to zero to ensure that $\mu_c^{\min} \le \hat\mu$. In practice, these details will not be important, since one does not expect an experimental sensitivity to the deviation from $|s_\alpha| = 1$ to be better than a few percent. A deviation of 1%, with $v_t = 1$ GeV, puts the value of k already around 600.

[11]We have kept in these expressions subleading terms of $\mathcal{O}(v_t^2)$ in order to handle as well the small parts of the λ_i's parameter space where the leading $\mathcal{O}(v_d^2)$ are suppressed.

[12]Although this expression of $\mu^\star$ is well defined for $\lambda_4 < 0$, one finds that the splitting $m_{H^{\pm\pm}}^2 - m_{h^0}^2$ is negative only in the domain defined by $\mu < (\lambda + 2\lambda_4)v_t/\sqrt2 + \mathcal{O}(v_t^3/v_d^2)$ and $-\lambda_4 v_d^2/(4\sqrt2 v_t) + \mathcal{O}(v_t) < \mu < (\lambda + \lambda_4)v_t/\sqrt2 + \mathcal{O}(v_t^3/v_d^2)$, which is clearly nonempty only for $\lambda_4 > 0$.
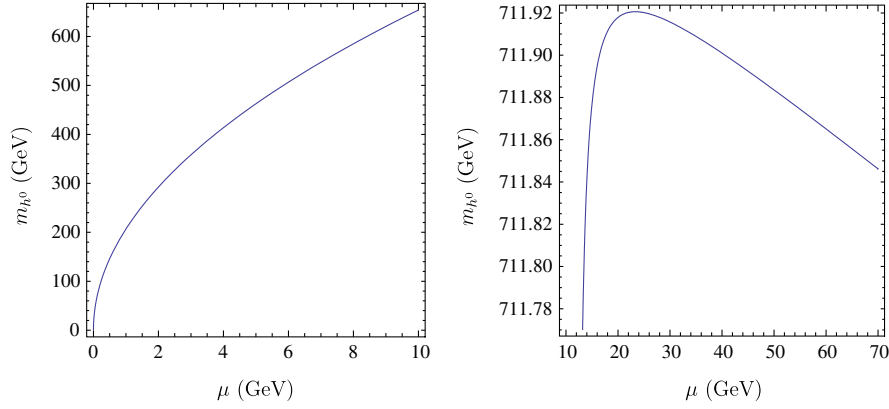
FIG. 4 (color online). Zoom on the variation of m_{h^0} with μ in the vicinity of $\mu_c^{(2)}$; $\lambda = \frac{16\pi}{3}$, $\lambda_2 = 10^{-1}$, $\lambda_3 = 2 \times 10^{-1}$, $\lambda_1 = -\frac{1}{2}$, $\lambda_4 = 1$, $v_t = 1$ GeV, $v = 246$ GeV, $v_d = \sqrt{v^2 - 2v_t^2}$, $\kappa = 8$, leading to $\mu_c^{(2)} \simeq 23$ GeV. See Eq. (7.5).

$$\mu_{\pm}^{h^0} = \frac{1}{8\sqrt{2}v_t}\left(\lambda v_d^2 + 8(\lambda_1 + \lambda_4)v_t^2 - 2(m_{h^0}^2)_{\text{exp}}\right.$$
$$\pm 2[(m_{(1)}^2 - (m_{h^0}^2)_{\text{exp}})(m_{(2)}^2 - (m_{h^0}^2)_{\text{exp}})]^{1/2}$$
$$\left.\times \left(1 + 16\frac{v_t^2}{v_d^2}\right)^{1/2}\right) \tag{7.30}$$

[and similarly for $\mu_{\pm}^{H^0}$ with $(m_{h^0})_{\text{exp}}$ replaced by $(m_{H^0})_{\text{exp}}$], for which m_{h^0} reaches $(m_{h^0})_{\text{exp}}$ [respectively, m_{H^0} reaches $(m_{H^0})_{\text{exp}}$]. Note that in the limit of no experimental bounds, i.e. $(m_{h^0,H^0}^2)_{\text{exp}} \to 0$, Eq. (7.30) gives back Eq. (A1). Furthermore, relying on the fact that m_{h^0} has a maximum and m_{H^0} has a minimum as functions of μ, cf. Eqs. (7.20) and (7.21), the phenomenological bounds read

$$\mu_{-}^{h^0} \leq \mu \leq \mu_{+}^{h^0} \text{ assuming } (m_{h^0})_{\text{exp}} \leq m_{h^0}^{\text{max}} \quad \text{and}$$
$$\mu \leq \mu_{-}^{H^0} \quad \text{or} \quad \mu_{+}^{H^0} \leq \mu \text{ assuming } (m_{H^0})_{\text{exp}} \geq m_{H^0}^{\text{min}}.$$
$$\tag{7.31}$$

Obviously $(m_{h^0})_{\text{exp}} > m_{h^0}^{\text{max}}$ would be an inconsistent assumption, while $(m_{H^0})_{\text{exp}} < m_{H^0}^{\text{min}}$ would be an empty assumption not leading to any constraint as far as μ is concerned.

In summary, the experimental lower bounds on the various Higgs masses will typically constrain the μ parameter to lie in a finite domain defined by the combination of Eqs. (3.14) and (7.31).

VIII. HIGGS PHENOMENOLOGY

Although previous studies in the literature typically assumed the triplet mass M_Δ and the mass parameter μ to be much larger than the electroweak scale, $M_\Delta \gg v_d$, more recently the possibility of having M_Δ, $\mu \lesssim 1$ TeV, where the Higgses of the DTHM might be accessible at the Tevatron and the LHC [17,39–46], has received more

attention. In this spirit, the results obtained in the previous sections help define educated strategies to extract constraints on the physical Higgs masses and model parameters from experimental data, rather than performing merely blind (and CPU time-consuming) scans on these parameters. The existing experimental exclusion limits on the SM-Higgs particle are readily translated into constraints on the DTHM in the parameter space region where h^0 becomes SM-like, i.e. when the mixing between the doublet and the triplet is very small. However, even when far from this region, existing exclusion limits for an extended Higgs sector (such as in two-Higgs-doublet models or in the minimal supersymmetric extension of the SM) can also be partially adapted to h^0, H^0, A^0, and $H^\pm$, while of course $H^{\pm\pm}$ has a distinctive experimental search.

In this section we give a quick overview of the Higgs sector phenomenology and experimental searches (for an extended overview on the phenomenology of triplet models, see Ref. [47]), followed by a preliminary analysis using our results. A detailed study taking into account all present-day experimental limits lies out of the scope of this paper and will be presented elsewhere.

A. Doubly charged Higgs

Observation of the doubly charged Higgs $H^{\pm\pm}$ would unambiguously signal physics beyond Higgs doublets, let alone physics beyond the SM-Higgs sector. Owing to charge conservation, it is obvious that $H^{\pm\pm}$ cannot couple to a pair of quarks; therefore, its possible decay modes are as follows:

(i) same sign charged lepton pair $H^{\pm\pm} \to l^\pm l^\pm$ that proceeds via lepton number violating coupling,

(ii) a pair of $W^\pm$ gauge bosons $H^{\pm\pm} \to W^\pm W^\pm$,

(iii) $H^{\pm\pm} \to W^\pm H^\pm$,

(iv) a pair of charged Higgs bosons $H^{\pm\pm} \to H^\pm H^\pm$.

We emphasize also that the doubly charged Higgs couples to the photon and to the Z boson through gauge couplings, Eqs. (C17) and (C18), while its coupling to a pair of $W^\pm$ is

proportional to the triplet VEV v_t; see Eqs. (C15). Therefore, the decay channel (ii) will be suppressed for $v_t \ll v_d$. The decay channel (iv) will also be suppressed for small v_t, as can be seen from the form of the coupling of $H^{\pm\pm}$ to a pair of charged Higgses $H^\pm$, Eq. (C16). Indeed, one has $\cos\beta' \simeq 1$ and $\sin\beta' \sim v_t/v_d$ from Eq. (2.19), and furthermore, the $\mu\sin^2\beta'$ is also of order v_t due to the μ upper bound $\mu_+ \sim v_d^2/v_t$, viz. Eq. (A1). In contrast, the coupling $H^{\pm\pm}W^\pm H^\pm$ is proportional to the gauge coupling and has no suppression factors. The decay channel (ii) will thus contribute substantially if kinematically open. Depending on the size of the Yukawa couplings of the leptons, the doubly charged Higgs can decay dominantly either to a pair of leptons or to $W^\pm$ and $H^\pm$, and subdominantly to a pair of $W^\pm$ and/or a pair of $H^\pm$ if kinematically allowed.

In e^+e^- collisions, the doubly charged Higgs can be pair produced through the γ and Z s channel,[13] $e^+e^- \rightarrow \gamma^*$, $Z^* \rightarrow H^{\pm\pm}H^{\mp\mp}$ [48–51]. One can also have access to the associate production of $H^\pm$ with $W^\mp$ through s-channel Z exchange [52–54]. If the e^-e^- option is available at the International Linear Collider, then the doubly charged Higgs can be produced in $W^\pm W^\pm$ fusion through $e^-e^- \rightarrow W^{-*}W^{-*} \rightarrow e^-e^-H^{++}$. Even if $H^{\pm\pm}W^\mp W^\mp$ has a v_t suppression, the rate for $W^\pm W^\pm$ fusion could be substantial, especially at higher energy options for e^-e^- [49].

At the Tevatron or the LHC, the two production mechanisms with potentially large cross sections are $p\bar{p}/pp \rightarrow \gamma^*, Z^* \rightarrow H^{\pm\pm}H^{\mp\mp}X$ or a single production through WW fusion, $p\bar{p}/pp \rightarrow W^{\pm*}W^{\pm*} \rightarrow H^{\pm\pm}X$ [55,56]. The latter process as well as the s channel $p\bar{p}/pp \rightarrow W^{\pm*} \rightarrow W^\mp H^{\pm\pm}$ depend on the coupling $H^{\pm\pm}W^\mp W^\mp$ which is proportional to the triplet VEV. However, the suppression due to the small value of v_t is somewhat compensated by the fact that $W^\pm W^\pm$ fusion could be substantial at high energies. Those processes have to be supplemented by the associated production of singly and doubly charged Higgs bosons $p\bar{p}/pp \rightarrow H^{\pm\pm}H^\mp X$ which could have a cross section comparable to $p\bar{p}/pp \rightarrow H^{\pm\pm}H^{\mp\mp}X$ [57,58].

Such doubly charged Higgses have been subject to many experimental searches. At LEP-II, the experiments L3, OPAL, and Delphi [59–61] performed a search for doubly charged Higgs bosons assuming that $H^{\pm\pm}$ decay dominantly to a pair of leptons, $H^{\pm\pm} \rightarrow l^\pm l^\pm$. Four lepton final states have been analyzed at L3, OPAL, and Delphi. L3 performed a search for the six possibilities: ee, $\mu\mu$, μe, $\mu\tau$, $e\tau$, and $\tau\tau$. No excess has been found, and lower limits in the range 95–100 GeV at the 95% confidence level on the doubly charged Higgs boson mass are derived. Those lower limits depend on the doubly charged Higgs decay modes. For example, if $H^{\pm\pm} \rightarrow e^\pm e^\pm$ is the dominant

decay, then the lower limit is 100 GeV, while if $H^{\pm\pm} \rightarrow \mu^\pm \tau^\pm$ is the dominant decay, then the lower limit is about 95 GeV.

At the Tevatron, D0 [62,63] and CDF [64,65] have searched for $p\bar{p} \rightarrow \gamma^*, Z^* \rightarrow H^{\pm\pm}H^{\mp\mp}X$ with $H^{\pm\pm} \rightarrow l^\pm l^\pm$. The D0 measurement [62] represents the first doubly charged Higgs search with the decay $H^{\pm\pm} \rightarrow \mu^\pm \mu^\pm$. Note that the D0 search was limited to $H^{\pm\pm} \rightarrow \mu^\pm \mu^\pm$ which is an almost background-free signal, while CDF explored the three final states $e^\pm e^\pm$, $\mu^\pm \mu^\pm$, and $e^\pm \mu^\pm$. Both D0 and CDF excluded a doubly charged Higgs with a mass in the range 100–150 GeV. We stress that all those bounds assume a 100% branching ratio for $H^{\pm\pm} \rightarrow l^\pm l^\pm$ decay, while in realistic cases one can easily find scenarios where $H^{\pm\pm} \rightarrow l^\pm l^\pm$ is suppressed while $H^{\pm\pm} \rightarrow W^{\pm*}W^{\pm*}$ is substantial [17,39,66,67], which could partially invalidate the CDF and D0 limits. However, the LHC has the capability to extend the above limits up to a mass of about 1 TeV for the high luminosity option [17,40,56,68]. Very recently CMS released the search results for doubly charged Higgs bosons using an integrated luminosity of 0.98 fb[1][69]. A lower limit of 313 GeV has been set on $H^{\pm\pm}$ which decays with a 100% branching ratio to $l^\pm l'^\pm$, l, $l' = \mu, e$. This limit is weakened to 266 GeV (respectively, 254 GeV) in the case of the $\mu^\pm \tau^\pm$ (respectively, $e^\pm \tau^\pm$) final state.

Note that the observation of doubly charged Higgs bosons at the LHC and measurement of its leptonic branching ratios will also shed some light on the neutrino mass pattern [17,39,44,51,58,66,67,70,71].

Finally, indirect limits on the mass and the bileptonic couplings of the doubly charged Higgs boson can be extracted from low energy lepton flavor violating processes, such as $\mu \rightarrow e\gamma$, $\mu \rightarrow 3e$, $\tau \rightarrow 3l, \ldots$ (see, for instance, [41,45]).

B. Singly charged Higgs

Let us now discuss briefly the couplings of the singly charged Higgs and its decay modes. The charged Higgs coupling to a lepton and a neutrino is proportional to $\approx m_\nu/v_t \approx Y_\nu$ [17], which could be of the order $\mathcal{O}(1)$ if v_t is very small. Similarly, the charged Higgs coupling to a pair of quarks, u and d, is proportional to $\tan\beta'$, which is suppressed by v_t/v_d [17]. In the case of $H^-\bar{t}b$, this coupling could enjoy some enhancement from the Yukawa coupling of the top quark. The suppression of the coupling $H^-\bar{t}b$ has three consequences:

(i) Given the suppression factor of the order v_t/v_d for $H^-\bar{t}b$, the charged Higgs mass cannot be subject to the $b \rightarrow s\gamma$ constraint, similarly to the type I two-Higgs-doublet model where the coupling is suppressed by $1/\tan\beta$.

(ii) Some of the conventional mechanisms for charged Higgs production at hadron colliders such as $bg \rightarrow tH^+$ and $gg \rightarrow tbH^+$ will be suppressed.

---

[13]The t channel mediated by a lepton is, in general, suppressed by the small Yukawa coupling.

(iii) Since the charged Higgs search at the Tevatron is based on the top decay $t \to H^+ b$, given the suppression of the $H^+ t\bar{b}$ coupling, the branching ratio of $t \to bH^+$ would also be suppressed. One concludes then that the CDF, CMS, and ATLAS [72–75] limits do not apply in this case.

Besides those processes which are suppressed, one can still produce charged Higgses through the associated production of singly and doubly charged Higgs $pp/p\bar{p} \to W^* \to H^{\pm\pm}H^{\mp}$ [57,58] with a spectacular signature from $H^{\pm\pm} \to l^{\pm}l^{\pm}$. Other mechanisms are as follows: the Drell-Yan process $(pp/p\bar{p} \to \gamma^*, \ Z^* \to H^+H^{\mp})$, the associated production of the charged Higgs and neutral Higgs $(pp/p\bar{p} \to W^* \to H^{\pm}h^0, \ pp/p\bar{p} \to W^* \to H^{\pm}H^0, \ pp/p\bar{p} \to W^* \to H^{\pm}A^0)$, and the associated production of the charged Higgs with a W gauge boson $(pp/p\bar{p} \to Z^* \to W^{\pm}H^{\mp})$. Note that among the latter processes, the ones with $W^{\pm}H^{\mp}$ or $H^{\mp}h^0$ final states are suppressed by a v_t/v_d factor as compared to the Drell-Yan process and the two other associated production processes that are controlled by gauge couplings, cf. Eqs. (C10)–(C13).

If the charged Higgs decays dominantly to leptons (for small v_t) we can apply the LEP mass lower bounds that are of the order of 80 GeV [76,77]. For large v_t, i.e. much larger than the neutrino masses but still well below the electroweak scale, the dominant decay is either $H^+ \to t\bar{b}$ or one of the bosonic decays $H^+ \to W^+Z$, $H^+ \to W^+h^0/W^+A^0$. For the first two decay modes there has been no explicit search at the LEP or at the Tevatron, while for the $H^+ \to W^+A^0$ decay (and possibly for $H^+ \to W^+h^0$ if h^0 decays similarly to A^0), one can use the LEP-II search performed in the framework of two-Higgs-doublet models. In this case the charged Higgs mass limit is again of the order of 80 GeV [77].

C. Neutral Higgses

The lighter $\mathcal{CP}_{\text{even}}$ Higgs boson h^0 is fully dominated by the doublet component (i.e. the mixing $|s_{\alpha}| \ll 1$) when $\mu > \bar{\mu}$, as discussed in Sec. VII and illustrated in Fig. 5. In this case the coupling of h^0 to a pair of neutrinos is suppressed, being proportional to s_{α}. Such a Higgs will completely mimic the SM-Higgs boson, and then the LEP and the recent Tevatron, CMS, and ATLAS limits would apply. In this scenario of very small mixing, the other neutral Higgses H^0 and A^0 would be fermiophobic to all charged leptons and quarks, but their coupling to a pair of neutrinos that is proportional to $\cos\alpha Y_{\nu} \approx Y_{\nu} = m_{\nu}/v_t$ could be enhanced for small v_t. Then the dominant decay mode for H^0 and A^0, for small v_t, would be a pair of neutrinos [17].

Note that A^0, being $\mathcal{CP}_{\text{odd}}$, does not couple to a pair of gauge bosons, while the couplings H^0ZZ and H^0WW in the small mixing case are suppressed by v_t/v_d, Eqs. (C4) and (C6). Thus the W and Z Higgsstrahlung productions of H^0 and A^0 are expected to be small. Furthermore, while the H^0A^0Z vertex is controlled by the gauge coupling, Eq. (C8), h^0A^0Z has an extra v_t/v_d suppression, Eq. (C7). This implies that in the small mixing case, one can still produce A^0 and H^0 through the Drell-Yan process $e^+e^-/pp/p\bar{p} \to Z^* \to H^0A^0$. For very small v_t, A and H^0 would decay essentially into a pair of neutrinos. At the LEP, the signal would then be a photon (from initial state radiation) and missing energy in the final state. A lower bound on m_H and m_A of the order of 55 GeV can be extracted in this case from LEP-II data, assuming mass degeneracy between A^0 and H^0 [78]. (In the nondegenerate case the lower bound translates into $m_H + m_A \gtrsim 110$ GeV.) Increasing v_t well above the neutrino masses significantly decreases $H^0/A^0 \to \nu\nu$, and the decay channels $H^0 \to b\bar{b}$, $A^0 \to b\bar{b}$, as well as $H^0 \to ZZ$, $A^0 \to Zh^0$
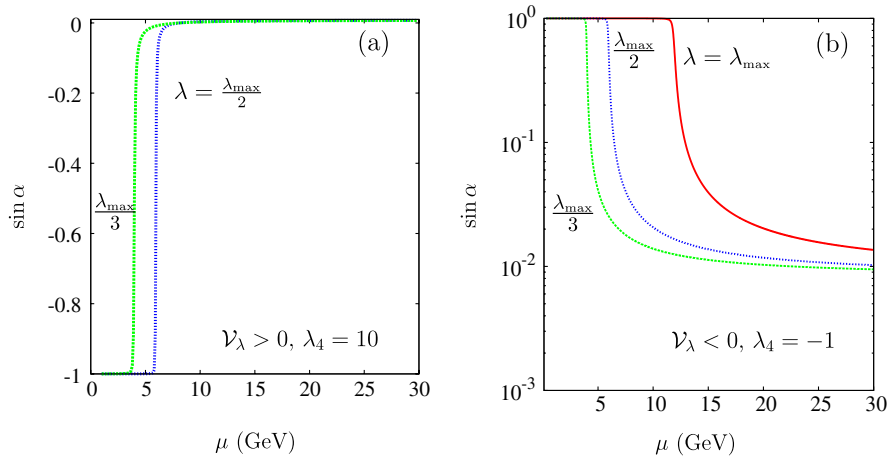

FIG. 5 (color online). The mixing angle as a function of μ, in the regimes $\mathcal{V}_{\lambda} > 0$ (a) and $\mathcal{V}_{\lambda} < 0$ (b); the other parameters are given by $v_t = 1$ GeV, $\lambda_{\text{max}} = 16\pi/3$, $\lambda_2 = \lambda_3 = 0.1$, $\lambda_1 = 0.5$, and $\epsilon_{\alpha} = +$. The log scale in (b) shows the asymptotic values at large μ. The same asymptotic values apply in (a). See text for further discussion.

if open [see Eqs. (C4) and (C7)], can become dominant. If $H^0 \to b\bar{b}$, $A^0 \to b\bar{b}$ dominate, the LEP-II Higgs search through $e^+e^- \to H^0 A^0$ in the two-Higgs-doublet model can apply to the DTHM in this case, and the limit is roughly $m_H + m_A \gtrsim 185$ GeV [79]. There is, however, a distinctive feature in the DTHM related to the $H^0 h^0 h^0$ coupling, Eq. (C9), the latter becoming substantial for increasing μ and thus for heavier H^0. The $H^0 \to h^0 h^0$ decay mode would then be important in both the large and small (with respect to the neutrino masses) v_t regimes.

In the case of maximal mixing $|s_\alpha| \approx 1$ which occurs for $\mu < \bar{\mu}$ (see Fig. 5), the roles of h^0 and H^0 are interchanged. H^0 is fully doublet and h^0 is fully triplet. Taking into account this interchange, the previous discussion applies here to H^0. However, since h^0 remains the lighter Higgs, which can now be far from SM-like, one expects weaker experimental constraints on its mass than the ones quoted above.

D. Top decay into a charged Higgs

A light charged Higgs of the order 100–200 GeV is still allowed by theoretical constraints, as well as by an experimental search. If the charged Higgs satisfies $m_{H^\pm} \lesssim m_t - m_b$, one could ask whether the decay $t \to bH^+$ can have a significant branching ratio to be observed at the LHC. As mentioned before, the coupling $H^+ tb$ has a v_t/v_d suppression, and the branching ratio for $t \to bH^+$ is expected to be small. We perform a systematic scan over the DTHM parameter space looking for charged Higgs masses that allow the $t \to bH^+$ decay to be open. In Fig. 6 we show the branching ratio for $t \to bH^+$, where we included $t \to bW^+$ and $t \to sW^+$ decay channels and the QCD corrections. It is obvious that a large effect on $t \to bH^+$ would appear for the largest possible values of v_t that are
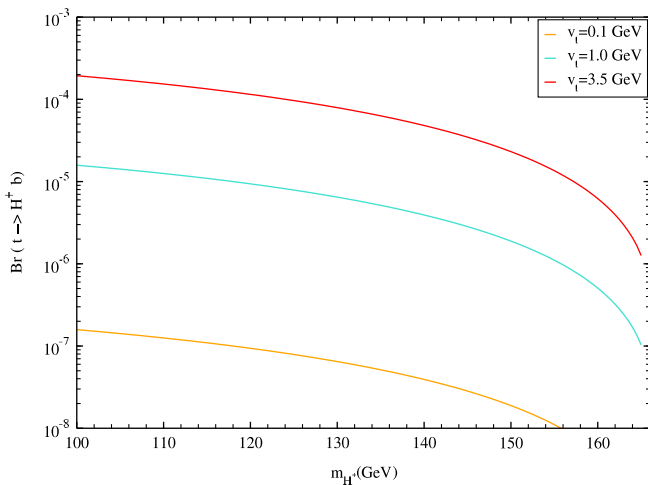

FIG. 6 (color online).   Branching ratio for $t \to bH^+$ as a function of the charged Higgs mass for three values of the triplet VEV v_t. The branching ratios increase with increasing values of v_t.

allowed by electroweak precision constraints and the theoretical constraints. Indeed, for a triplet VEV v_t in the range $0.1 \to 3.5$ GeV and a charged Higgs mass less than 165 GeV, one finds $\mathrm{Br}(t \to bH^+)$ in the range 10^{-5}–10^{-4}.

However, it is well known that the LHC will act as a top factory. With low luminosity 10 fb^{-1}, 8×10^6 $t\bar{t}$ pairs per experiment per year will be produced. This number will increase by 1 order of magnitude with the high luminosity option. Therefore, the properties of top quarks can be examined with significant precision at the LHC. For instance, it has been shown that for top decays through flavor changing neutral processes, it is possible to reach $\mathrm{Br}(t \to cH^0) \lesssim 4.5 \times 10^{-5}$ at the LHC [80]. For $t \to bH^+$, no such studies are available. But it is clear that if we let one top decay to bW and the other one decay to bH with a branching ratio in the range 10^{-5}–10^{-4}, this would lead to 800–8000 raw $bW^+\bar{b}H^-$ (or $\bar{b}W^-bH^+$) events in the case of the high luminosity option, which may be enough to extract a charged Higgs and measure its coupling to the top. Note also that high sensitivity to the charged or neutral Higgses of top decays through loop induced flavor changing neutral currents can also be attained at the International Linear Collider [81–83].

E. DTHM spectrum and theoretical constraints

We illustrate, in Figs. 7(a) and 8(a), the correlations among μ, $\sin\alpha$, and v_t for fixed values of the λ_i's and λ, and in Figs. 7(b), 8(b), and 8(c), the correlations among μ, $\sin\alpha$, and the $\mathcal{CP}_{\text{even}}$ Higgs masses (or equivalently λ), for fixed values of the λ_i's and v_t, where we take into account the boundedness from below and unitarity constraints discussed in the previous sections. Note that the chosen numbers in the figures are such that $\mathcal{V}_\lambda < 0$ in Fig. 7 and $\mathcal{V}_\lambda > 0$ in Fig. 8(a), while Figs. 8(b) and 8(c) interpolate between these two regimes; see Eq. (7.1). For fixed μ, increasing the magnitude of v_t decreases m_{h^0} and increases the mixing parameter $|s_\alpha|$, as can be seen from Figs. 7(a) and 8(a). The upper-left white areas in these plots correspond to $m_{h^0} \lesssim 115$ GeV, where we took the latter value as a fiducial lower bound for a SM-like Higgs. Such a bound corresponds to $\lambda^{\text{SM}} \simeq 0.44$, for $v_t < 1$ GeV, while the upper bound for m_{h^0} is around 120 GeV, corresponding to the value $\lambda = 0.48$ chosen in the figures, cf. Eqs. (7.2) and (7.4). It thus follows that the colored areas in the plots, indicating mainly very small s_α values, i.e. h^0 behaving like a SM Higgs, correspond to the small Higgs mass range $115 \text{ GeV} \lesssim m_{h^0} \lesssim 120$ GeV. Increasing the value of λ, keeping λ^{SM} fixed, would result in an increase of the Higgs mass range as well as of the regions with larger $|s_\alpha|$ (the dark gray areas on the plots). In fact, there are two regions corresponding to $m_{h^0} \lesssim 115$ GeV—the white area in the upper-left corner corresponding to small values of μ delimited by the thin dark gray area, and another region at very large values of μ [$\gtrsim \mathcal{O}(1)$–$\mathcal{O}(10^3)$ TeV]—which are out of the scope of the μ range shown on the plots,

delimited by the light gray to black areas. One should note that, in the former region, $|s_\alpha|$ reaches 1 quickly, so that h^0 carries essentially a triplet component and is thus not excluded by a fiducial SM-like Higgs mass lower bound, even if it is lighter than this bound. In contrast, in the latter region where $|s_\alpha|$ remains very small, a SM-Higgs mass lower bound applies to h^0. It follows that such a bound does not put lower bounds on μ, while it leads typically to very large upper bounds on μ as a function of v_t. In the small μ region, H^0 carries mainly the SM-like component and should respect a SM-Higgs mass lower bound. However, due to the very low sensitivity to μ in this regime (see Fig. 3), such a bound will translate merely into a lower bound on λ. Therefore, exclusion of very small values of μ can only originate from exclusion limits on the lightest non-SM-like $\mathcal{CP}_{\mathrm{even}}$ or $\mathcal{CP}_{\mathrm{odd}}$ Higgses, which could be extracted, for instance, from existing limits for the minimal supersymmetric extension of the SM in the nondecoupling regime [84].

Complementary features, now with a fixed v_t and varying λ, are illustrated in Figs. 7(b), 8(b), and 8(c). The gross features of Figs. 7(b) and 8(b) are in agreement with the previous discussion on the phenomenological bounds, related to Eqs. (7.30) and (7.31). They illustrate how information on m_{h^0} constrains the allowed range for μ without any prior knowledge on λ. For a given m_{h^0}, the allowed range of λ is theoretically bounded from below by some $\lambda_{\min}$, in order to satisfy $m_{h^0} \leq m_{h^0}^{\max}$; see Eq. (7.31). Then for each value of λ in the domain $\lambda_{\min} \leq \lambda \leq \lambda_{\max} \equiv \frac{16\pi}{3}$ there corresponds two values of μ consistent with a given m_{h^0}, according to Eq. (7.30). Then it is easy to see, from the shape of the $m_{h^0}(\mu)$ plots shown in Fig. 3, that the largest spread between $\mu_+^{h^0}$ and $\mu_-^{h^0}$ is reached for $\lambda = \lambda_{\max}$, since increasing λ results in shifting these plots upwards. The two branches of the envelope of the domains in Figs. 7(b) and 8(b) correspond to $\mu_\pm^{h^0}(\lambda_{\max})$. Furthermore, increasing

m_{h^0} with fixed $\lambda = \lambda_{\max}$ results in an increase of μ_- and a decrease of μ_+, as can again be seen from the shape of the $m_{h^0}(\mu)$ plots shown in Fig. 3, till the two branches join and terminate when m_{h^0} reaches its unitarity bound, Eq. (7.26). With the numbers chosen on the plots, μ is bounded to lie between $\mu_- \approx 0.3$ GeV and $\mu_+ \approx 10^5$ GeV. One can see that for small $\mu \leq 1$ GeV, m_{h^0} must be less than about 200 GeV. The latter bound on m_{h^0} increases quickly to reach the unitarity bound, Eq. (7.26), when μ increases from 1 GeV to 10 GeV. Above, $\mu = 10$ GeV, m_{h^0} can be any number between the LEP limit (114 GeV) and this unitarity bound. As noted previously, one should take into account the actual doublet content of h^0 when reading out exclusion domains from these plots. In the plot, we have illustrated the size of $|s_\alpha|$. In most of the cases the mixing angle is very small (black to light gray areas), which means that h^0 is dominated by a doublet component. In these regions where a SM-Higgs exclusion limit can be readily applied, one might still need to combine this information with the search limits for the other charged, doubly charged, and $\mathcal{CP}_{\mathrm{odd}}$ Higgs states, in order to further reduce the otherwise large allowed domain for μ; see Eq. (3.13). However, due to the v_t suppression in Eq. (3.13) of the lower bound $\mu_{\min}$, such a reduction is not expected to be significant unless the experimental lower bounds, $(m_{H^{\pm\pm}})_{\exp}$ or $(m_{H^\pm})_{\exp}$ or $(m_{H^{A0}})_{\exp}$, become sufficiently higher than the electroweak scale. In contrast, bounds on m_{h^0} alone would significantly shrink the spread of the μ range whenever $|s_\alpha| > 10^{-2}$ (the light gray/dark gray areas), reducing as well the order of magnitude of the size of μ. In such a regime of small μ one starts being sensitive to the actual values of the λ_i's, as can be seen through the slight difference, in the light gray area, between Figs. 7(b) and 8(b). This effect will, of course, increase for higher values of the λ_i's consistent with unitarity and BFB constraints.
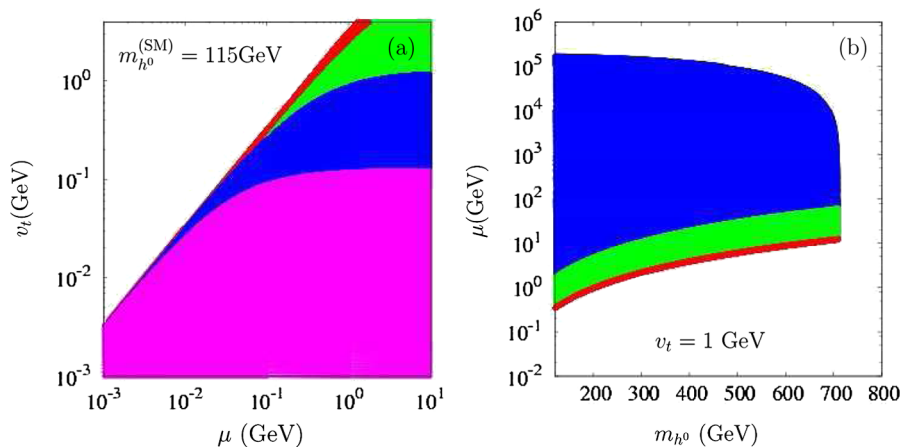

FIG. 7 (color online). (a) Correlation between μ and v_t with $m_{h^0} > m_{h^0}^{(\mathrm{SM})} = 115$ GeV and $\lambda = 0.48$; (b) correlation between μ and m_{h^0}, scanning over λ in the range $0.44 \leq \lambda \leq 16\pi/3$, with $v_t = 1$ GeV. The color code is as follows: $10^{-1} \leq s_\alpha \leq 1$ (dark gray), $10^{-2} \leq s_\alpha \leq 10^{-1}$ (light gray), $10^{-3} \leq s_\alpha \leq 10^{-2}$ (black), and $s_\alpha \leq 10^{-3}$ (gray). The other parameters are $\lambda_1 = -\lambda_4 = 1$, $\lambda_2 = \lambda_3 = 0$, and $\kappa = 8$. $\mathcal{V}_\lambda < 0$ for both figures.
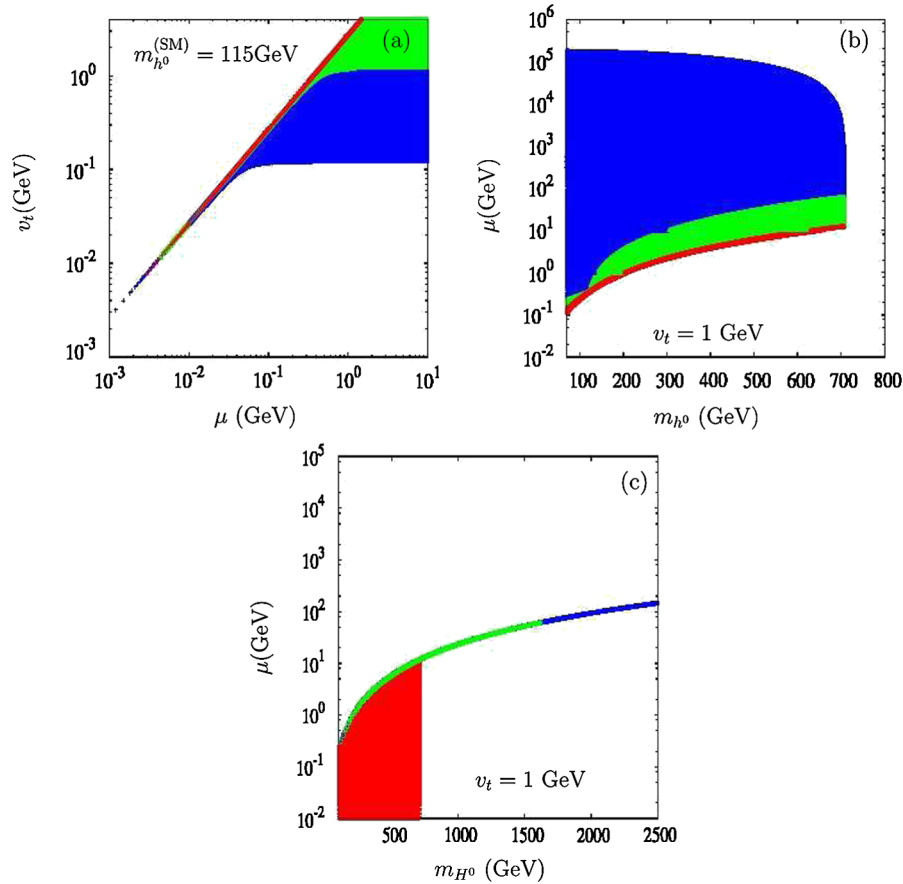
FIG. 8 (color online). (a) Correlation between μ and v_t with $m_{h^0} > m_{h^0}^{(SM)} = 115$ GeV and $\lambda = 0.48$; (b) correlation between μ and the light $\mathcal{CP}_{\text{even}}$ Higgs mass; (c) correlation between μ and the heavy $\mathcal{CP}_{\text{even}}$ Higgs mass, scanning over λ in the range $0.44 \leq \lambda \leq 16\pi/3$, with $v_t = 1$ GeV. The color code is as follows: $10^{-1} \leq |s_\alpha| \leq 1$ (dark gray), $10^{-2} \leq |s_\alpha| \leq 10^{-1}$ (light gray), $10^{-3} \leq |s_\alpha| \leq 10^{-2}$ (black), and $|s_\alpha| \leq 10^{-3}$ [white bottom area in (a)]. The other parameters are given by $\lambda_1 = 1.5$, $\lambda_2 = \lambda_3 = 0.1$, $\lambda_4 = -1$, and $\kappa = 8$. $\mathcal{V}_\lambda > 0$ in (a), while in (b) and (c) $\mathcal{V}_\lambda$ changes sign with increasing Higgs masses.

Figure 8(c) illustrates the behavior of m_{H^0} as a function of μ and λ which, as compared to Fig. 8(b), shows a striking difference from the behavior of m_{h^0}. According to the previous discussion on neutral Higgses (see also Fig. 5), $|s_\alpha|$ is essentially either very small or very close to 1. Thus, the dark gray area corresponds to an H^0 behaving essentially like the SM Higgs. The dual sizes of the dark gray areas in both plots can be understood again from the mass shapes of Fig. 3: For small $\mu (<\bar{\mu})$, m_{h^0} changes very quickly with μ while m_{H^0} is almost insensitive to μ. It follows that a variation of λ, that amounts to shifting these mass shapes upwards or downwards in Fig. 3, results in a small change in μ for a fixed m_{h^0} and a big change in μ for a fixed m_{H^0}, hence the narrow dark gray strip in Fig. 8(b) and the large dark gray area in Fig. 8(c). [One can similarly understand the dual sizes of the black and light gray areas for large $\mu (>\bar{\mu})$.] These features suggest a useful complementary strategy when using present or future exclusion limits, depending on whether one interprets these limits in the small or large $|s_\alpha|$ regimes. We discuss this strategy only qualitatively here, summarizing its main points as follows:

(I) In the *small* $|s_\alpha|$ regime, akin to moderate to large μ values, the typical Higgs spectrum features a $\mathcal{CP}_{\text{even}}$ lightest state h^0 behaving like a SM Higgs, the remaining Higgs states being much heavier, as illustrated in Figs. 3 and 9(a). Interpreting the exclusion limits within this regime amounts to applying a SM-Higgs mass lower bound $m_h^{(SM)}$ to m_{h^0} that leads to a lower bound on λ; see Eq. (7.31). A lower, $\mu_-^{h^0}$, and an upper, $\mu_+^{h^0}$, bound on μ will correspond to any λ above this bound. The lower bound $\mu_-^{h^0}$ is, however, typically too small to be consistent with the small $|s_\alpha|$ regime and should be superseded by a larger value $\mathcal{O}(\max\{\mu_c^{(1)}, \mu_c^{(2)}\})$. Furthermore, one should keep in mind that $\mu_+^{h^0}$ is extremely sensitive to m_{h^0} and decreases quickly with increasing m_{h^0}. This implies the important feature that a slight improvement of the exclusion limit $m_h^{(SM)}$ results in a substantial *decrease* of the upper bound on μ. The heavier $\mathcal{CP}_{\text{even}}$ state H^0 is not expected to bring significant constraints. Indeed, in the considered regime, this state carries essentially the triplet

component with suppressed couplings to the SM sector. Its mass can thus be bounded only by $m_h^{(\text{non-SM})}$, the exclusion mass limit on non-SM-like Higgs particles. Since such an exclusion mass limit is expected to be weaker than the SM-like limit due to lower statistics, that is, $m_h^{(\text{non-SM})} < m_h^{(\text{SM})}$, then taking into account that one theoretically has $m_{H^0} > m_{h^0}$, one is trivially led to $m_h^{(\text{non-SM})} < m_{H^0}^{\min}$, which implies no new constraints [cf. the discussion following Eq. (7.31)]. As stated previously, exclusion limits on the remaining Higgs states can also be used independently to improve the lower bound on μ based on Eq. (3.13). One can, however, get further information within the present regime depending on whether these exclusion limits are higher or lower than $m_h^{(\text{SM})}$. In particular, if $(m_{H^{\pm\pm}})_{\exp} \gtrsim m_h^{(\text{SM})}$, which excludes an $H^{\pm\pm}$ lighter than h^0, then one excludes all the $\lambda_4 > 0$ region, or else puts a stronger lower bound on μ, namely, $\mu > \mu^*$. [See Eq. (7.29) and discussion thereof.] In the case where $(m_{H^{\pm\pm}})_{\exp} \lesssim m_h^{(\text{SM})}$, which is the present experimental situation, there is a small window $\mu_{\min} < \mu < \mu^*$ with $\lambda_4 > 0$; otherwise, $\mu^* < \mu < \mu_+^{h^0}$ irrespective of the sign of λ_4, and for all the allowed values of λ discussed above. We have illustrated in Fig. 9(b) a case where $H^{\pm\pm}$ can be the lightest Higgs state.

(II) In the *large* $|s_\alpha|$ regime, akin to small μ values, H^0 is the heaviest among all the Higgs states of the model and behaves like a SM Higgs. This is a rather unusual configuration that should help constrain more efficiently, or perhaps exclude, this regime. Also in this small μ regime, and in contrast with the previous regime where only λ was playing a role, there can now be a somewhat increased sensitivity

to the λ_i's as well, in particular, $\lambda_1 + \lambda_4$. The reason for this is that the size of the μ domain is of order $\hat\mu$, Eq. (7.24), where in the latter, λ_1, λ_4 do not suffer a v_t suppression as compared to λ. However, as discussed in Sec. VII, the parameter k will characterize the sensitivity to the deviation of H^0 from a pure SM-Higgs state, which can lead, for realistic experimental sensitivities, to a significant reduction of the sensitivity on $\lambda_1 + \lambda_4$.

One then has to consider two cases:

(a) $m_h^{(\text{SM})} < m_{H^0}^{\min}$.—This case implies essentially a lower bound on λ through Eq. (7.21), but no constraint on μ apart from the defining region in this regime, namely, $0 < \mu \le \hat\mu$, whose size depends mainly on λ and, to a lesser extent, on $\lambda_1 + \lambda_4$. The latter couplings are bounded by the combined unitarity and BFB constraints of Sec. VI, so that there is an indirect sensitivity to λ_2 and λ_3 as well. The dark gray area in Fig. 8(c) gives an illustration of this least-constrained case. The μ domain extends over all the dark gray area, while the vertical boundary of this area is determined by the maximal value of $\lambda = \frac{16\pi}{3}$ given by unitarity. This boundary corresponds to the unitarity upper bound on the SM-Higgs mass as well as the one on m_{h^0}, Eq. (7.26). Of course H^0 can escape this bound but at the expense of switching consistently to the small $|s_\alpha|$ regime as seen in Fig. 8(c).

(b) $m_h^{(\text{SM})} \gtrsim m_{H^0}^{\min}$.—In this case not only do we have an upper bound on λ through Eq. (7.21), but we actually have a lower bound also. Indeed, a too small λ, leading to a too low $m_{H^0}^{\min}$ with respect to $m_h^{(\text{SM})}$, will eventually put $m_h^{(\text{SM})}$ just above all the values of m_{H^0} corresponding to the *large* $|s_\alpha|$ regime, thus ruling out this regime altogether. Furthermore, this
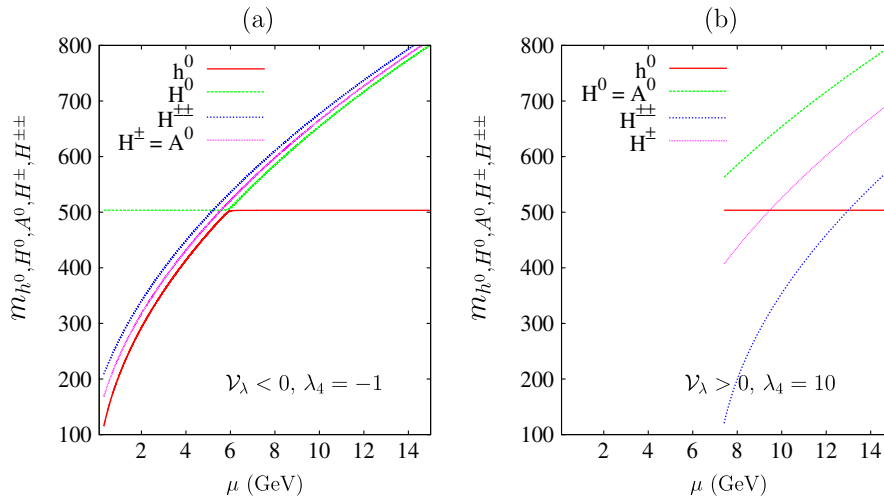

FIG. 9 (color online). Higgs boson masses as a function of μ with $v_t = 1$ GeV, $\lambda = 8\pi/3$, $\lambda_1 = 0.5$, $\lambda_2 = \lambda_3 = 0.1$, for $\mathcal{V}_\lambda < 0$, $\lambda_4 = -1$ (left panel) and $\mathcal{V}_\lambda > 0$, $\lambda_4 = 10$ (right panel). We note that in the left (right) panel one has $m_{H^\pm} \simeq m_{A^0}$ ($m_{H^0} \simeq m_{A^0}$).

configuration will immediately rule out the *small* $|s_\alpha|$ regime as well, since $m_h^{(\text{SM})}$ is, by definition, applicable only to SM-like states and we have $m_h^{(\text{SM})} \gtrsim m_{H^0}^{\min} > m_{h^0}$ for all m_{h^0}. Consequently, a too small λ would exclude the whole μ parameter space. One concludes that λ should lie in a very narrow strip such that $m_{H^0}^{\min} \lesssim m_h^{(\text{SM})} \lesssim m_{H^0}(\mu = 0)$. This strip is essentially giving the lower bound on λ of case (a) and thus does not provide significantly new information. [Note, though, that for values of $\lambda_1 + \lambda_4$ close to its unitarity bound, and taking, for instance, $m_h^{(\text{SM})} \simeq 114$ GeV and $v_t = 1$ GeV, case (b) can still reduce the lower bound on λ, from $\lambda \simeq 0.43$ to $\lambda \simeq 0.38$. But the effect will be smaller for smaller values of v_t.] One should, however, keep in mind that due to the high flatness of m_{H^0} as a function of μ in the region $0 < \mu \le \hat\mu$, the slightest variation of λ within the above-noted strip would result in the exclusion of significant parts of the $0 < \mu \le \hat\mu$ region. For instance, with $\lambda_1 = 1.5$, $\lambda_2 = \lambda_3 = 0.1$, $\lambda_4 = -1$ and taking the SM-Higgs lower bound $m_h^{(\text{SM})} = 114$ GeV, if one reduces the lower bound of λ (for which the whole range $0 < \mu \le \hat\mu \approx 0.3$ of the *large* $|s_\alpha|$ regime is allowed) by just $1‰$, then the SM-Higgs lower bound would imply $\mu < -5$ GeV or $\mu > 0.3$ GeV, thus ruling out the whole *large* $|s_\alpha|$ regime.

For all practical purposes and barring the fine-tuned effects just mentioned, the above discussion of cases (a) and (b) shows that an experimental lower bound on the SM-like Higgs mass cannot, by itself, cut into the *large* $|s_\alpha|$/small μ regime; it either excludes it or allows all of it, depending on whether λ is, respectively, below or above the value $\bar\lambda$ that satisfies $m_h^{(\text{SM})} = m_{H^0}^{\min}(\lambda = \bar\lambda)$. Thus, the size of the μ domain $[0, \hat\mu]$ that is controlled mainly by λ (but can also be sensitive to $\lambda_1 + \lambda_4$) for each given value of v_t [see Eq. (7.24)] will not be reduced by the actual value of the experimental bound $m_h^{(\text{SM})}$. Moreover, an extra constraint from an experimental lower bound on the mass of a non-SM-like $\mathcal{CP}_{\text{even}}$ Higgs state would have a marginal effect since m_{h^0} decreases very quickly in the region $\mu \lesssim \hat\mu$. An efficient reduction of the μ domain can come only from experimental lower bounds on the masses of the charged, doubly charged, and $\mathcal{CP}_{\text{odd}}$ Higgs states. Indeed, these bounds translate into a lower bound on μ typically of the same size as $\hat\mu$, Eq. (3.13). As long as these experimental bounds are of the same order, $(m_{A^0}^2)_{\text{exp}} \simeq (m_{H^\pm}^2)_{\text{exp}} \simeq (m_{H^{\pm\pm}}^2)_{\text{exp}}$, the relevant bound will be given by A^0 (respectively, $H^{\pm\pm}$) when $\lambda_4 < 0$ (respectively, $\lambda_4 > 0$).

Comparing $\mu_{\min}$ and $\hat\mu$, one easily determines the necessary and sufficient conditions for which the *large* $|s_\alpha|$ regime would be excluded. They read as follows:
$$(m_{A^0}^2)_{\text{exp}} \ge (k\lambda - 2(\lambda_1 + \lambda_4) - \sqrt{2k}|\lambda - \lambda_1 - \lambda_4|) \times$$

$\frac{v_d^2}{2(k-2)} + \mathcal{O}(v_t^2)$, for $\lambda_4 < 0$, and $(m_{H^{\pm\pm}}^2)_{\text{exp}} \ge (k(\lambda - \lambda_4) - 2\lambda_1 - \sqrt{2k}|\lambda - \lambda_1 - \lambda_4|)\frac{v_d^2}{2(k-2)} + \mathcal{O}(v_t^2)$, for $\lambda_4 > 0$, where we have taken into account the twofold structure as discussed after Eq. (7.24).

IX. CONCLUSION

We have carried out a detailed study of the renormalizable Higgs potential relevant to the type II seesaw model, keeping the full set of seven free parameters of the potential. We determined analytically the unitarity constraints on the various scalar couplings and fully solved the *all directions* conditions for boundedness from below. These combined theoretical constraints delineate efficiently the physically allowed regions of the parameter space and should be taken into account in phenomenological studies. We also examined the vacuum structure of the potential and determined general consistency constraints on the μ parameter, as well as theoretical upper (respectively, lower) bounds on the lighter (respectively, heavier) $\mathcal{CP}_{\text{even}}$ Higgs particle mass that can further constrain the phenomenological analyses. We also identified two distinct regimes, respectively, for large and small μ. In the first regime the lightest Higgs particle is the h^0, behaving as a SM-like Higgs, the remaining Higgses being typically too heavy to be of any phenomenological relevance. In the second regime, it is the heaviest Higgs H^0 that behaves as a SM-like Higgs; the lighter charged, doubly charged; and $\mathcal{CP}_{\text{odd}}$ states become accessible to the colliders, with the $H^{\pm\pm}$ possibly being the lightest state, while the lighter $\mathcal{CP}_{\text{even}}$ decouples quickly from the SM sector. We also initiated the study of possible consequences from existing experimental exclusion limits.

Although we did not commit to any underlying GUT assumptions, thus allowing μ to vary between a few GeV and possibly the GUT scale, we do retrieve, as a consequence of the (model-independent) dynamical constraints on μ, a seesaw-like behavior that leads to tiny v_t if μ is taken very large.

Finally, since the results of this study have been obtained at the tree level, one should keep in mind that modifications due to quantum corrections to the effective potential can possibly be substantial in some cases. The inclusion of such corrections is, however, beyond the scope of the present paper, given the nontrivial form of the constraints already at the tree-level.

APPENDIX A

As stated in Sec. III, the positivity of $m_{h^0}^2$ constrains μ to lie in the range $\mu_- \leq \mu \leq \mu_+$ so as to satisfy Eq. (3.9). We give here the full expression for $\mu_\pm$:

$$\mu_\pm = \frac{\lambda v_d^2 + 8(\lambda_1 + \lambda_4)v_t^2 \pm \sqrt{\lambda(\lambda v_d^4 + 16v_t^2((\lambda_1 + \lambda_4)v_d^2 + 4(\lambda_2 + \lambda_3)v_t^2))}}{8\sqrt{2}v_t}. \tag{A1}$$

Note that due to the negative coefficient of μ^2 in Eq. (3.9), $\mu_\pm$ should always be real valued, otherwise Eq. (3.9) is not satisfied and h^0 is tachyonic for *all* values of μ. As can be seen from Eq. (A1), this requirement leads, in principle, to an extra constraint on top of Eqs. (3.8), (3.9), and (3.10), that is,

$$\lambda(\lambda v_d^4 + 16v_t^2((\lambda_1 + \lambda_4)v_d^2 + 4(\lambda_2 + \lambda_3)v_t^2)) \geq 0. \tag{A2}$$

However, we show here that this extra constraint is automatically satisfied due to the BFB constraints: Since $\lambda > 0$, cf. Eq. (6.1), it suffices to show that $(\lambda v_d^4 + 16v_t^2((\lambda_1 + \lambda_4)v_d^2 + 4(\lambda_2 + \lambda_3)v_t^2)) \geq 0$. Now using the first inequality of Eq. (6.3), one obtains

$$\lambda v_d^4 + 16v_t^2((\lambda_1 + \lambda_4)v_d^2 + 4(\lambda_2 + \lambda_3)v_t^2)$$

$$\geq (\lambda v_d^4 + 16v_t^2(-\sqrt{\lambda(\lambda_2 + \lambda_3)}v_d^2 + 4(\lambda_2 + \lambda_3)v_t^2))$$

$$\geq (\sqrt{\lambda}v_d^2 - 8\sqrt{(\lambda_2 + \lambda_3)}v_t^2)^2, \tag{A3}$$

which proves our statement.

APPENDIX B

In this appendix we give the form of the Higgs potential in the field subspaces where only two or three fields are nonvanishing, dubbed, respectively, two-field and three-field directions. We identify exhaustively ten different directions for each of these two classes and give their corresponding BFB conditions.

The ten two-field directions:

$$_2V_{\text{dir.1}}^{(4)} = \frac{\lambda}{4}(|\phi^0|^2 + |\phi^+|^2)^2, \tag{B1}$$

$$_2V_{\text{dir.2}}^{(4)} = (\lambda_2 + \lambda_3)|\delta^{++}|^4 + (\lambda_1 + \lambda_4)|\delta^{++}|^2|\phi^+|^2$$
$$+ \frac{\lambda}{4}|\phi^+|^4, \tag{B2}$$

$$_2V_{\text{dir.3}}^{(4)} = (\lambda_2 + \lambda_3)|\delta^{++}|^4 + \lambda_1|\delta^{++}|^2|\phi^0|^2 + \frac{\lambda}{4}|\phi^0|^4, \tag{B3}$$

$$_2V_{\text{dir.4}}^{(4)} = \left(\lambda_2 + \frac{\lambda_3}{2}\right)|\delta^+|^4 + \left(\lambda_1 + \frac{\lambda_4}{2}\right)|\delta^+|^2|\phi^+|^2$$
$$+ \frac{\lambda}{4}|\phi^+|^4, \tag{B4}$$

$$_2V_{\text{dir.5}}^{(4)} = \left(\lambda_2 + \frac{\lambda_3}{2}\right)|\delta^+|^4 + \left(\lambda_1 + \frac{\lambda_4}{2}\right)|\delta^+|^2|\phi^0|^2$$
$$+ \frac{\lambda}{4}|\phi^0|^4, \tag{B5}$$

$$_2V_{\text{dir.6}}^{(4)} = \left(\lambda_2 + \frac{\lambda_3}{2}\right)|\delta^+|^4 + 2(\lambda_2 + \lambda_3)|\delta^+|^2|\delta^{++}|^2$$
$$+ (\lambda_2 + \lambda_3)|\delta^{++}|^4, \tag{B6}$$

$$_2V_{\text{dir.7}}^{(4)} = (\lambda_2 + \lambda_3)|\delta^0|^4 + \lambda_1|\delta^0|^2|\phi^+|^2 + \frac{\lambda}{4}|\phi^+|^4, \tag{B7}$$

$$_2V_{\text{dir.8}}^{(4)} = (\lambda_2 + \lambda_3)|\delta^0|^4 + (\lambda_1 + \lambda_4)|\delta^0|^2|\phi^0|^2$$
$$+ \frac{\lambda}{4}|\phi^0|^4, \tag{B8}$$

$$_2V_{\text{dir.9}}^{(4)} = (\lambda_2 + \lambda_3)|\delta^0|^4 + 2\lambda_2|\delta^0|^2|\delta^{++}|^2 + (\lambda_2$$
$$+ \lambda_3)|\delta^{++}|^4, \tag{B9}$$

$$_2V_{\text{dir.10}}^{(4)} = (\lambda_2 + \lambda_3)|\delta^0|^4 + 2(\lambda_2 + \lambda_3)|\delta^0|^2|\delta^+|^2$$
$$+ \left(\lambda_2 + \frac{\lambda_3}{2}\right)|\delta^+|^4, \tag{B10}$$

$$\text{direction } 1: \lambda > 0, \tag{B11}$$

$$\text{directions } 2 \text{ and } 8: \lambda > 0, \lambda_2 + \lambda_3 > 0, \lambda_1 + \lambda_4$$
$$+ \sqrt{\lambda(\lambda_2 + \lambda_3)} > 0, \tag{B12}$$

$$\text{directions } 3 \text{ and } 7: \lambda > 0, \lambda_2 + \lambda_3 > 0, \lambda_1$$
$$+ \sqrt{\lambda(\lambda_2 + \lambda_3)} > 0, \tag{B13}$$

$$\text{directions } 4 \text{ and } 5: \lambda > 0, \lambda_2 + \frac{\lambda_3}{2} > 0, \lambda_1 + \frac{\lambda_4}{2}$$
$$+ \sqrt{\lambda\left(\lambda_2 + \frac{\lambda_3}{2}\right)} > 0, \tag{B14}$$

directions 6, 9 and 10: $\lambda_2 + \lambda_3 > 0$, $\lambda_2 + \dfrac{\lambda_3}{2} > 0$,

$$\text{(B15)}$$

The ten three-field directions:

$$_3V^{(4)}_{\text{dir.1}} = (\lambda_2 + \lambda_3)|\delta^0|^4 + 2(\lambda_2 + \lambda_3)|\delta^0|^2|\delta^+|^2$$
$$+ \left(\lambda_2 + \frac{\lambda_3}{2}\right)|\delta^+|^4 + 2\lambda_2|\delta^0|^2|\delta^{++}|^2$$
$$+ 2(\lambda_2 + \lambda_3)|\delta^+|^2|\delta^{++}|^2 + (\lambda_2 + \lambda_3)|\delta^{++}|^4$$
$$- \lambda_3 \frac{\delta^{--}}{\delta^0(\delta^-)^2}|\delta^0|^2|\delta^+|^4 - \lambda_3 \frac{\delta^0(\delta^-)^2}{\delta^{--}}|\delta^{++}|^2,$$

$$\text{(B16)}$$

$$_3V^{(4)}_{\text{dir.2}} = (\lambda_2 + \lambda_3)|\delta^0|^4 + 2(\lambda_2 + \lambda_3)|\delta^0|^2|\delta^+|^2$$
$$+ \left(\lambda_2 + \frac{\lambda_3}{2}\right)|\delta^+|^4 + (\lambda_1 + \lambda_4)|\delta^0|^2|\phi^0|^2$$
$$+ \left(\lambda_1 + \frac{\lambda_4}{2}\right)|\delta^+|^2|\phi^0|^2 + \frac{\lambda}{4}|\phi^0|^4,$$

$$\text{(B17)}$$

$$_3V^{(4)}_{\text{dir.3}} = (\lambda_2 + \lambda_3)|\delta^0|^4 + 2(\lambda_2 + \lambda_3)|\delta^0|^2|\delta^+|^2$$
$$+ \left(\lambda_2 + \frac{\lambda_3}{2}\right)|\delta^+|^4 + \lambda_1|\delta^0|^2|\phi^+|^2$$
$$+ \left(\lambda_1 + \frac{\lambda_4}{2}\right)|\delta^+|^2|\phi^+|^2 + \frac{\lambda}{4}|\phi^+|^4,$$

$$\text{(B18)}$$

$$_3V^{(4)}_{\text{dir.4}} = (\lambda_2 + \lambda_3)|\delta^0|^4 + 2\lambda_2|\delta^0|^2|\delta^{++}|^2$$
$$+ (\lambda_2 + \lambda_3)|\delta^{++}|^4 + (\lambda_1 + \lambda_4)|\delta^0|^2|\phi^0|^2$$
$$+ \lambda_1|\delta^{++}|^2|\phi^0|^2 + \frac{\lambda}{4}|\phi^0|^4,$$

$$\text{(B19)}$$

$$_3V^{(4)}_{\text{dir.5}} = (\lambda_2 + \lambda_3)|\delta^0|^4 + 2\lambda_2|\delta^0|^2|\delta^{++}|^2$$
$$+ (\lambda_2 + \lambda_3)|\delta^{++}|^4 + \lambda_1|\delta^0|^2|\phi^+|^2$$
$$+ (\lambda_1 + \lambda_4)|\delta^{++}|^2|\phi^+|^2 + \frac{\lambda}{4}|\phi^+|^4,$$

$$\text{(B20)}$$

$$_3V^{(4)}_{\text{dir.6}} = (\lambda_2 + \lambda_3)|\delta^0|^4 + (\lambda_1 + \lambda_4)|\delta^0|^2|\phi^0|^2$$
$$+ \frac{\lambda}{4}|\phi^0|^4 + \lambda_1|\delta^0|^2|\phi^+|^2 + \frac{\lambda}{2}|\phi^0|^2|\phi^+|^2$$
$$+ \frac{\lambda}{4}|\phi^+|^4,$$

$$\text{(B21)}$$

$$_3V^{(4)}_{\text{dir.7}} = \left(\lambda_2 + \frac{\lambda_3}{2}\right)|\delta^+|^4 + 2(\lambda_2 + \lambda_3)|\delta^+|^2|\delta^{++}|^2$$
$$+ (\lambda_2 + \lambda_3)|\delta^{++}|^4 + \left(\lambda_1 + \frac{\lambda_4}{2}\right)|\delta^+|^2|\phi^0|^2$$
$$+ \lambda_1|\delta^{++}|^2|\phi^0|^2 + \frac{\lambda}{4}|\phi^0|^4,$$

$$\text{(B22)}$$

$$_3V^{(4)}_{\text{dir.8}} = \left(\lambda_2 + \frac{\lambda_3}{2}\right)|\delta^+|^4 + 2(\lambda_2 + \lambda_3)|\delta^+|^2|\delta^{++}|^2$$
$$+ (\lambda_2 + \lambda_3)|\delta^{++}|^4 + \left(\lambda_1 + \frac{\lambda_4}{2}\right)|\delta^+|^2|\phi^+|^2$$
$$+ (\lambda_1 + \lambda_4)|\delta^{++}|^2|\phi^+|^2 + \frac{\lambda}{4}|\phi^+|^4,$$

$$\text{(B23)}$$

$$_3V^{(4)}_{\text{dir.9}} = \left(\lambda_2 + \frac{\lambda_3}{2}\right)|\delta^+|^4 + \left(\lambda_1 + \frac{\lambda_4}{2}\right)|\delta^+|^2|\phi^0|^2$$
$$+ \frac{\lambda}{4}|\phi^0|^4 + \left(\lambda_1 + \frac{\lambda_4}{2}\right)|\delta^+|^2|\phi^+|^2$$
$$+ \frac{\lambda}{2}|\phi^0|^2|\phi^+|^2 + \frac{\lambda}{4}|\phi^+|^4,$$

$$\text{(B24)}$$

$$_3V^{(4)}_{\text{dir.10}} = (\lambda_2 + \lambda_3)|\delta^{++}|^4 + \lambda_1|\delta^{++}|^2|\phi^0|^2$$
$$+ \frac{\lambda}{4}|\phi^0|^4 + (\lambda_1 + \lambda_4)|\delta^{++}|^2|\phi^+|^2$$
$$+ \frac{\lambda}{2}|\phi^0|^2|\phi^+|^2 + \frac{\lambda}{4}|\phi^+|^4,$$

$$\text{(B25)}$$

The corresponding BFB conditions read

direction 1: $2\lambda_2 + \lambda_3 > 0 \wedge \lambda_2 + \lambda_3 > 0 \wedge (\lambda_3^2 < 4(\lambda_2 + \lambda_3)^2 \vee \lambda_3 < 0)$,

$$\text{(B26)}$$

direction 2: $\lambda > 0 \wedge \lambda_2 + \lambda_3 > 0 \wedge 2\lambda_2 + \lambda_3 > 0 \wedge \sqrt{\lambda(\lambda_2 + \lambda_3)} + \lambda_1 + \lambda_4 > 0 \wedge \Bigg(\bigg(2\lambda(2\lambda_2 + \lambda_3) > (2\lambda_1 + \lambda_4)^2$

$$\wedge \left((\sqrt{2}\sqrt{\lambda_3(\lambda_2 + \lambda_3)((2\lambda_1 + \lambda_4)^2 - 2\lambda(2\lambda_2 + \lambda_3))} + 2\lambda_2\lambda_4 > 2\lambda_1\lambda_3 \wedge \lambda_3 < 0\right)$$

$$\vee \left(\frac{(2\lambda_2 + \lambda_3)((2\lambda_1 + \lambda_4)(2\lambda_1 + 3\lambda_4) - 4\lambda(\lambda_2 + \lambda_3))}{2\lambda_1 + \lambda_4} > 0 \wedge 2\lambda_1 + \lambda_4 < 0\right)\bigg)\bigg) \vee 2\lambda_1 + \lambda_4 > 0\Bigg),$$

$$\text{(B27)}$$

direction 3: $\lambda > 0 \wedge \lambda_2 + \lambda_3 > 0 \wedge 2\lambda_2 + \lambda_3 > 0 \wedge \sqrt{\lambda(\lambda_2 + \lambda_3)} + \lambda_1 > 0 \wedge \Big(\Big(2\lambda(2\lambda_2 + \lambda_3) > (2\lambda_1 + \lambda_4)^2$

$$\wedge \Big(\Big(2\lambda_1 + \lambda_4 < 0 \wedge \frac{(2\lambda_2 + \lambda_3)(4\lambda(\lambda_2 + \lambda_3) - 4\lambda_1^2 + \lambda_4^2)}{2\lambda_1 + \lambda_4} < 0 \Big) \vee \Big((\lambda_2 + \lambda_3)(2\lambda_2 + \lambda_3 - 2) > 0$$

$$\wedge \sqrt{2}\sqrt{\lambda_3(\lambda_2 + \lambda_3)((2\lambda_1 + \lambda_4)^2 - 2\lambda(2\lambda_2 + \lambda_3))} > 2\lambda_1\lambda_3 + 2\lambda_4(\lambda_2 + \lambda_3) \Big) \Big) \Big) \vee 2\lambda_1 + \lambda_4 > 0 \Big), \tag{B28}$$

direction 4: $\lambda > 0 \wedge \lambda_2 + \lambda_3 > 0 \wedge \sqrt{\lambda(\lambda_2 + \lambda_3)} + \lambda_1 + \lambda_4 > 0 \wedge \Big(\Big(\dfrac{(\lambda_2 + \lambda_3)(-\lambda\lambda_2^2 + \lambda_1^2(\lambda_2 - \lambda_3) + 2\lambda_1\lambda_2\lambda_4)}{\lambda_1\lambda_2} > 0$

$$\wedge ((\lambda_2 > 0 \wedge \lambda(\lambda_2 + \lambda_3) > \lambda_1^2 \wedge \lambda_1 < 0) \vee (\lambda_1 > 0 \wedge \lambda_3(2\lambda_2 + \lambda_3) > 0 \wedge \lambda_2 < 0))) \vee (\lambda_1 > 0 \wedge \lambda_2 > 0)$$

$$\vee (\lambda(\lambda_2 + \lambda_3) > \lambda_1^2 \wedge \lambda_3(2\lambda_2 + \lambda_3) > 0 \wedge \sqrt{\lambda_3(2\lambda_2 + \lambda_3)(\lambda(\lambda_2 + \lambda_3) - \lambda_1^2)} + \lambda_1\lambda_3 + \lambda_4(\lambda_2 + \lambda_3) > 0 \Big) \Big), \tag{B29}$$

direction 5: $\lambda > 0 \wedge \lambda_2 + \lambda_3 > 0 \wedge \sqrt{\lambda(\lambda_2 + \lambda_3)} + \lambda_1 > 0$

$$\wedge \Big(\Big(\frac{(\lambda_2 + \lambda_3)(\lambda\lambda_2^2 + \lambda_1^2(\lambda_3 - \lambda_2) + 2\lambda_1\lambda_3\lambda_4 + \lambda_4^2(\lambda_2 + \lambda_3))}{\lambda_2(\lambda_1 + \lambda_4)} < 0 \wedge ((\lambda_3(2\lambda_2 + \lambda_3) > 0 \wedge \lambda_1$$

$$+ \lambda_4 > 0 \wedge \lambda_2 < 0) \vee (\lambda_2 > 0 \wedge \lambda(\lambda_2 + \lambda_3) > (\lambda_1 + \lambda_4)^2 \wedge \lambda_1 + \lambda_4 < 0) \Big) \Big) \vee (\lambda_2 > 0 \wedge \lambda_1 + \lambda_4 > 0)$$

$$\vee (\lambda(\lambda_2 + \lambda_3) > (\lambda_1 + \lambda_4)^2 \wedge \lambda_3(2\lambda_2 + \lambda_3) > 0 \wedge \sqrt{-\lambda_3(2\lambda_2 + \lambda_3)((\lambda_1 + \lambda_4)^2 - \lambda(\lambda_2 + \lambda_3))} + \lambda_1\lambda_3 > \lambda_2\lambda_4)), \tag{B30}$$

direction 6: $\lambda > 0 \wedge \lambda_2 + \lambda_3 > 0 \wedge \sqrt{\lambda(\lambda_2 + \lambda_3)} + \lambda_1 > 0 \wedge (\lambda_1 + \lambda_4 > 0 \vee (\lambda(\lambda_2 + \lambda_3) > (\lambda_1 + \lambda_4)^2 \wedge \lambda_4 < 0)), \tag{B31}$

direction 7: $\lambda > 0 \wedge 2\lambda_2 + \lambda_3 > 0 \wedge \lambda_2 + \lambda_3 > 0 \wedge \sqrt{\lambda(4\lambda_2 + 2\lambda_3)} + 2\lambda_1 + \lambda_4 > 0 \wedge \Big(\Big(\lambda(\lambda_2 + \lambda_3) > \lambda_1^2$

$$\wedge \Big(\Big(\lambda_1(2\lambda_2 + 3\lambda_3) + 2\lambda_4(\lambda_2 + \lambda_3) > \frac{2\lambda(\lambda_2 + \lambda_3)^2}{\lambda_1} \wedge \lambda_1 < 0 \Big)$$

$$\vee \sqrt{2}\sqrt{\lambda_3(\lambda_2 + \lambda_3)(\lambda_1^2 - \lambda(\lambda_2 + \lambda_3))} + \lambda_4(\lambda_2 + \lambda_3) > 0 \Big) \Big) \vee \lambda_1 > 0 \Big), \tag{B32}$$

direction 8: $\lambda > 0 \wedge 2\lambda_2 + \lambda_3 > 0 \wedge \lambda_2 + \lambda_3 > 0 \wedge \sqrt{\lambda(4\lambda_2 + 2\lambda_3)} + 2\lambda_1 + \lambda_4 > 0$

$$\wedge \Big(\Big(\lambda(\lambda_2 + \lambda_3) > (\lambda_1 + \lambda_4)^2 \wedge \Big((\sqrt{2}\sqrt{\lambda_3(\lambda_2 + \lambda_3)((\lambda_1 + \lambda_4)^2 - \lambda(\lambda_2 + \lambda_3))} > \lambda_4(\lambda_2 + \lambda_3) \wedge \lambda_3 < 0)$$

$$\vee \Big(2\lambda_1\lambda_2 + 3\lambda_1\lambda_3 + \lambda_3\lambda_4 > \frac{2\lambda(\lambda_2 + \lambda_3)^2}{\lambda_1 + \lambda_4} \wedge \lambda_1 + \lambda_4 < 0 \Big) \Big) \Big) \vee \lambda_1 + \lambda_4 > 0 \Big), \tag{B33}$$

direction 9: $\lambda > 0 \wedge 2\lambda_2 + \lambda_3 > 0 \wedge \sqrt{\lambda(4\lambda_2 + 2\lambda_3)} + 2\lambda_1 + \lambda_4 > 0 \wedge (2\lambda(2\lambda_2 + \lambda_3) > (2\lambda_1 + \lambda_4)^2 \vee 2\lambda_1 + \lambda_4 > 0), \tag{B34}$

direction 10: $\lambda > 0 \wedge \lambda_2 + \lambda_3 > 0 \wedge \sqrt{\lambda(\lambda_2 + \lambda_3)} + \lambda_1 + \lambda_4 > 0 \wedge (\lambda_1 > 0 \vee \lambda(\lambda_2 + \lambda_3) > \lambda_1^2 \vee \lambda_4 > 0). \tag{B35}$

We emphasize that all the above BFB conditions are contained in the general solution given by Eqs. (6.1), (6.2), and (6.3).

APPENDIX C

For completeness, we give in Appendixes C 1 and C 2a partial list of the couplings in the DTHM that are relevant, respectively, to the discussion in Sec. VIII and to the derivation of the results of Sec. V.

1. Higgs-gauge boson couplings and triple Higgs couplings

Shifting the neutral fields according to Eq. (2.26), and using the relations between the physical and nonphysical state bases,

$$\begin{pmatrix} h \\ \xi^0 \end{pmatrix} = \mathcal{R}_\alpha \begin{pmatrix} h^0 \\ H^0 \end{pmatrix}, \qquad \begin{pmatrix} Z_1 \\ Z_2 \end{pmatrix} = \mathcal{R}_\beta \begin{pmatrix} G^0 \\ A^0 \end{pmatrix}, \quad \text{(C1)}$$

$$\begin{pmatrix} \phi^\pm \\ \delta^\pm \end{pmatrix} = \mathcal{R}_{\beta'} \begin{pmatrix} G^\pm \\ H^\pm \end{pmatrix} \quad \text{(C2)}$$

with $\mathcal{R}_\alpha$, $\mathcal{R}_\beta$, and $\mathcal{R}_{\beta'}$ as defined in Eqs. (2.12) and (2.23), one extracts from the kinetic terms and the covariant derivatives, Eqs. (2.1), (2.2), and (2.3), the couplings involving Higgs bosons and gauge bosons, and from the potential, Eq. (2.4), the triple Higgs couplings.

We list below some of the resulting Feynman rules and provide also approximate expressions in the limit of very small mixing between the triplet and doublet Higgs multiplets [i.e. $s_\alpha = \mathcal{O}(v_t^2/v_d^2)$, $c_{\alpha,\beta,\beta'} = 1 + \mathcal{O}(v_t^2/v_d^2)$, $s_\beta = 2v_t/v_d + \mathcal{O}(v_t^2/v_d^2)$, and $s_{\beta'} = \sqrt{2}v_t/v_d + \mathcal{O}(v_t^2/v_d^2)$].

$$h^0 ZZ = +i\frac{g}{c_W}m_Z(c_\alpha c_\beta + 2s_\alpha s_\beta)g_{\mu\nu} \approx i\frac{g}{c_W}m_Z g_{\mu\nu},$$
$$\text{(C3)}$$

$$H^0 ZZ = -i\frac{g}{c_W}m_Z(s_\alpha c_\beta - 2c_\alpha s_\beta)g_{\mu\nu}$$
$$\approx 4i\frac{g}{c_W}\frac{v_t}{v_d}m_Z g_{\mu\nu}, \quad \text{(C4)}$$

$$h^0 W^+ W^- = igc_W m_Z(c_\alpha c_\beta + s_\alpha s_\beta)g_{\mu\nu} \approx igm_W g_{\mu\nu},$$
$$\text{(C5)}$$

$$H^0 W^+ W^- = -igm_W(s_\alpha c_\beta - c_\alpha s_\beta)g_{\mu\nu}$$
$$\approx 2igm_W\frac{v_t}{v_d}g_{\mu\nu}, \quad \text{(C6)}$$

$$h^0 A^0 Z = -\frac{g}{2c_W}(c_\alpha s_\beta - 2c_\beta s_\alpha)(p_h - p_A)_\mu$$
$$\approx -\frac{g}{c_W}\frac{v_t}{v_d}(p_h - p_A)_\mu, \quad \text{(C7)}$$

$$H^0 A^0 Z = \frac{g}{2c_W}(s_\alpha s_\beta + 2c_\alpha c_\beta)(p_H - p_A)_\mu$$
$$\approx \frac{g}{c_W}(p_H - p_A)_\mu, \quad \text{(C8)}$$

$$h^0 h^0 H^0 = i\left(\left(\frac{3}{2}\lambda c_\alpha^2 - \lambda_{14}^+\right)s_\alpha v_d - 6\lambda_{23}^+ c_\alpha s_\alpha^2 v_t \right.$$
$$\left. + (c_\alpha^2 - 2s_\alpha^2)(\sqrt{2}c_\alpha\mu - \lambda_{14}^+(s_\alpha v_d + c_\alpha v_t))\right)$$
$$\approx i(\sqrt{2}\mu + (3\lambda - 5(\lambda_1 + \lambda_4))v_t) + \mathcal{O}(v_t^2), \quad \text{(C9)}$$

$$h^0 W^+ H^- = i\frac{g}{2}(c_\alpha s_{\beta'} - \sqrt{2}s_\alpha c_{\beta'})(p_h - p_{H^-})_\mu$$
$$\approx +i\frac{g}{\sqrt{2}}\frac{v_t}{v_d}(p_h - p_{H^-})_\mu, \quad \text{(C10)}$$

$$H^0 W^+ H^- = -i\frac{g}{2}(s_\alpha s_{\beta'} + \sqrt{2}c_\alpha c_{\beta'})(p_H - p_{H^-})_\mu$$
$$\approx -i\frac{g}{\sqrt{2}}(p_H - p_{H^-})_\mu, \quad \text{(C11)}$$

$$A^0 W^+ H^- = \frac{g}{2}(\sqrt{2}c_{\beta'}c_\beta + s_{\beta'}s_\beta)(p_{A^0} - p_{H^-})_\mu$$
$$\approx \frac{g}{\sqrt{2}}(p_{A^0} - p_{H^-})_\mu, \quad \text{(C12)}$$

$$Z_\mu W_\nu^+ H^- = gm_Z\left(c_\beta s_{\beta'}s_W^2 - \frac{s_\beta c_{\beta'}}{\sqrt{2}}(1 + s_W^2)\right)g_{\mu\nu}$$
$$\approx -\sqrt{2}g\frac{m_Z v_t}{v_d}g_{\mu\nu}, \quad \text{(C13)}$$

$$H^{++} H^- W_\mu^- = igc_{\beta'}(p_{H^{++}} - p_{H^-})_\mu$$
$$\approx ig(p_{H^{++}} - p_{H^-})_\mu, \quad \text{(C14)}$$

$$H^{++} W_\mu^- W_\nu^- = -i\sqrt{2}g^2 v_t g_{\mu\nu}, \quad \text{(C15)}$$

$$H^{++} H^- H^- = -i(2\mu s_{\beta'}^2 + c_{\beta'}(\lambda_4 s_{\beta'}v_d - \sqrt{2}\lambda_3 c_{\beta'}v_t)),$$
$$\text{(C16)}$$

$$H^{++} H^{--} VV' = 8ie_V e_{V'}g_{\mu\nu}, \quad \text{(C17)}$$

$$H^{++} H^{--} V = -2ie_V(p_{H^{++}} - p_{H^{--}})_\mu, \quad \text{(C18)}$$

$$H^+ H^- VV' = 2ie_V e_{V'}g_{\mu\nu}, \quad \text{(C19)}$$

$$H^+ H^- V = -ie_V(p_{H^+} - p_{H^-})_\mu, \quad \text{(C20)}$$

$$G^+ G^- VV' = 2ie_V e_{V'}g_{\mu\nu}, \quad \text{(C21)}$$

$$G^+ G^- V = -ie_V(p_{G^+} - p_{G^-})_\mu, \quad \text{(C22)}$$

where in Eqs. (C17)–(C22) we denote by V and V' the γ or Z gauge boson, with the couplings satisfying $e_\gamma \equiv e$ and $e_Z \equiv e\cot 2\theta_W$. We also adopted the convention that all momenta are incoming at each vertex.

2. Quartic scalar couplings in the doublet-triplet basis

Here we give the complete list of Feynman rules for the quartic scalar couplings in the unrotated basis which were used in Sec. V to determine the unitarity constraints:

$$\delta^+\delta^+\delta^-\delta^- = -2i(2\lambda_2 + \lambda_3), \qquad Z_2 Z_2 \phi^- \phi^+ = -i(\lambda_1),$$

$$\delta^+\delta^-\delta^{--}\delta^{++} = -2i(\lambda_2 + \lambda_3), \qquad Z_1 Z_1 \phi^- \phi^+ = -i\frac{1}{2}\lambda,$$

$$\delta^{++}\delta^{++}\delta^{--}\delta^{--} = -4i(\lambda_2 + \lambda_3), \qquad \phi^-\phi^-\phi^+\phi^+ = -i\lambda,$$

$$\delta^+\delta^+\delta^{--}Z_2 = \sqrt{2}\lambda_3, \qquad \delta^+\delta^+\delta^{--}\xi^0 = i\sqrt{2}\lambda_3,$$

$$\delta^-\delta^-\delta^{++}Z_2 = -\sqrt{2}\lambda_3, \qquad \delta^-\delta^-\delta^{++}\xi^0 = i\sqrt{2}\lambda_3,$$

$$\delta^-\delta^+ Z_2 Z_2 = -2i(\lambda_2 + \lambda_3), \qquad \delta^+ Z_1 \phi^- \xi^0 = \frac{\lambda_4}{2\sqrt{2}},$$

$$Z_2 Z_2 Z_2 Z_2 = -6i(\lambda_2 + \lambda_3), \qquad \delta^- Z_1 \phi^+ \xi^0 = \frac{-\lambda_4}{2\sqrt{2}},$$

$$\delta^{++}\delta^{--}Z_2 Z_2 = -2i\lambda_2, \qquad \delta^-\delta^+\xi^0\xi^0 = -2i(\lambda_2 + \lambda_3), \qquad \delta^+\delta^- Z_1 Z_1 = -\frac{i}{2}(2\lambda_1 + \lambda_4),$$

$$\delta^{--}\delta^{++}\xi^0\xi^0 = -2i\lambda_2, \qquad \delta^{++}\delta^{--}Z_1 Z_1 = -i(\lambda_1), \qquad Z_2 Z_2 \xi^0 \xi^0 = -2i(\lambda_2 + \lambda_3),$$

$$Z_2 Z_2 Z_1 Z_1 = -i(\lambda_1 + \lambda_4), \qquad Z_1 Z_1 \xi^0 \xi^0 = -i(\lambda_1 + \lambda_4), \qquad Z_1 Z_1 Z_1 Z_1 = -\frac{3}{2}i\lambda,$$

$$\phi^-\phi^+\xi^0\xi^0 = -i(\lambda_1), \qquad \delta^{++}\delta^- Z_1 \phi^- = -\frac{\lambda_4}{2}, \qquad \xi^0\xi^0\xi^0\xi^0 = -6i(\lambda_2 + \lambda_3),$$

$$\delta^+\phi^- Z_1 Z_2 = -\frac{i\lambda_4}{2\sqrt{2}}, \qquad \delta^-\delta^{++}\phi^- h = \frac{i\lambda_4}{2}, \qquad \delta^+\delta^{--}\phi^+ Z_1 = \frac{\lambda_4}{2},$$

$$\delta^+\phi^- Z_2 h = -\frac{\lambda_4}{2\sqrt{2}}, \qquad \delta^-\phi^+ Z_2 Z_1 = -\frac{i\lambda_4}{2\sqrt{2}}, \qquad \delta^+\delta^{--}\phi^+ h = \frac{i\lambda_4}{2},$$

$$\delta^-\delta^+\phi^+\phi^- = -\frac{i}{2}(2\lambda_1 + \lambda_4), \qquad \delta^- Z_2 \phi^+ h = \frac{\lambda_4}{2\sqrt{2}}, \qquad \delta^{--}\delta^{++}\phi^+\phi^- = -i(\lambda_1 + \lambda_4),$$

$$\delta^+\xi^0 h\phi^- = -\frac{i\lambda_4}{2\sqrt{2}}, \qquad \delta^-\phi^+\xi^0 h = -\frac{i\lambda_4}{2\sqrt{2}}, \qquad Z_2 Z_2 hh = -i(\lambda_4 + \lambda_1),$$

$$\delta^-\delta^+ hh = -\frac{i}{2}(2\lambda_1 + \lambda_4), \qquad Z_1 Z_1 hh = -i\frac{\lambda}{2}, \qquad \delta^{--}\delta^{++} hh = -i(\lambda_1),$$

$$\phi^+\phi^- hh = -i\frac{\lambda}{2}, \qquad hh\xi^0\xi^0 = -i(\lambda_1 + \lambda_4), \qquad hhhh = -i\frac{3\lambda}{2}.$$

One can read off from this list the μ-independent part of the triple scalar couplings, by making the substitutions $Z_1 \to -iv_d$, $h \to v_d$ or $Z_2 \to -iv_t$, $\xi^0 \to v_t$ [cf. Eq. (2.26)] in the appropriate vertices and modifying accordingly the symmetry factors for identical fields.

---

[1] Guido Altarelli, Proc. Sci., HRMS2010 (2010) 022 [arXiv:1011.5342].

[2] S. Weinberg, Phys. Rev. Lett. **43**, 1566 (1979).

[3] M. Gell-Mann, P. Ramond, and R. Slansky, in *Supergravity*, edited by D. Freedman *et al.* (North-Holland, Amsterdam, 1979).

[4] Tsutomu Yanagida, in Proceedings of the Workshop on the Baryon Number of the Universe and Unified Theories, Tsukuba, Japan, 1979.

[5] R. N. Mohapatra and G. Senjanovic, Phys. Rev. Lett. **44**, 912 (1980).

[6] W. Konetschny and W. Kummer, Phys. Lett. **70B**, 433 (1977).

[7] T. P. Cheng and Ling-Fong Li, Phys. Rev. D **22**, 2860 (1980).

[8] G. Lazarides, Q. Shafi, and C. Wetterich, Nucl. Phys. **B181**, 287 (1981).

[9] J. Schechter and J. W. F. Valle, Phys. Rev. D **22**, 2227 (1980).

[10] R. N. Mohapatra and G. Senjanovic, Phys. Rev. D **23**, 165 (1981).

[11] R. Foot, H. Lew, X. G. He, and C. Girish, Z. Phys. C **44**, 441 (1989).

[12] E. Ma, Phys. Rev. Lett. **81**, 1171 (1998).

[13] B. Bajc and G. Senjanovic, J. High Energy Phys. 08 (2007) 014.

[14] P. Fileviez Perez, Phys. Lett. B **654**, 189 (2007).

[15] P. Fileviez Perez, Phys. Rev. D **76**, 071701 (2007).

[16] A. Abada, C. Biggio, F. Bonnet, M. B. Gavela, and T. Hambye, J. High Energy Phys. 12 (2007) 061.

[17] P. Fileviez Perez, T. Han, G.-Y. Huang, Tong Li, and K. Wang, Phys. Rev. D **78**, 015018 (2008).

[18] P. Dey, A. Kundu, and B. Mukhopadhyaya, J. Phys. G **36**, 025002 (2009).

[19] C. Amsler et al., Phys. Lett. B **667**, 1 (2008).

[20] M.-C. Chen, S. Dawson, and T. Krupovnickas, Phys. Rev. D **74**, 035001 (2006).

[21] T. Blank and W. Hollik, Nucl. Phys. **B514**, 113 (1998).

[22] P. H. Chankowski, S. Pokorski, and J. Wagner, Eur. Phys. J. C **50**, 919 (2007).

[23] M.-C. Chen, S. Dawson, and C. B. Jackson, Phys. Rev. D **78**, 093001 (2008).

[24] S. R. Coleman, Phys. Rev. D **15**, 2929 (1977).

[25] C. G. Callan, Jr. and S. R. Coleman, Phys. Rev. D **16**, 1762 (1977).

[26] M. Sher, Phys. Rep. **179**, 273 (1989).

[27] A. Wahab El Kaffas and W. Khater, Nucl. Phys. **B775**, 45 (2007).

[28] T. Appelquist and J. D. Bjorken, Phys. Rev. D **4**, 3726 (1971).

[29] J. M. Cornwall, D. N. Levin, and G. Tiktopoulos, Phys. Rev. D **10**, 1145 (1974).

[30] B. W. Lee, C. Quigg, and H. B. Thacker, Phys. Rev. D **16**, 1519 (1977).

[31] S. Kanemura, T. Kubota, and E. Takasugi, Phys. Lett. B **313**, 155 (1993).

[32] A. G. Akeroyd, A. Arhrib, and E.-M. Naimi, Phys. Lett. B **490**, 119 (2000).

[33] M. Aoki and S. Kanemura, Phys. Rev. D **77**, 095009 (2008).

[34] I. Gogoladze, N. Okada, and Q. Shafi, Phys. Lett. B **668**, 121 (2008).

[35] H. M. Pilkuhn, Relativistic Particle Physics (Springer-Verlag, Berlin, 1979).

[36] M. Luscher and P. Weisz, Phys. Lett. B **212**, 472 (1988).

[37] W. J. Marciano, G. Valencia, and S. Willenbrock, Phys. Rev. D **40**, 1725 (1989).

[38] A. G. Akeroyd and C.-W. Chiang, Phys. Rev. D **81**, 115007 (2010).

[39] A. G. Akeroyd, M. Aoki, and H. Sugiyama, Phys. Rev. D **77**, 075010 (2008).

[40] F. del Aguila and J. A. Aguilar-Saavedra, Nucl. Phys. **B813**, 22 (2009).

[41] A. G. Akeroyd, M. Aoki, and H. Sugiyama, Phys. Rev. D **79**, 113010 (2009).

[42] T. Fukuyama, H. Sugiyama, and K. Tsumura, J. High Energy Phys. 03 (2010) 044.

[43] A. G. Akeroyd and C.-W. Chiang, Phys. Rev. D **80**, 113010 (2009).

[44] S. T. Petcov, H. Sugiyama, and Y. Takanishi, Phys. Rev. D **80**, 015005 (2009).

[45] T. Fukuyama, H. Sugiyama, and K. Tsumura, Phys. Rev. D **82**, 036004 (2010).

[46] A. G. Akeroyd, C.-W. Chiang, and N. Gaur, J. High Energy Phys. 11 (2010) 005.

[47] E. Accomando et al., arXiv:hep-ph/0608079.

[48] A. G. Akeroyd, Phys. Lett. B **353**, 519 (1995).

[49] J. F. Gunion, C. Loomis, and K. T. Pitts, arXiv:hep-ph/9610237.

[50] J. F. Gunion, R. Vega, and J. Wudka, Phys. Rev. D **42**, 1673 (1990).

[51] C.-S. Chen, C.-Q. Geng, and D. V. Zhuridov, Eur. Phys. J. C **60**, 119 (2009).

[52] D. K. Ghosh, R. M. Godbole, and B. Mukhopadhyaya, Phys. Rev. D **55**, 3150 (1997).

[53] K.-M. Cheung, R. J. N. Phillips, and A. Pilaftsis, Phys. Rev. D **51**, 4731 (1995).

[54] R. Godbole, B. Mukhopadhyaya, and M. Nowakowski, Phys. Lett. B **352**, 388 (1995).

[55] K. Huitu, J. Maalampi, A. Pietila, and M. Raidal, Nucl. Phys. **B487**, 27 (1997).

[56] G. Azuelos, K. Benslama, and J. Ferland, J. Phys. G **32**, 73 (2006).

[57] V. D. Barger, H. Baer, W.-Y. Keung, and R. J. N. Phillips, Phys. Rev. D **26**, 218 (1982).

[58] A. G. Akeroyd and M. Aoki, Phys. Rev. D **72**, 035011 (2005).

[59] P. Achard et al., Phys. Lett. B **576**, 18 (2003).

[60] G. Abbiendi et al., Phys. Lett. B **526**, 221 (2002).

[61] J. Abdallah et al., Phys. Lett. B **552**, 127 (2003).

[62] V. M. Abazov et al., Phys. Rev. Lett. **93**, 141801 (2004).

[63] V. M. Abazov et al., Phys. Rev. Lett. **101**, 071803 (2008).

[64] D. E. Acosta et al., Phys. Rev. Lett. **93**, 221802 (2004).

[65] T. Aaltonen et al., Phys. Rev. Lett. **101**, 121801 (2008).

[66] J. Garayoa and T. Schwetz, J. High Energy Phys. 03 (2008) 009.

[67] M. Kadastik, M. Raidal, and L. Rebane, Phys. Rev. D **77**, 115023 (2008).

[68] T. Rommerskirchen and T. Hebbeker, J. Phys. G **34**, N47 (2007).

[69] S. Chatrchyan et al., Report No. CMS-HIG-11-007.

[70] E. J. Chun, K. Y. Lee, and S. C. Park, Phys. Lett. B **566**, 142 (2003).

[71] P. Ren and Z.-Z. Xing, Phys. Lett. B **666**, 48 (2008).

[72] V. M. Abazov et al., Phys. Lett. B **682**, 278 (2009).

[73] T. Aaltonen et al., Phys. Rev. Lett. **103**, 101803 (2009).

[74] S. Chatrchyan et al., Report No. CMS-HIG-11-008.

[75] G. Aad et al., Report No. ATLAS-CONF-2011-138.

[76] P. Achard et al., Phys. Lett. B **575**, 208 (2003).

[77] J. Abdallah et al., Eur. Phys. J. C **34**, 399 (2004).

[78] A. Datta and A. Raychaudhuri, Phys. Rev. D **62**, 055002 (2000).

[79] J. Abdallah *et al.*, Eur. Phys. J. C **38**, 1 (2004).

[80] J. A. Aguilar-Saavedra and G. C. Branco, Phys. Lett. B **495**, 347 (2000).

[81] M. Beneke *et al.*, arXiv:hep-ph/0003033.

[82] J. A. Aguilar-Saavedra, Phys. Lett. B **502**, 115 (2001).

[83] J. A. Aguilar-Saavedra, Acta Phys. Pol. B **35**, 2695 (2004).

[84] K Nakamura *et al.*, J. Phys. G **37**, 075021 (2010).